Confronting electroweak MSSM through one-loop renormalized neutralino-Higgs interactions for dark matter direct detection and the muon $g-2$

Subhadip Bisal,[1,2,*] Arindam Chatterjee,[3,†] Debottam Das,[1,2,‡] and Syed Adil Pasha[3,§]

[1]*Institute of Physics, Sachivalaya Marg, Bhubaneswar 751 005, India*
[2]*Homi Bhabha National Institute, Training School Complex, Anushakti Nagar, Mumbai 400 094, India*
[3]*Shiv Nadar Institution of Eminence Deemed to be University, Gautam Buddha Nagar, Uttar Pradesh, 201314, India*

(Received 26 November 2023; accepted 29 May 2024; published 18 July 2024)

We compute the next-to-leading order (NLO) corrections to the vertices where a pair of the lightest neutralino couples to *CP*-even (light or heavy) Higgs scalars. In particular, the lightest neutralino is assumed to be a dominantly binolike mixed state, composed of bino and Higgsino or bino, wino, and Higgsino. After computing all the three-point functions in the electroweak minimal supersymmetric Standard Model (MSSM), we detail the contributions from the counterterms that arise in renormalizing these vertices in one-loop order. The amendment of the renormalized vertices impacts the spin-independent direct detection cross sections of the scattering of nucleons with dark matter. We perform a comprehensive numerical scan over the parameter space where all the points satisfy the present *B*-physics constraints and accommodate the muon's anomalous magnetic moment. Finally, we exemplify a few benchmark points, which indulge the present searches of supersymmetric particles. After including the renormalized one-loop vertices, the spin-independent DM-nucleon cross sections may be enhanced up to 20% compared to its tree-level results. Finally, with the NLO cross section, we use the recent LUX-ZEPLIN (LZ) results on the neutralino-nucleon scattering to display the relative rise in the lowest allowed band of the Higgsino mass parameter in the M_1-μ plane of the electroweak MSSM.

DOI: 10.1103/PhysRevD.110.015021

I. INTRODUCTION

One of the main motivations of the supersymmetric (SUSY) Standard Model (SM) with minimal field content or the minimal supersymmetric SM (MSSM) is the prediction of the lightest supersymmetric particle (LSP) in the form of the lightest neutralino, which is neutral and weakly interacting with the SM particles. If *R*-parity is conserved, in most parts of the MSSM parameter space, the lightest neutralino ($\tilde{\chi}_1^0$) becomes stable, thus forming a good dark matter (DM) candidate (see, e.g., [1,2]). In the MSSM, $\tilde{\chi}_1^0$ can be dominated by one of the interaction states—bino, wino, or Higgsino—or by any of their suitable admixtures. For instance, the LSP can be mixed bino-Higgsino, bino-wino, or even bino-wino-Higgsino-like. Such mixed LSP scenarios are also known as "well-tempered" neutralinos in Ref. [3]. The bino with mass M_1 carries no gauge charge and thus does not couple to gauge bosons. Over the parameter space of the MSSM, a dominantly binolike LSP results in an overabundance of dark matter except for a few fine-tuned strips characterized by, e.g., (a) slepton coannihilations ($\tilde{\chi}_1^0\tilde{l} \xrightarrow{l} l\gamma$) and (b) resonant annihilation ($\tilde{\chi}_1^0\tilde{\chi}_1^0 \xrightarrow{A} b\bar{b}, t\bar{t}, l^+l^-$). A nonzero value of the Higgsino components will be necessary for the latter. Moreover, a somewhat precise relation will be required between the masses of the annihilating LSP and the mediator for the *s*-channel resonance or between the coannihilating supersymmetric state and the lightest neutralino for satisfying the observed relic abundance. The DM relic density of the Higgsino [4–12] (wino [11,13–24]) is primarily realized through the pair annihilation of $\tilde{H}\,\tilde{H}(\tilde{W}\,\tilde{W}) \to WW, f\bar{f}, \ldots$ With isospins $= 1/2$ and 1, Higgsino (wino)like states can be observed to produce the correct abundance with mass term $\mu \simeq 1$ $(M_2 = 2)$ TeV respectively. Otherwise, in most of the MSSM parameter space, the relic density falls below the experimental value $\Omega_{\rm DM}h^2 \sim 0.12$ [25,26]. This is also supplemented by the fact that the second lightest neutralino

*subhadip.b@iopb.res.in
†arindam.chatterjee@snu.edu.in
‡debottam@iopb.res.in
§sp855@snu.edu.in

Published by the American Physical Society under the terms of the Creative Commons Attribution 4.0 International license. Further distribution of this work must maintain attribution to the author(s) and the published article's title, journal citation, and DOI. Funded by SCOAP³.

$\tilde{\chi}_2^0$ and the lightest chargino $\tilde{\chi}_1^\pm$ can be degenerate with $\tilde{\chi}_1^0$, thus causing too strong coannihilations to have too small DM relic density. An exception may be observed in the unconstrained MSSM (pMSSM), with coannihilations may help to lower the effective thermally averaged annihilation cross sections $\langle \sigma_{\rm eff} v \rangle$ thereby causing an increase in the DM relic density [27]. On the other hand, a well-tempered or a mixed LSP dominated by the bino component is expected to give cosmologically compatible DM relic density in an intermediate-mass (sub-TeV) range [27–39]. It may be added here that a Higgsino or a mixed bino-Higgsino DM naturally appears in most of the hyperbolic branch/focus point region of minimal supergravity (mSUGRA) inspired models [4,5,28–30,40,41] where the scalars may become considerably heavier (multi-TeV) satisfying the universal boundary conditions at the gauge coupling unification scale ($M_G \sim 2 \times 10^{16}$ GeV).[1] Similarly, a winolike LSP arises naturally in the anomaly mediated supersymmetry breaking (AMSB) model [46,47] where the gaugino and scalar masses are calculated from supergravity breaking in the hidden sector via super-Weyl anomaly contributions [48].

In this era of LHC, with strongly interacting squarks and gluino heavier than a few TeV [49,50], a sub-TeV neutralino or chargino (will be referred to as an electroweakino) becomes the torchbearer for the TeV scale SUSY. On the one hand, unlike the colored sparticles, LHC constraints are much weaker for electroweak (EW) particles due to a smaller production cross section [49–51] (for heavier Higgsino searches at the LHC, see [52]). On the other hand, the pursuance of explaining muon anomalous magnetic moment $a_\mu = (g-2)_\mu/2$ through SUSY contributions is another instance where lighter electroweak sparticles are highly welcome. The measured value (combining the BNL E821 [53] and the Fermilab muon $g-2$ [54] experiments) deviates by 4.2σ from the SM [55–75]. The recent update released by Fermilab using Run-2 and Run-3 data, the new experimental average predicts 5.1σ deviations from the SM [76]. In the MSSM, lighter smuons and electroweakinos, e.g., $\tilde{\chi}^- - \tilde{\nu}_\mu$ and $\tilde{\mu} - \tilde{\chi}^0$ contribute to $\delta a_\mu = a_\mu^{\rm Exp} - a_\mu^{\rm SM}$ at one-loop level. A dominantly binolike light $\tilde{\chi}_1^0$ accompanying light sleptons seems to be favored by δa_μ, especially if the observed DM abundance has to come entirely from the lightest neutralino in the R-parity conserving MSSM. For a mixed $\tilde{\chi}_1^0$, such as bino-Higgsino DM, stringent limits from the direct dark matter detection experiments (DD) [77–86] can be placed [87–90]. The spin-independent (SI) searches are particularly severe, as it directly curbs the gaugino-Higgsino-Higgs coupling in the $\tilde{\chi}_1^0 \tilde{\chi}_1^0 h(H)$ (h and H indicate the light and heavy Higgs bosons) vertex. Following Ref. [88], one finds that even with the maximal mixing, a narrow strip is still viable for $\tan\beta \lesssim 3$ (with stop mass $m_{\tilde{t}_1} \sim 25$ TeV). Otherwise, pockets exist in the parameter space where small DD cross sections can be realized to comply with the DM-initiated recoils. In one example, "blind spots" can be realized when the tree-level couplings of $\tilde{\chi}_1^0$ to Z or the Higgs bosons may be highly suppressed or even zero identically [91,92] or through the destructive interference between light and heavy CP-even Higgs bosons, as first noticed in [93]. Another example follows when the SM-like Yukawa couplings of the light quarks are relaxed [94]. For a bino-wino scenario (i.e., with negligible Higgsino fraction), the SI and spin-dependent (SD) DD rates vanish (see, e.g., [95]). This is because the Higgs coupling to the LSP pair is proportional to the product of their Higgsino and gaugino components, and the Z boson coupling to the LSP pair is proportional to the square of its Higgsino components $|\mathcal{N}_{13}|^2 - |\mathcal{N}_{14}|^2$ (but vanishes for pure Higgsinos).

More recently, Ref. [90] zoom out the regions of the allowed MSSM parameter space, compatible with the muon $g-2$ anomaly, DM relic density, DD limits, and the latest LHC Run-2 data. It turns out that a binolike light $\tilde{\chi}_1^0$ with minimal Higgsino contributions where sleptons are not far from the LSP or to a compressed scenario of bino, wino, and sleptons are still viable for future searches. The leading-order (LO) process is only considered for evaluating DM observables, specifically for the DD cross section.

It is known that the next-to-leading order (NLO) corrections may lead to important effects in specific examples of DM phenomenology. For instance, heavy quarks (t, b) and their superpartners can induce mass splitting between the Higgsino-like states [96], which in turn can influence the estimate of the LSP relic density [97]. Latter follows from the fact that (i) the coannihilation rate is weighted by the exponential factors, thereby suppressed with the relative mass splitting of the Higgsino-like states, and (ii) gaugino and Higgsino components may get changed, which may affect the LSP couplings to the gauge and Higgs bosons. References [97–99] also presented the important SUSY corrections in the cross section of a Higgsino-like neutralino DM with the nucleon. In [100], wino/Higgsino-nucleon one-loop cross sections generated by the gauge interactions were calculated. References [101,102] considered the SUSY QCD corrections for the DD of neutralino DM. The DM-nucleon cross section at one one-loop level for a general class of weakly interacting massive particles was considered in Refs. [103,104]. At the same time, the interaction of gluon with the DM was noted in Refs. [105,106]. However, none of the analyses considers the renormalization of chargino/neutralino sector, which we employ here to explicitly estimate the Higgs interactions with $\tilde{\chi}_1^0$ pairs. Adopting a suitable renormalization scheme, the vertex counterterms are calculated and added to the

[1]A relatively small value of μ parameter ≤ 1 TeV, is typically favored in most of the SUSY models guided by "naturalness" (for recent searches of the natural SUSY see [42–45]).

three-point vertex corrections. Here, we recall that in the limit of vanishing mixings among the different constituents in $\tilde{\chi}_1^0$, counterterms may be calculated to vanish. Since for a pure $\tilde{\chi}_1^0$, there is no tree-level interaction that an SM-like Higgs scalar can couple to $\tilde{\chi}_1^0$ pairs, the renormalization of $\tilde{\chi}_1^0\tilde{\chi}_1^0 h$ or $\tilde{\chi}_1^0\tilde{\chi}_1^0 H$ coupling at the NLO is neither needed nor possible.[2] For a general and dominantly binolike $\tilde{\chi}_1^0$, as in this case, tree-level coupling exists, and counterterms may boost the DM-nucleon scattering. Based on this lesson, we explore the MSSM regions through the muon $g-2$ anomaly, DM relic density, and the spin-independent DM direct detections (SI-DD) at the one-loop level. The latest LHC Run-2 data is also considered. The relic density constraint is not always respected in the analysis; thus, thermal relic abundance of the LSP may satisfy (i) the observed cosmological dark matter abundance, (ii) falls below the dark matter abundance (known as underabundant neutralinos), (iii) overshoots the observed cosmological data (over-abundant neutralino). Since our primary interest is to find out the role of the NLO corrections to the neutralino-Higgs vertices and the SI-DD cross section in compliance with $(g-2)_\mu$; we relax the relic density constraint in the first place.[3] In particular, two regions with a dominantly binolike $\tilde{\chi}_1^0$, but having (i) a minimal Higgsino ($M_1 \ll \mu$) component and (ii) a minimal wino-Higgsino ($M_1 < M_2 \lesssim \mu$) component (assuming M_1, M_2, and μ to be real and positive in both the scenarios) will come out as interesting for future searches. Henceforth, we refer them as $\tilde{B}_{\tilde{H}}$ and $\tilde{B}_{\tilde{W}\tilde{H}}$ zones of the MSSM parameter space.

The rest of the paper is organized as follows. In Sec. II, we briefly review the neutralino and chargino sectors of the MSSM. We fix the notation and convention for the masses and mixing matrices and then discuss the different possibilities of the mixed neutralino states. We present the effective Lagrangian for the neutralino-nucleon scattering in Sec. III. In Sec. IV A, we show the generic triangular topologies of the relevant Feynman diagrams and present analytical results, while Sec. IV B covers the important aspects of renormalizations of the chargino and neutralino sectors. In Sec. V A and Sec. V B, we summarize the supersymmetric contributions to anomalous magnetic moments of muon (δa_μ) and the limits from the SUSY searches at the collider experiments. Section VI illustrates the methodology adopted for the numerical calculations, followed by the evaluation of the neutralino-nucleon scattering cross section in Sec. VII. Finally, we conclude in Sec. VIII.

II. THE NEUTRALINO AND CHARGINO SECTORS OF THE MSSM

In the MSSM, the supersymmetric partner of the neutral gauge bosons, known as bino, $\tilde{B}$ [the supersymmetric partner of the $U(1)_Y$ gauge boson B] and wino, $\tilde{W}^0$ (the supersymmetric partner of the $SU(2)_L$ neutral gauge boson W^0) mix with the supersymmetric partners of the two MSSM Higgs bosons, known as down-type and up-type Higgsinos $\tilde{H}_d^0$ and $\tilde{H}_u^0$, respectively. The 4×4 neutralino mass matrix in the basis $(\tilde{B}, \tilde{W}^0, \tilde{H}_d^0, \tilde{H}_u^0)$ can be written as

$$\bar{\mathbb{M}}_{\tilde{\chi}^0} = \begin{pmatrix} M_1 & 0 & -M_Z s_W c_\beta & M_Z s_W s_\beta \\ 0 & M_2 & M_Z c_W c_\beta & -M_Z c_W s_\beta \\ -M_Z s_W c_\beta & M_Z c_W c_\beta & 0 & -\mu \\ M_Z s_W s_\beta & -M_Z c_W s_\beta & -\mu & 0 \end{pmatrix}, \tag{1}$$

where M_Z is the mass of the Z boson, β represents the mixing angle between the two Higgs vacuum expectation values, and $s_\beta = \sin\beta$, $c_\beta = \cos\beta$. Here, $c_W = \cos\theta_W$ and $s_W = \sin\theta_W$ are the cosine and sine of the Weinberg angle θ_W, respectively. The mass parameters M_1, M_2, and μ can generally be complex, allowing the CP-violating interactions in MSSM. But we restrict to the case of CP-conserving interactions; hence, M_1, M_2, and μ are real in our scenario.

Besides, the mass matrix of charginos can be read from the mass eigenstates of the 2×2 complex mass matrix, $\bar{\mathbb{M}}_{\tilde{\chi}^\pm}$ in the wino-Higgsino basis,

$$\bar{\mathbb{M}}_{\tilde{\chi}^\pm} = \begin{pmatrix} M_2 & \sqrt{2}s_\beta M_W \\ \sqrt{2}c_\beta M_W & \mu \end{pmatrix}, \tag{2}$$

which can be diagonalized by two unitary 2×2 matrices $\mathbf{U}$ and $\mathbf{V}$.

The neutralino mass matrix in Eq. (1) can be diagonalized by a 4×4 unitary matrix $\mathbb{N}$ (in this case $\mathbb{N}$ is orthogonal),

$$\mathbb{N}\bar{\mathbb{M}}_{\tilde{\chi}^0}\mathbb{N}^{-1} = \mathbb{M}_{\tilde{\chi}^0}, \quad [\text{since } \mathbb{N}^* = \mathbb{N}], \tag{3}$$

where $\mathbb{M}_{\tilde{\chi}^0} = \text{diag}\,(m_{\tilde{\chi}_1^0}, m_{\tilde{\chi}_2^0}, m_{\tilde{\chi}_3^0}, m_{\tilde{\chi}_4^0})$ refer to the physical masses of the neutralinos with $\tilde{\chi}_1^0$ being the lightest, and $\mathcal{N}_{ij}$ are the elements of the neutralino mixing matrix $\mathbb{N}$. The Lagrangian for the neutralino-neutralino-scalar interaction is given by [107],

[2]However, due to the off-diagonal terms in the neutralino mass matrix (generated after EWSB), a small admixture of the gauge eigenstates is inevitable even when the respective mass parameters are $\mathcal{O}(1\text{ TeV})$.

[3]However, scenario (ii) and (iii) can be made viable in the presence of different DM components or through modifying the standard cosmological thermal history.

$$\mathcal{L}_{\tilde{\chi}^0_\ell \tilde{\chi}^0_n \phi} \supset \frac{g_2}{2} h \bar{\tilde{\chi}}^0_n [\mathbf{P_L}(Q''^*_{\ell n} s_\alpha + S''^*_{\ell n} c_\alpha) + \mathbf{P_R}(Q''_{n\ell} s_\alpha + S''_{n\ell} c_\alpha)]\tilde{\chi}^0_\ell - \frac{g_2}{2} H \bar{\tilde{\chi}}^0_n [\mathbf{P_L}(Q''^*_{\ell n} c_\alpha - S''^*_{\ell n} s_\alpha) + \mathbf{P_R}(Q''_{n\ell} c_\alpha - S''_{n\ell} s_\alpha)]\tilde{\chi}^0_\ell - i\frac{g_2}{2} A \bar{\tilde{\chi}}^0_n [\mathbf{P_L}(S''^*_{\ell n} c_\beta - Q''^*_{\ell n} s_\beta) + \mathbf{P_R}(Q''_{n\ell} s_\beta - S''_{n\ell} c_\beta)]\tilde{\chi}^0_\ell, \quad (4)$$

where $\phi = h_i, A$, with h_i, for $i = 1$ and 2 refer to an SM-like scalar h and a heavy CP-even Higgs boson H, respectively. Similarly, $\mathbf{P_{L,R}} = \frac{1\mp\gamma 5}{2}$ as usual. The neutral CP-odd Higgs is denoted by A, α is the Higgs mixing angle, and g_2 is the $SU(2)_L$ gauge coupling strength. Couplings $Q''_{n\ell}$ and $S''_{n\ell}$ are defined in Appendix A.

Similarly, the neutralino-neutralino-Z interaction can be read from

$$\mathcal{L}_{\tilde{\chi}^0_\ell \tilde{\chi}^0_n Z} \supset \frac{g_2}{2c_W} Z_\mu \bar{\tilde{\chi}}^0_\ell \gamma^\mu (N^L_{\ell n} \mathbf{P_L} + N^R_{\ell n} \mathbf{P_R}) \tilde{\chi}^0_n, \quad (5)$$

where $N^L_{\ell n}$ and $N^R_{\ell n}$ are defined in Appendix A.

A few interesting limits can now be observed. A pure Higgsino-like $\tilde{\chi}^0_1$; it refers to a limit $\mathcal{N}_{11} = \mathcal{N}_{12} = 0$ or the soft masses M_1 and M_2 are large and decoupled. A pure gauginolike $\tilde{\chi}^0_1$: it refers to a limit $\mathcal{N}_{13} = \mathcal{N}_{14} = 0$. In this pure limit, the coupling $\tilde{\chi}^0_1 \tilde{\chi}^0_1 \phi$ (with $\phi = h, H, A$) vanishes since $Q''_{11} = S''_{11} = 0$. In the mixed LSP scenarios, as said before, we are interested in bino-Higgsino ($\tilde{B}_{\tilde{H}}$) and bino-wino-Higgsino ($\tilde{B}_{\tilde{W}\tilde{H}}$) DM scenarios with a predominantly bino component. A qualitative understanding of the neutralino masses and their mixings (mainly $\mathcal{N}_{1j}$) can be instructive here, which we detail in Appendix B (see also [108–110]). In fact, using the expressions derived for the mixing matrices in Appendix B, we can rewrite the $\tilde{\chi}^0_1 \tilde{\chi}^0_1 h$ and $\tilde{\chi}^0_1 \tilde{\chi}^0_1 H$ couplings for $\tilde{B}_{\tilde{W}\tilde{H}}$ DM as

$$\mathcal{L}_{\tilde{\chi}^0_1 \tilde{\chi}^0_1 \phi} = \phi \bar{\tilde{\chi}}^0_1 [\mathbf{P_L} C^{\rm LO}_L + \mathbf{P_R} C^{\rm LO}_R] \tilde{\chi}^0_1. \quad (6)$$

For $\phi = h$,

$$C^{\rm LO}_L = C^{\rm LO}_R = \frac{g_2}{2}(Q''_{11} s_\alpha + S''_{11} c_\alpha) = -\frac{g_2}{2}\frac{M_Z s_W}{\mu^2 - M_1^2}(\mu s_\alpha - M_1 c_\alpha)\left[\frac{M_1 M_Z^2 s_{2W}}{2(M_2 - M_1)} + t_W\right], \quad (7)$$

and for $\phi = H$,

$$C^{\rm LO}_L = C^{\rm LO}_R = -\frac{g_2}{2}(Q''_{11} c_\alpha - S''_{11} s_\alpha) = \frac{g_2}{2}\frac{M_Z s_W}{\mu^2 - M_1^2}(\mu c_\alpha + M_1 s_\alpha)\left[\frac{M_1 M_Z^2 s_{2W}}{2(M_2 - M_1)} + t_W\right]. \quad (8)$$

Similarly, the couplings for $\tilde{B}_{\tilde{H}}$ DM are given as follows. For $\phi = h$,

$$C^{\rm LO}_L = C^{\rm LO}_R = -\frac{g_2}{2} t_W \frac{M_Z s_W}{\mu^2 - M_1^2}(\mu s_\alpha - M_1 c_\alpha), \quad (9)$$

and for $\phi = H$,

$$C^{\rm LO}_L = C^{\rm LO}_R = \frac{g_2}{2} t_W \frac{M_Z s_W}{\mu^2 - M_1^2}(\mu c_\alpha + M_1 s_\alpha). \quad (10)$$

The coefficients of $\mathbf{P_L}$ and $\mathbf{P_R}$ are equal due to the Majorana nature of the neutralinos. Recall that, in the above expressions, $s_\beta \to 1$ and $c_\beta \to 0$ are assumed. If instead we keep the $\tan\beta$ dependence, one can obtain the $\tilde{\chi}^0_1 \tilde{\chi}^0_1 h(H)$ coupling goes as $\propto [M_1 + \mu s_{2\beta}](\mu c_{2\beta})$.

III. EFFECTIVE LAGRANGIAN FOR NEUTRALINO-NUCLEON SCATTERING

This section presents the effective Lagrangian governing the neutralino-nucleon scattering process and provides the corresponding formulas for the cross section ([1,2,98,111–118]). In the realm of nonrelativistic neutralinos, the effective interactions between $\tilde{\chi}^0_1$ and the light quarks and gluons, at the renormalization scale $\bar{\mu}_0 \simeq m_p$, can be elegantly described as follows [98,100,119–121]:

$$\mathcal{L}^{\rm eff} = \sum_{q=u,d,s} \mathcal{L}^{\rm eff}_q + \mathcal{L}^{\rm eff}_g, \quad (11)$$

where

$$\mathcal{L}^{\rm eff}_q = \eta_q \bar{\tilde{\chi}}^0_1 \gamma^\mu \gamma_5 \tilde{\chi}^0_1 \bar{q} \gamma_\mu \gamma_5 q + \lambda_q m_q \bar{\tilde{\chi}}^0_1 \tilde{\chi}^0_1 \bar{q} q + \frac{g^{(1)}_q}{m_{\tilde{\chi}^0_1}} \bar{\tilde{\chi}}^0_1 i\partial^\mu \gamma^\nu \tilde{\chi}^0_1 \mathcal{O}^q_{\mu\nu} + \frac{g^{(2)}_q}{m^2_{\tilde{\chi}^0_1}} \bar{\tilde{\chi}}^0_1 (i\partial^\mu)(i\partial^\nu) \tilde{\chi}^0_1 \mathcal{O}^q_{\mu\nu},$$

$$\mathcal{L}^{\rm eff}_g = \lambda_G \bar{\tilde{\chi}}^0_1 \tilde{\chi}^0_1 G^a_{\mu\nu} G^{a\mu\nu} + \frac{g^{(1)}_G}{m_{\tilde{\chi}^0_1}} \bar{\tilde{\chi}}^0_1 i\partial^\mu \gamma^\nu \tilde{\chi}^0_1 \mathcal{O}^g_{\mu\nu} + \frac{g^{(2)}_G}{m^2_{\tilde{\chi}^0_1}} \bar{\tilde{\chi}}^0_1 (i\partial^\mu)(i\partial^\nu) \tilde{\chi}^0_1 \mathcal{O}^g_{\mu\nu}. \quad (12)$$

The terms up to the second derivative of the neutralino field have been incorporated in the above. The spin-dependent interaction refers to the first term of $\mathcal{L}^{\rm eff}_q$ while the spin-independent "coherent" contributions arising from the remaining terms in $\mathcal{L}^{\rm eff}_q$ and $\mathcal{L}^{\rm eff}_g$. The third and fourth terms in $\mathcal{L}^{\rm eff}_q$ and the second and third terms in $\mathcal{L}^{\rm eff}_g$ are

governed by the twist-2 operators (traceless part of the energy-momentum tensor) for the quarks and gluons [98,100]. Note that the contributions of the twist-2 operators of gluon are suppressed by the strong coupling constant α_s, thus not included in the subsequent sections. Finally, the SI scattering cross section of the neutralino with target nuclei can be expressed as

$$\sigma_{\rm SI} = \frac{4}{\pi}\left(\frac{m_{\tilde{\chi}_1^0} M_A}{m_{\tilde{\chi}_1^0} + M_A}\right)^2 [\{Z f_p + (A-Z) f_n\}^2], \tag{13}$$

where Z and A represent its atomic and mass numbers, respectively.

The spin-independent coupling of the neutralino with nucleon (of mass m_N), f_N ($N = p, n$) in Eq. (13) can be expressed as (neglecting the contributions from twist-2 operators and also from squark loops)

$$\frac{f_N}{m_N} = \sum_{q=u,d,s} \lambda_q f_q^{(N)} - \frac{8\pi}{9\alpha_s}\lambda_G f_G^{(N)}, \tag{14}$$

where the matrix elements of nucleon are defined as

$$f_q^{(N)} \equiv \frac{1}{m_N}\langle N|m_q \bar{q} q|N\rangle. \tag{15}$$

The second term in Eq. (14) involves effective interactions between the weakly interacting massive particles, heavy quarks, and gluons, which can be evaluated utilizing the trace anomaly of the energy-momentum tensor in QCD [98,122]. Here, one finds heavy quark form factors are related to that of gluons,

$$\begin{aligned}\langle N|m_Q \bar{Q} Q|N\rangle &= -\frac{\alpha_s}{12\pi} c_Q \langle N|G^a_{\mu\nu} G^{a\mu\nu}|N\rangle, \\ m_N f_G^{(N)} &= -9\frac{\alpha_s}{8\pi}\langle N|G^a_{\mu\nu} G^{a\mu\nu}|N\rangle,\end{aligned} \tag{16}$$

with $\alpha_s = g_s^2/4\pi$ and the leading order QCD correction $c_Q = 1 + 11\alpha_s(m_Q)/4\pi$ is considered. The coefficient λ_G in Eq. (14) is related to heavy quarks,

$$\lambda_G = -\frac{\alpha_s}{12\pi}\sum_{Q=c,b,t} c_Q \lambda_Q, \tag{17}$$

with λ_Q often involves $\phi Q\bar{Q}$ vertex at the tree level. Here, λ_q and λ_Q contains all SUSY model-dependent information.

The parameters, $f_q^{(N)}$ ($q \in u, d, s$) can be determined from lattice QCD calculations [123]. We use the following central values of $f_q^{(N)}$ [123,124]:

$$\begin{aligned} f_u^{(p)} &= 0.0153, \quad f_d^{(p)} = 0.0191, \quad f_s^{(p)} = 0.0447, \\ f_u^{(n)} &= 0.0110, \quad f_d^{(n)} = 0.0273, \quad f_s^{(n)} = 0.0447, \end{aligned} \tag{18}$$

which leads to $f_G^{(N)} \sim 0.921$.[4] It should be noted that the above numerical values are subject to some uncertainties as they are evaluated using the hadronic data [115,128].

The scalar cross section depends on t-channel Higgs exchange (h, H) (neglecting squark contributions) ($\sigma_{\rm SI} \propto \frac{1}{m^4_{h,H}}$). Apart from the masses of the Higgs scalar, the cross section depends strongly on the $\tilde{\chi}_1^0\tilde{\chi}_1^0 h(H)$ couplings [Eqs. (7)–(10)] and also on the $q\bar{q}h(H)$ coupling (through λ_q and λ_Q). Note that for down-type fermions $q\bar{q}h$ coupling goes as $\sim \tan\beta\cos(\beta-\alpha)$ while $q\bar{q}H$ coupling goes as $\sim \tan\beta\sin(\beta-\alpha)$. For H scalar, $\tilde{\chi}_1^0\tilde{\chi}_1^0 H$ and $q\bar{q}H$ couplings assume larger values compared to that of the SM-like Higgs scalar in the decoupling region ($M_A^2 \gg M_Z^2$) and with large $\tan\beta$. This makes the heavier Higgs boson contributions in the direct detection quite important.

IV. SPIN-INDEPENDENT $\tilde{\chi}_1^0$-NUCLEON SCATTERING AT ONE-LOOP: THEORY AND IMPLEMENTATION

As already discussed, in general, a tree-level $\tilde{\chi}_1^0\tilde{\chi}_1^0 h_i$ coupling depends on the product of gaugino and Higgsino components. The one-loop correction to this vertex leads to a UV-divergent result. Therefore, one has to renormalize the vertex to get a UV-finite result. Here, we systematically analyze the vertex corrections' generic triangular topologies along with the renormalization procedure.

A. Vertex corrections

We start by classifying different triangular topologies for $\tilde{\chi}_1^0$-nucleon elastic scattering in Fig. 1 where the $\tilde{\chi}_1^0\tilde{\chi}_1^0 h_i$ vertex has been modified by the one-loop radiative corrections from the SM and SUSY particles. We adopt a general notation $S, S' = h, H, A, H^\pm, G^0, G^\pm, \tilde{\ell}$, and $\tilde{\nu}_\ell$ (where $\ell = e, \mu, \tau$); $F, F' = \ell, \nu_\ell, \tilde{\chi}_n^0$, and $\tilde{\chi}_k^\pm$ (where $n = 1, \ldots, 4$ and $k = 1, 2$); $V = W^\pm$ and Z. The squark contributions can be ignored because we set them as heavy ≥4 TeV. For explicit calculations, we find a total of 468 diagrams where 234 diagrams for the $\tilde{\chi}_1^0\tilde{\chi}_1^0 h$ vertex and another 234 diagrams for the $\tilde{\chi}_1^0\tilde{\chi}_1^0 H$ vertex at the particle level.

The analytical expressions for the one-loop diagrams are calculated using PACKAGE-X-2.1.1 [129,130] and given in terms of the Passarino-Veltman functions. The Higgs propagator (h/H), which connects the quark line to the one-loop vertex, has been taken as off-shell with four-momentum q, known as the momentum transfer. The momentum transfer q is generally very small [$q^2 \sim \mathcal{O}(10^{-6})$ GeV^2 for $v_{\chi_1^0} \sim 10^{-3}$] for the elastic scattering process. It may be noted here that $q^2 \sim 0$ is assumed for numerical estimation. In Appendix A,

[4] One gets slightly different values from chiral perturbation theory [125–127].

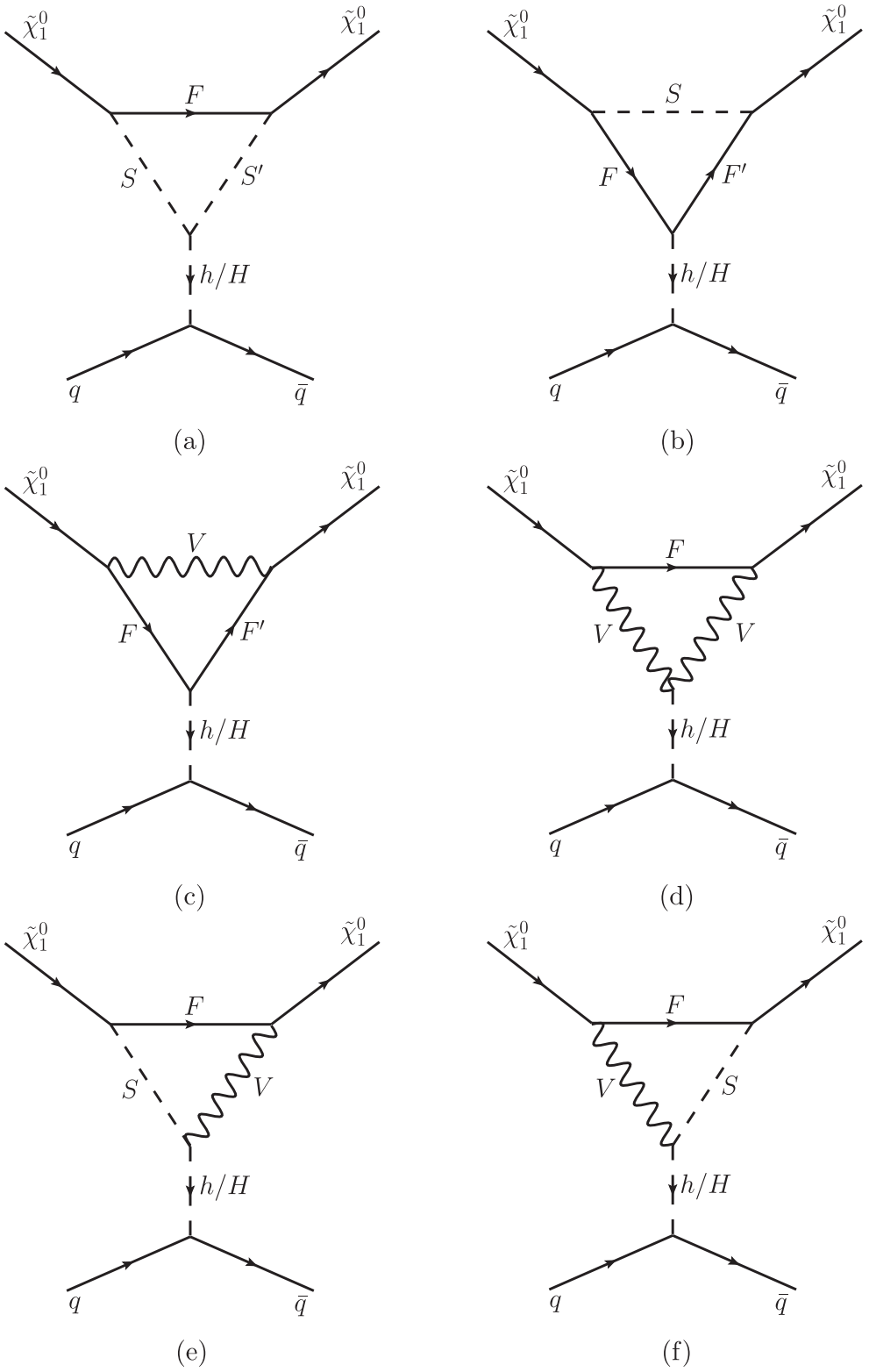

FIG. 1. Relevant topologies for the one-loop correction to the $\tilde{\chi}_1^0\tilde{\chi}_1^0 h_i$ vertex which in turn yields the one-loop correction to the $\tilde{\chi}_1^0\tilde{\chi}_1^0 q\bar{q}$ scattering. Here, $S,S' \in \{h,H,A,H^{\pm},G^0,G^{\pm},\tilde{\ell},\tilde{\nu}_\ell\,(\text{where}\,\ell = e,\mu,\tau)\}$; $F,F' \in \{\tilde{\chi}_n^0,\tilde{\chi}_k^{\pm}\,(\text{where}\,n = 1,\ldots,4\,\text{and}\,k = 1,2),\ell,\nu_\ell; V \in W^{\pm},Z\}$.

we present the prefactors of different topologies for the MSSM.

Topology-1(a):

$$i\Gamma^{(a)}_{\tilde{\chi}^0_1\tilde{\chi}^0_1 h_i} = -\frac{i}{16\pi^2}[\mathbf{P_L}\{\xi_{LL} m_F \mathbf{C}_0 - \xi_{LR} m_{\tilde{\chi}^0_1}\mathbf{C}_1 - \xi_{RL} m_{\tilde{\chi}^0_1}\mathbf{C}_2\} + \mathbf{P_R}\{\xi_{RR} m_F \mathbf{C}_0 - \xi_{RL} m_{\tilde{\chi}^0_1}\mathbf{C}_1 - \xi_{LR} m_{\tilde{\chi}^0_1}\mathbf{C}_2\}], \quad (19)$$

where $\mathbf{C}_i = \mathbf{C}_i(m^2_{\tilde{\chi}^0_1}, q^2, m^2_{\tilde{\chi}^0_1}; m_F, m_S, m_{S'})$ and

$$\xi_{LL} = \lambda_{h_i SS'}\mathcal{G}^L_{\tilde{\chi}^0_1 FS'}\mathcal{G}^L_{\tilde{\chi}^0_1 FS}, \qquad \xi_{LR} = \lambda_{h_i SS'}\mathcal{G}^L_{\tilde{\chi}^0_1 FS'}\mathcal{G}^R_{\tilde{\chi}^0_1 FS},$$
$$\xi_{RL} = \lambda_{h_i SS'}\mathcal{G}^R_{\tilde{\chi}^0_1 FS'}\mathcal{G}^L_{\tilde{\chi}^0_1 FS}, \qquad \xi_{RR} = \lambda_{h_i SS'}\mathcal{G}^R_{\tilde{\chi}^0_1 FS'}\mathcal{G}^R_{\tilde{\chi}^0_1 FS}.$$

Topology-1(b):

$$\begin{aligned} i\Gamma^{(b)}_{\tilde{\chi}^0_1\tilde{\chi}^0_1 h_i} = -\frac{i}{16\pi^2}[&\mathbf{P_L}\{\zeta_{LLL} m_F m_{F'}\mathbf{C}_0 + \zeta_{LLR} m_{\tilde{\chi}^0_1} m_{F'}(\mathbf{C}_0+\mathbf{C}_1) + \zeta_{LRL}\{\mathbf{B}_0 + m_S^2\mathbf{C}_0 + m^2_{\tilde{\chi}^0_1}(\mathbf{C}_1+\mathbf{C}_2)\} \\ &+ \zeta_{LRR} m_{\tilde{\chi}^0_1} m_F \mathbf{C}_1 + \zeta_{RLL} m_{\tilde{\chi}^0_1} m_F(\mathbf{C}_1+\mathbf{C}_2) + \zeta_{RLR} m^2_{\tilde{\chi}^0_1}(\mathbf{C}_0+\mathbf{C}_1+\mathbf{C}_2) + \zeta_{RRL} m_{\tilde{\chi}^0_1} m_{F'}\mathbf{C}_2\} \\ &+ \mathbf{P_R}\{\zeta_{LLR} m_{\tilde{\chi}^0_1} m_{F'}\mathbf{C}_2 + \zeta_{LRL} m^2_{\tilde{\chi}^0_1}(\mathbf{C}_0+\mathbf{C}_1+\mathbf{C}_2) + \zeta_{LRR} m_{\tilde{\chi}^0_1} m_F(\mathbf{C}_1+\mathbf{C}_2) + \zeta_{RLL} m_{\tilde{\chi}^0_1} m_F \mathbf{C}_1 \\ &+ \zeta_{RLR}\{\mathbf{B}_0 + m_S^2\mathbf{C}_0 + m^2_{\tilde{\chi}^0_1}(\mathbf{C}_1+\mathbf{C}_2)\} + \zeta_{RRL} m_{\tilde{\chi}^0_1} m_{F'}(\mathbf{C}_0+\mathbf{C}_1) + \zeta_{RRR} m_F m_{F'}\mathbf{C}_0\}], \end{aligned} \quad (20)$$

where $\mathbf{B}_0 = \mathbf{B}_0(q^2; m_F, m_{F'})$, $\mathbf{C}_i = \mathbf{C}_i(m^2_{\tilde{\chi}^0_1}, q^2, m^2_{\tilde{\chi}^0_1}; m_S, m_F, m_{F'})$, and

$$\zeta_{LLL} = \mathcal{G}^L_{\tilde{\chi}^0_1 F'S}\mathcal{G}^L_{FF'h_i}\mathcal{G}^L_{\tilde{\chi}^0_1 FS}, \qquad \zeta_{LLR} = \mathcal{G}^L_{\tilde{\chi}^0_1 F'S}\mathcal{G}^L_{FF'h_i}\mathcal{G}^R_{\tilde{\chi}^0_1 FS},$$
$$\zeta_{LRL} = \mathcal{G}^L_{\tilde{\chi}^0_1 F'S}\mathcal{G}^R_{FF'h_i}\mathcal{G}^L_{\tilde{\chi}^0_1 FS}, \qquad \zeta_{LRR} = \mathcal{G}^L_{\tilde{\chi}^0_1 F'S}\mathcal{G}^R_{FF'h_i}\mathcal{G}^R_{\tilde{\chi}^0_1 FS},$$
$$\zeta_{RLL} = \mathcal{G}^R_{\tilde{\chi}^0_1 F'S}\mathcal{G}^L_{FF'h_i}\mathcal{G}^L_{\tilde{\chi}^0_1 FS}, \qquad \zeta_{RLR} = \mathcal{G}^R_{\tilde{\chi}^0_1 F'S}\mathcal{G}^L_{FF'h_i}\mathcal{G}^R_{\tilde{\chi}^0_1 FS},$$
$$\zeta_{RRL} = \mathcal{G}^R_{\tilde{\chi}^0_1 F'S}\mathcal{G}^R_{FF'h_i}\mathcal{G}^L_{\tilde{\chi}^0_1 FS}, \qquad \zeta_{RRR} = \mathcal{G}^R_{\tilde{\chi}^0_1 F'S}\mathcal{G}^R_{FF'h_i}\mathcal{G}^R_{\tilde{\chi}^0_1 FS}.$$

Topology-1(c):

$$\begin{aligned} i\Gamma^{(c)}_{\tilde{\chi}^0_1\tilde{\chi}^0_1 h_i} = \frac{i}{16\pi^2}\Big[&\mathbf{P_L}\{\Lambda_{LLL} m_{\tilde{\chi}^0_1} m_{F'}(2-d)\mathbf{C}_2 + \Lambda_{LRL} m_{\tilde{\chi}^0_1} m_F(2-d)(\mathbf{C}_0+\mathbf{C}_2) + \Lambda_{LRR} m^2_{\tilde{\chi}^0_1}(d-4)(\mathbf{C}_0+\mathbf{C}_1+\mathbf{C}_2) \\ &+ \Lambda_{RLL}\{d\mathbf{B}_0 + (4m^2_{\tilde{\chi}^0_1} + m_V^2 d - 2q^2)\mathbf{C}_0 + (4m^2_{\tilde{\chi}^0_1} + m^2_{\tilde{\chi}^0_1} d - 2q^2)(\mathbf{C}_1+\mathbf{C}_2)\} \\ &+ \Lambda_{RLR} m_{\tilde{\chi}^0_1} m_F(2-d)\mathbf{C}_1 + \Lambda_{RRL} m_F m_{F'} d\mathbf{C}_0 + \Lambda_{RRR} m_{\tilde{\chi}^0_1} m_{F'}(2-d)(\mathbf{C}_0+\mathbf{C}_1)\} \\ &+ \mathbf{P_R}\{\Lambda_{LLL} m_{\tilde{\chi}^0_1} m_{F'}(2-d)(\mathbf{C}_0+\mathbf{C}_1) + \Lambda_{LLR} m_F m_{F'} d\mathbf{C}_0 + \Lambda_{LRL} m_{\tilde{\chi}^0_1} m_F(2-d)\mathbf{C}_1 + \Lambda_{LRR} \\ &\times \{d\mathbf{B}_0 + (4m^2_{\tilde{\chi}^0_1} + m_V^2 d - 2q^2)\mathbf{C}_0 + (4m^2_{\tilde{\chi}^0_1} + m^2_{\tilde{\chi}^0_1} d - 2q^2)(\mathbf{C}_1+\mathbf{C}_2)\} + \Lambda_{RLL} m^2_{\tilde{\chi}^0_1}(d-4)(\mathbf{C}_0+\mathbf{C}_1+\mathbf{C}_2) \\ &+ \Lambda_{RLR} m_{\tilde{\chi}^0_1} m_F(2-d)(\mathbf{C}_0+\mathbf{C}_2) + \Lambda_{RRR} m_{\tilde{\chi}^0_1} m_{F'}(2-d)\mathbf{C}_2\}\Big], \end{aligned} \quad (21)$$

where $\mathbf{B}_0 = \mathbf{B}_0(q^2, m_F, m_{F'})$, $\mathbf{C}_i = \mathbf{C}_i(m^2_{\tilde{\chi}^0_1}, q^2, m^2_{\tilde{\chi}^0_1}; m_V, m_F, m_{F'})$ and

$$\Lambda_{LLL} = \mathcal{G}^L_{\tilde{\chi}^0_1 F'V}\mathcal{G}^L_{FF'h_i}\mathcal{G}^L_{\tilde{\chi}^0_1 FV}, \qquad \Lambda_{LLR} = \mathcal{G}^L_{\tilde{\chi}^0_1 F'V}\mathcal{G}^L_{FF'h_i}\mathcal{G}^R_{\tilde{\chi}^0_1 FV},$$
$$\Lambda_{LRL} = \mathcal{G}^L_{\tilde{\chi}^0_1 F'V}\mathcal{G}^R_{FF'h_i}\mathcal{G}^L_{\tilde{\chi}^0_1 FV}, \qquad \Lambda_{LRR} = \mathcal{G}^L_{\tilde{\chi}^0_1 F'V}\mathcal{G}^R_{FF'h_i}\mathcal{G}^R_{\tilde{\chi}^0_1 FV},$$
$$\Lambda_{RLL} = \mathcal{G}^R_{\tilde{\chi}^0_1 F'V}\mathcal{G}^L_{FF'h_i}\mathcal{G}^L_{\tilde{\chi}^0_1 FV}, \qquad \Lambda_{RLR} = \mathcal{G}^R_{\tilde{\chi}^0_1 F'V}\mathcal{G}^L_{FF'h_i}\mathcal{G}^R_{\tilde{\chi}^0_1 FV},$$
$$\Lambda_{RRL} = \mathcal{G}^R_{\tilde{\chi}^0_1 F'V}\mathcal{G}^R_{FF'h_i}\mathcal{G}^L_{\tilde{\chi}^0_1 FV}, \qquad \Lambda_{RRR} = \mathcal{G}^R_{\tilde{\chi}^0_1 F'V}\mathcal{G}^R_{FF'h_i}\mathcal{G}^R_{\tilde{\chi}^0_1 FV}.$$

Topology-1(d):

$$
\begin{aligned}
i\Gamma^{(d)}_{\tilde{\chi}^0_1\tilde{\chi}^0_1 h_i} = -\frac{i}{16\pi^2}[&\mathbf{P_L}\{\eta_{LL} m_{\tilde{\chi}^0_1}(d-2)\mathbf{C}_2 \\
&+ \eta_{RL} m_F d\mathbf{C}_0 + \eta_{RR} m_{\tilde{\chi}^0_1}(d-2)\mathbf{C}_1\} \\
&+ \mathbf{P_R}\{\eta_{LL} m_{\tilde{\chi}^0_1}(d-2)\mathbf{C}_1 + \eta_{LR} m_F d\mathbf{C}_0 \\
&+ \eta_{RR} m_{\tilde{\chi}^0_1}(d-2)\mathbf{C}_2\}], \qquad (22)
\end{aligned}
$$

where $\mathbf{C}_i = \mathbf{C}_i(m^2_{\tilde{\chi}^0_1}, q^2, m^2_{\tilde{\chi}^0_1}; m_F, m_V, m_V)$ and

$$
\begin{aligned}
\eta_{LL} &= \mathcal{G}_{VVh_i}\mathcal{G}^L_{\tilde{\chi}^0_1 FV}\mathcal{G}^L_{\tilde{\chi}^0_1 FV}, \qquad \eta_{LR} = \mathcal{G}_{VVh_i}\mathcal{G}^L_{\tilde{\chi}^0_1 FV}\mathcal{G}^R_{\tilde{\chi}^0_1 FV}, \\
\eta_{RL} &= \mathcal{G}_{VVh_i}\mathcal{G}^R_{\tilde{\chi}^0_1 FV}\mathcal{G}^L_{\tilde{\chi}^0_1 FV}, \qquad \eta_{RR} = \mathcal{G}_{VVh_i}\mathcal{G}^R_{\tilde{\chi}^0_1 FV}\mathcal{G}^R_{\tilde{\chi}^0_1 FV}.
\end{aligned}
$$

Topology-1(e):

$$
\begin{aligned}
i\Gamma^{(e)}_{\tilde{\chi}^0_1\tilde{\chi}^0_1 h_i} = \frac{i}{16\pi^2}[&\mathbf{P_L}\{\psi_{LL} m_{\tilde{\chi}^0_1} m_F(\mathbf{C}_2 - \mathbf{C}_0) + \psi_{LR} m^2_{\tilde{\chi}^0_1}(\mathbf{C}_1 + 2\mathbf{C}_2) + \psi_{RL}\{-d\mathbf{C}_{00} - m^2_{\tilde{\chi}^0_1}(\mathbf{C}_{22} + 2\mathbf{C}_{12} \\
&+ \mathbf{C}_{11} + 2\mathbf{C}_1) + q^2\mathbf{C}_{12} + (2q^2 - 3m^2_{\tilde{\chi}^0_1})\mathbf{C}_2\} + \psi_{RR} m_{\tilde{\chi}^0_1} m_F(\mathbf{C}_1 + 2\mathbf{C}_0)\} + \mathbf{P_R}\{\psi_{LL} m_{\tilde{\chi}^0_1} m_F \\
&\times (\mathbf{C}_1 + 2\mathbf{C}_0) + \psi_{LR}\{-d\mathbf{C}_{00} - m^2_{\tilde{\chi}^0_1}(\mathbf{C}_{22} + 2\mathbf{C}_{12} + \mathbf{C}_{11} + 2\mathbf{C}_1) + q^2\mathbf{C}_{12} + (2q^2 - 3m^2_{\tilde{\chi}^0_1})\mathbf{C}_2\} \\
&+ \psi_{RL} m^2_{\tilde{\chi}^0_1}(\mathbf{C}_1 + 2\mathbf{C}_2) + \psi_{RR} m_{\tilde{\chi}^0_1} m_F(\mathbf{C}_2 - \mathbf{C}_0)\}], \qquad (23)
\end{aligned}
$$

where $\mathbf{C}_i = \mathbf{C}_i(m^2_{\tilde{\chi}^0_1}, q^2, m^2_{\tilde{\chi}^0_1}; m_F, m_S, m_V)$, $\mathbf{C}_{ij} = \mathbf{C}_{ij}(m^2_{\tilde{\chi}^0_1}, q^2, m^2_{\tilde{\chi}^0_1}; m_F, m_S, m_V)$, and

$$
\begin{aligned}
\psi_{LL} &= \mathcal{G}_{h_i SV}\mathcal{G}^L_{\tilde{\chi}^0_1 FV}\mathcal{G}^L_{\tilde{\chi}^0_1 FS}, \qquad \psi_{LR} = \mathcal{G}_{h_i SV}\mathcal{G}^L_{\tilde{\chi}^0_1 FV}\mathcal{G}^R_{\tilde{\chi}^0_1 FS}, \\
\psi_{RL} &= \mathcal{G}_{h_i SV}\mathcal{G}^R_{\tilde{\chi}^0_1 FV}\mathcal{G}^L_{\tilde{\chi}^0_1 FS}, \qquad \psi_{RR} = \mathcal{G}_{h_i SV}\mathcal{G}^R_{\tilde{\chi}^0_1 FV}\mathcal{G}^R_{\tilde{\chi}^0_1 FS}.
\end{aligned}
$$

Topology-1(f):

$$
\begin{aligned}
i\Gamma^{(f)}_{\tilde{\chi}^0_1\tilde{\chi}^0_1 h_i} = \frac{i}{16\pi^2}[&\mathbf{P_L}\{\Xi_{LL}\{d\mathbf{C}_{00} + m^2_{\tilde{\chi}^0_1}(\mathbf{C}_{22} + 2\mathbf{C}_{12} + \mathbf{C}_{11} + 2\mathbf{C}_2 + 3\mathbf{C}_1) - q^2(\mathbf{C}_{12} + 2\mathbf{C}_1)\} + \Xi_{LR} \\
&\times m_{\tilde{\chi}^0_1} m_F(\mathbf{C}_0 - \mathbf{C}_1) - \Xi_{RL} m_{\tilde{\chi}^0_1} m_F(\mathbf{C}_2 + 2\mathbf{C}_0) - \Xi_{RR} m^2_{\tilde{\chi}^0_1}(\mathbf{C}_2 + 2\mathbf{C}_1)\} + \mathbf{P_R}\{-\Xi_{LL} m^2_{\tilde{\chi}^0_1} \\
&\times (\mathbf{C}_2 + 2\mathbf{C}_1) - \Xi_{LR} m_{\tilde{\chi}^0_1} m_F(\mathbf{C}_2 + 2\mathbf{C}_0) + \Xi_{RL} m_{\tilde{\chi}^0_1} m_F(\mathbf{C}_0 - \mathbf{C}_1) + \Xi_{RR}\{d\mathbf{C}_{00} + m^2_{\tilde{\chi}^0_1}(\mathbf{C}_{22} \\
&+ 2\mathbf{C}_{12} + \mathbf{C}_{11} + 2\mathbf{C}_2 + 3\mathbf{C}_1) - q^2(\mathbf{C}_{12} + 2\mathbf{C}_1)\}\}], \qquad (24)
\end{aligned}
$$

where $\mathbf{C}_i = \mathbf{C}_i(m^2_{\tilde{\chi}^0_1}, q^2, m^2_{\tilde{\chi}^0_1}; m_F, m_V, m_S)$, $\mathbf{C}_{ij} = \mathbf{C}_{ij}(m^2_{\tilde{\chi}^0_1}, q^2, m^2_{\tilde{\chi}^0_1}; m_F, m_V, m_S)$ and

$$
\begin{aligned}
\Xi_{LL} &= \mathcal{G}_{h_i SV}\mathcal{G}^L_{\tilde{\chi}^0_1 FS}\mathcal{G}^L_{\tilde{\chi}^0_1 FV}, \qquad \Xi_{LR} = \mathcal{G}_{h_i SV}\mathcal{G}^L_{\tilde{\chi}^0_1 FS}\mathcal{G}^R_{\tilde{\chi}^0_1 FV}, \\
\Xi_{RL} &= \mathcal{G}_{h_i SV}\mathcal{G}^R_{\tilde{\chi}^0_1 FS}\mathcal{G}^L_{\tilde{\chi}^0_1 FV}, \qquad \Xi_{RR} = \mathcal{G}_{h_i SV}\mathcal{G}^R_{\tilde{\chi}^0_1 FS}\mathcal{G}^R_{\tilde{\chi}^0_1 FV}.
\end{aligned}
$$

In the above, $\mathbf{B_0}$, $\mathbf{C}_i$, and $\mathbf{C}_{ij}$ represent the Passarino-Veltman functions and can be evaluated using LOOPTOOLS [131] or PACKAGE-X [129,130]. Now, the total vertex corrections can be obtained as

$$
\begin{aligned}
\Gamma_{\tilde{\chi}^0_1\tilde{\chi}^0_1 h_i} &= \Gamma^{(a)}_{\tilde{\chi}^0_1\tilde{\chi}^0_1 h_i} + \Gamma^{(b)}_{\tilde{\chi}^0_1\tilde{\chi}^0_1 h_i} + \Gamma^{(c)}_{\tilde{\chi}^0_1\tilde{\chi}^0_1 h_i} + \Gamma^{(d)}_{\tilde{\chi}^0_1\tilde{\chi}^0_1 h_i} \\
&\quad + \Gamma^{(e)}_{\tilde{\chi}^0_1\tilde{\chi}^0_1 h_i} + \Gamma^{(f)}_{\tilde{\chi}^0_1\tilde{\chi}^0_1 h_i} \\
&= C^{1L}_L \mathbf{P_L} + C^{1L}_R \mathbf{P_R}, \qquad (25)
\end{aligned}
$$

where $C^{1L}_{L,R}$ refers to total one-loop corrections to the coefficients of the left- and right-handed projection operators in the $\tilde{\chi}^0_1\tilde{\chi}^0_1 h_i$ vertex.

B. Renormalization of the chargino and neutralino sectors: A brief reprisal

In this part, we briefly discuss the various schemes used to renormalize the chargino and neutralino sectors of the MSSM. The details of the renormalization, which include counterterms and renormalization constants, can be found in Refs. [132–140]. The SUSY parameters that define charged and neutral fermions are the electroweak gaugino mass parameters M_1, M_2, and the supersymmetric Higgsino mass parameter μ. The mass matrices involve the masses of the electroweak gauge bosons with mixing angle θ_W and $\tan\beta$; all these parameters are renormalized independently from the chargino and neutralino sectors. The implementation parts have been discussed in Ref. [141], which also covers the Feynman rules of the counterterms for a general Complex MSSM. Although we consider *CP*-conserving MSSM, we keep our discussion general following Ref. [140]. We start with the Fourier-transformed MSSM Lagrangian, which is bilinear in the chargino and neutralino fields,

$$\begin{aligned}\mathcal{L}_{\tilde{\chi}^\pm\tilde{\chi}^0} = &\bar{\tilde{\chi}}_i^\pm \not{p}\mathbf{P_L}\tilde{\chi}_i^\pm + \bar{\tilde{\chi}}_i^\pm \not{p}\mathbf{P_R}\tilde{\chi}_i^\pm - \bar{\tilde{\chi}}_i^\pm [\mathbb{V}^*\bar{\mathbb{M}}^{\mathrm{T}}_{\tilde{\chi}^\pm}\mathbb{U}^\dagger]_{ij}\mathbf{P_L}\tilde{\chi}_j^\pm \\ &- \bar{\tilde{\chi}}_i^\pm [\mathbb{U}\bar{\mathbb{M}}^*_{\tilde{\chi}^\pm}\mathbb{V}^{\mathrm{T}}]_{ij}\mathbf{P_R}\tilde{\chi}_j^\pm \\ &+ \frac{1}{2}(\bar{\tilde{\chi}}_m^0 \not{p}\mathbf{P_L}\tilde{\chi}_m^0 + \bar{\tilde{\chi}}_m^0 \not{p}\mathbf{P_R}\tilde{\chi}_m^0 \\ &- \bar{\tilde{\chi}}_m^0 [\mathbb{N}^*\bar{\mathbb{M}}_{\tilde{\chi}^0}\mathbb{N}^\dagger]_{mn}\mathbf{P_L}\tilde{\chi}_n^0 \\ &- \bar{\tilde{\chi}}_m^0 [\mathbb{N}\bar{\mathbb{M}}^*_{\tilde{\chi}^0}\mathbb{N}^{\mathrm{T}}]_{mn}\mathbf{P_R}\tilde{\chi}_n^0), \end{aligned} \tag{26}$$

where $i, j = 1, 2, m, n = 1, \ldots, 4$. We recall that, $\mathbb{U}$, $\mathbb{V}$, and $\mathbb{N}$ diagonalize the chargino and neutralino mass matrices $\bar{\mathbb{M}}_{\tilde{\chi}^\pm}$ and $\bar{\mathbb{M}}_{\tilde{\chi}^0}$, respectively (see Sec. II).

We note the following replacements of the parameters and fields.

$$M_1 \to M_1 + \delta M_1, \tag{27}$$

$$M_2 \to M_2 + \delta M_2, \tag{28}$$

$$\mu \to \mu + \delta\mu, \tag{29}$$

$$\mathbf{P_L}\tilde{\chi}_i^\pm \to \left[\mathbb{1} + \frac{1}{2}\delta\mathbb{Z}^L_{\tilde{\chi}^\pm}\right]_{ij}\mathbf{P_L}\tilde{\chi}_j^\pm, \tag{30}$$

$$\mathbf{P_R}\tilde{\chi}_i^\pm \to \left[\mathbb{1} + \frac{1}{2}\delta\mathbb{Z}^R_{\tilde{\chi}^\pm}\right]_{ij}\mathbf{P_R}\tilde{\chi}_j^\pm, \tag{31}$$

$$\mathbf{P_L}\tilde{\chi}_m^0 \to \left[\mathbb{1} + \frac{1}{2}\delta\mathbb{Z}_{\tilde{\chi}^0}\right]_{mn}\mathbf{P_L}\tilde{\chi}_n^0, \tag{32}$$

$$\mathbf{P_R}\tilde{\chi}_m^0 \to \left[\mathbb{1} + \frac{1}{2}\delta\mathbb{Z}^*_{\tilde{\chi}^0}\right]_{mn}\mathbf{P_R}\tilde{\chi}_n^0, \tag{33}$$

where $\delta\mathbb{Z}_{\tilde{\chi}^\pm\tilde{\chi}^0}$ refer to field renormalization constants for the physical states, general 2×2 or 4×4 matrices respectively. The parameter counterterms are generally complex; we need two renormalization conditions to fix those counterterms (one for the real part and another for the complex part). The transformation matrices are not renormalized; therefore, one can write the matrix in terms of the renormalized one and a counterterm matrix in the following way:

$$\bar{\mathbb{M}}_{\tilde{\chi}^\pm} \to \bar{\mathbb{M}}_{\tilde{\chi}^\pm} + \delta\bar{\mathbb{M}}_{\tilde{\chi}^\pm}, \tag{34}$$

$$\bar{\mathbb{M}}_{\tilde{\chi}^0} \to \bar{\mathbb{M}}_{\tilde{\chi}^0} + \delta\bar{\mathbb{M}}_{\tilde{\chi}^0}, \tag{35}$$

with

$$\delta\bar{\mathbb{M}}_{\tilde{\chi}^\pm} = \begin{pmatrix} \delta M_2 & \sqrt{2}\delta(M_W s_\beta) \\ \sqrt{2}\delta(M_W c_\beta) & \delta\mu \end{pmatrix}, \tag{36}$$

and

$$\delta\bar{\mathbb{M}}_{\tilde{\chi}^0} = \begin{pmatrix} \delta M_1 & 0 & -\delta(M_Z s_W c_\beta) & \delta(M_Z s_W s_\beta) \\ 0 & \delta M_2 & \delta(M_Z c_W c_\beta) & -\delta(M_Z c_W s_\beta) \\ -\delta(M_Z s_W c_\beta) & \delta(M_Z c_W c_\beta) & 0 & -\delta\mu \\ \delta(M_Z s_W s_\beta) & -\delta(M_Z c_W s_\beta) & -\delta\mu & 0 \end{pmatrix}. \tag{37}$$

Also the replacements of the diagonalized matrices $\mathbb{M}_{\tilde{\chi}^\pm}$ and $\mathbb{M}_{\tilde{\chi}^0}$ can be written as

$$\mathbb{M}_{\tilde{\chi}^\pm} \to \mathbb{M}_{\tilde{\chi}^\pm} + \delta\mathbb{M}_{\tilde{\chi}^\pm} = \mathbb{M}_{\tilde{\chi}^\pm} + \mathbb{V}^*\delta\bar{\mathbb{M}}^{\mathrm{T}}_{\tilde{\chi}^\pm}\mathbb{U}^\dagger, \tag{38}$$

$$\mathbb{M}_{\tilde{\chi}^0} \to \mathbb{M}_{\tilde{\chi}^0} + \delta\mathbb{M}_{\tilde{\chi}^0} = \mathbb{M}_{\tilde{\chi}^0} + \mathbb{N}^*\delta\bar{\mathbb{M}}^{\mathrm{T}}_{\tilde{\chi}^0}\mathbb{N}^\dagger. \tag{39}$$

We can decompose the self energies into left- and right-handed vector and scalar coefficients in the following way:

$$\begin{aligned}[\Sigma_{\tilde{\chi}}(p^2)]_{\ell m} = &\not{p}\mathbf{P_L}[\Sigma^L_{\tilde{\chi}}(p^2)]_{\ell m} + \not{p}\mathbf{P_R}[\Sigma^R_{\tilde{\chi}}(p^2)]_{\ell m} \\ &+ \mathbf{P_L}[\Sigma^{SL}_{\tilde{\chi}}(p^2)]_{\ell m} + \mathbf{P_R}[\Sigma^{SR}_{\tilde{\chi}}(p^2)]_{\ell m}. \end{aligned} \tag{40}$$

The coefficients of the renormalized self-energies can be written as

$$[\hat{\Sigma}^L_{\tilde{\chi}^\pm}(p^2)]_{ij} = [\Sigma^L_{\tilde{\chi}^\pm}(p^2)]_{ij} + \frac{1}{2}[\delta\mathbb{Z}^L_{\tilde{\chi}^\pm} + \delta\mathbb{Z}^{L\dagger}_{\tilde{\chi}^\pm}]_{ij}, \tag{41}$$

$$[\hat{\Sigma}^R_{\tilde{\chi}^\pm}(p^2)]_{ij} = [\Sigma^R_{\tilde{\chi}^\pm}(p^2)]_{ij} + \frac{1}{2}[\delta\mathbb{Z}^R_{\tilde{\chi}^\pm} + \delta\mathbb{Z}^{R\dagger}_{\tilde{\chi}^\pm}]_{ij}, \tag{42}$$

$$\begin{aligned}[\hat{\Sigma}^{SL}_{\tilde{\chi}^\pm}(p^2)]_{ij} = &[\Sigma^{SL}_{\tilde{\chi}^\pm}(p^2)]_{ij} \\ &- \left[\frac{1}{2}\delta\mathbb{Z}^{R\dagger}_{\tilde{\chi}^\pm}\mathbb{M}_{\tilde{\chi}^\pm} + \frac{1}{2}\mathbb{M}_{\tilde{\chi}^\pm}\delta\mathbb{Z}^L_{\tilde{\chi}^\pm} + \delta\mathbb{M}_{\tilde{\chi}^\pm}\right]_{ij}, \end{aligned} \tag{43}$$

$$\begin{aligned}[\hat{\Sigma}^{SR}_{\tilde{\chi}^\pm}(p^2)]_{ij} = &[\Sigma^{SR}_{\tilde{\chi}^\pm}(p^2)]_{ij} \\ &- \left[\frac{1}{2}\delta\mathbb{Z}^{L\dagger}_{\tilde{\chi}^\pm}\mathbb{M}^\dagger_{\tilde{\chi}^\pm} + \frac{1}{2}\mathbb{M}^\dagger_{\tilde{\chi}^\pm}\delta\mathbb{Z}^R_{\tilde{\chi}^\pm} + \delta\mathbb{M}^\dagger_{\tilde{\chi}^\pm}\right]_{ij}, \end{aligned} \tag{44}$$

$$[\hat{\Sigma}^L_{\tilde{\chi}^0}(p^2)]_{n\ell} = [\Sigma^L_{\tilde{\chi}^0}(p^2)]_{n\ell} + \frac{1}{2}[\delta\mathbb{Z}_{\tilde{\chi}^0} + \delta\mathbb{Z}^\dagger_{\tilde{\chi}^0}]_{n\ell}, \tag{45}$$

$$[\hat{\Sigma}^R_{\tilde{\chi}^0}(p^2)]_{n\ell} = [\Sigma^R_{\tilde{\chi}^0}(p^2)]_{n\ell} + \frac{1}{2}[\delta\mathbb{Z}^*_{\tilde{\chi}^0} + \delta\mathbb{Z}^{\mathrm{T}}_{\tilde{\chi}^0}]_{n\ell}, \tag{46}$$

$$[\hat{\Sigma}^{SL}_{\tilde{\chi}^0}(p^2)]_{n\ell} = [\Sigma^{SL}_{\tilde{\chi}^0}(p^2)]_{n\ell} - \left[\frac{1}{2}\delta\mathbb{Z}^{\mathrm{T}}_{\tilde{\chi}^0}\mathbb{M}_{\tilde{\chi}^0} + \frac{1}{2}\mathbb{M}_{\tilde{\chi}^0}\delta\mathbb{Z}_{\tilde{\chi}^0} + \delta\mathbb{M}_{\tilde{\chi}^0}\right]_{n\ell}, \quad (47)$$

$$[\hat{\Sigma}^{SR}_{\tilde{\chi}^0}(p^2)]_{n\ell} = [\Sigma^{SR}_{\tilde{\chi}^0}(p^2)]_{n\ell} - \left[\frac{1}{2}\delta\mathbb{Z}^{\dagger}_{\tilde{\chi}^0}\mathbb{M}^{\dagger}_{\tilde{\chi}^0} + \frac{1}{2}\mathbb{M}^{\dagger}_{\tilde{\chi}^0}\delta\mathbb{Z}^{*}_{\tilde{\chi}^0} + \delta\mathbb{M}^{\dagger}_{\tilde{\chi}^0}\right]_{n\ell}. \quad (48)$$

With the above machinery, in the on-shell renormalization scheme for the charginos and neutralinos, we may evaluate the counterterms δM_1, $\delta\mu$, and δM_2 by requiring that the masses of $\tilde{\chi}^{\pm}_{1,2}$ and one of the neutralino $\tilde{\chi}^0_n$ ($n \in \{1,\ldots,4\}$) are defined as the poles of the corresponding tree-level propagators. This scheme is called CCN[n] where "C" stands for chargino, "N" for neutralino, and "n" in the square bracket indicates that $\tilde{\chi}^0_n$ is taken as on shell. One of the choices can be CCN[1] scheme where the mass of the dominantly binolike lightest neutralino should be chosen on shell to ensure numerical stability [142] while a large unphysical contribution may be observed for non-binolike lightest neutralino [143] if taken as on shell. The scheme fits well even for bino-dominated mixed LSP scenarios, such as bino-Higgsino or even for a bino-wino-Higgsino neutralino. For other hierarchical mass patterns, e.g., $|M_2| < |M_1|, |\mu|$, or $|\mu| < |M_1|, |M_2|$, CCN[1] scheme may fail to yield numerically stable results; thus, different renormalization schemes like CCN[2] or CCN[4] may need to be adopted [140,144]. Wino in the first case and Higgsino for the latter are chosen to be on shell. On the other hand, in the "CNN" scheme, one of the two charginos and two neutralinos $\tilde{\chi}^0_\ell$ and $\tilde{\chi}^0_m$ are taken to be on shell [136,142,144]. Since we are interested in the bino-dominated LSP scenarios, we stick to imposing on shell conditions for the two charginos and one bino-like neutralino.

The above field renormalization constants can be used in evaluating the vertex counterterms. Finally, we can write the expression for the vertex counterterm as follows [see Fig. 2(a) and Fig. 2(b)]:

$$\delta\Gamma_{\tilde{\chi}^0_1\tilde{\chi}^0_1 h_i} = \mathbf{P_L}\delta C^L_{\tilde{\chi}^0_1\tilde{\chi}^0_1 h_i} + \mathbf{P_R}\delta C^R_{\tilde{\chi}^0_1\tilde{\chi}^0_1 h_i}, \quad (49)$$

where, for the lightest CP-even scalar,

$$\begin{aligned}\delta C^L_{\tilde{\chi}^0_1\tilde{\chi}^0_1 h} = -\frac{e}{4c_W s^2_W}\Bigg[&\frac{4}{c^2_W}\{(c^2_W\delta Z_e + s_W\delta s_W)s^2_W\mathcal{N}^*_{11} + c_W c^2_W(\delta s_W - s_W\delta Z_e)\mathcal{N}^*_{12}\}(s_\alpha\mathcal{N}^*_{13} + c_\alpha\mathcal{N}^*_{14})\\ &+ s_W\{2(s_W\mathcal{N}^*_{11} - c_W\mathcal{N}^*_{12})\{(2[\delta\mathbf{Z}^L_{\tilde{\chi}^0}]_{11} + \delta Z_{hh})(s_\alpha\mathcal{N}^*_{13} + c_\alpha\mathcal{N}^*_{14}) - \delta Z_{hH}(c_\alpha\mathcal{N}^*_{13} - s_\alpha\mathcal{N}^*_{14})\}\\ &+ ([\delta\mathbf{Z}^L_{\tilde{\chi}^0}]_{12} + [\delta\mathbf{Z}^L_{\tilde{\chi}^0}]_{21})\{(s_\alpha\mathcal{N}^*_{13} + c_\alpha\mathcal{N}^*_{14})(s_W\mathcal{N}^*_{21} - c_W\mathcal{N}^*_{22}) + (s_W\mathcal{N}^*_{11} - c_W\mathcal{N}^*_{12})(s_\alpha\mathcal{N}^*_{23}\\ &+ c_\alpha\mathcal{N}^*_{24})\} + ([\delta\mathbf{Z}^L_{\tilde{\chi}^0}]_{13} + [\delta\mathbf{Z}^L_{\tilde{\chi}^0}]_{31})\{(s_\alpha\mathcal{N}^*_{13} + c_\alpha\mathcal{N}^*_{14})(s_W\mathcal{N}^*_{31} - c_W\mathcal{N}^*_{32}) + (s_W\mathcal{N}^*_{11} - c_W\mathcal{N}^*_{12})\\ &\times(s_\alpha\mathcal{N}^*_{33} + c_\alpha\mathcal{N}^*_{34})\} + ([\delta\mathbf{Z}^L_{\tilde{\chi}^0}]_{14} + [\delta\mathbf{Z}^L_{\tilde{\chi}^0}]_{41})\{(s_\alpha\mathcal{N}^*_{13} + c_\alpha\mathcal{N}^*_{14})(s_W\mathcal{N}^*_{41} - c_W\mathcal{N}^*_{42}) + (s_W\mathcal{N}^*_{11}\\ &- c_W\mathcal{N}^*_{12})(s_\alpha\mathcal{N}^*_{43} + c_\alpha\mathcal{N}^*_{44})\}\}\Bigg]\end{aligned} \quad (50)$$

and

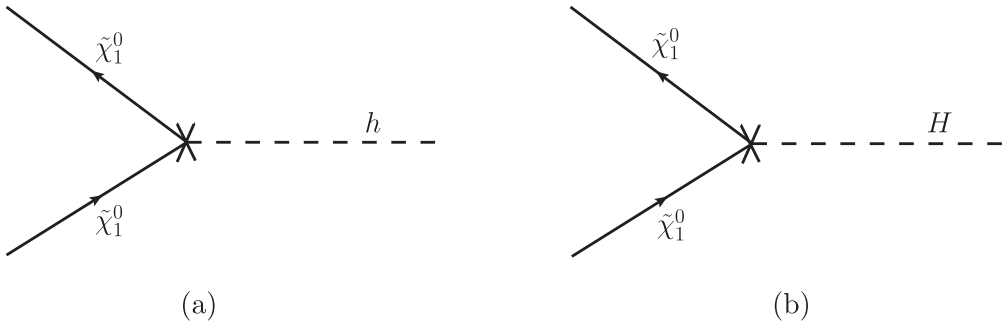

FIG. 2. Counterterm diagrams for the $\tilde{\chi}^0_1\tilde{\chi}^0_1 h$ and $\tilde{\chi}^0_1\tilde{\chi}^0_1 H$ vertices which should be added to the one-loop corrected $\tilde{\chi}^0_1\tilde{\chi}^0_1 h$ and $\tilde{\chi}^0_1\tilde{\chi}^0_1 H$ vertices, respectively to get the UV-finite results.

$$\delta C^{R}_{\tilde{\chi}^0_1\tilde{\chi}^0_1 h} = -\frac{e}{4c_W s_W^2}\Bigg[\frac{4}{c_W^2}\{(c_W^2\delta Z_e + s_W\delta s_W)s_W^2\mathcal{N}_{11} + c_W c_W^2(\delta s_W - s_W\delta Z_e)\mathcal{N}_{12}\}(s_\alpha\mathcal{N}_{13} + c_\alpha\mathcal{N}_{14}) + s_W\{2(s_W\mathcal{N}_{11} - c_W\mathcal{N}_{12})\{(s_\alpha\delta Z_{hh} - c_\alpha\delta Z_{hH})\mathcal{N}_{13} + (c_\alpha\delta Z_{hh} + s_\alpha\delta Z_{hH})\mathcal{N}_{14} + (2[\delta\mathbf{Z}^R_{\tilde{\chi}^0}]_{11}) \times (s_\alpha\mathcal{N}_{13} + c_\alpha\mathcal{N}_{14})\} + ([\delta\mathbf{Z}^R_{\tilde{\chi}^0}]_{12} + [\delta\mathbf{Z}^R_{\tilde{\chi}^0}]_{21})\{(s_\alpha\mathcal{N}_{13} + c_\alpha\mathcal{N}_{14})(s_W\mathcal{N}_{21} - c_W\mathcal{N}_{22}) + (s_W\mathcal{N}_{11} - c_W\mathcal{N}_{12})(s_\alpha\mathcal{N}_{23} + c_\alpha\mathcal{N}_{24})\} + ([\delta\mathbf{Z}^R_{\tilde{\chi}^0}]_{13} + [\delta\mathbf{Z}^R_{\tilde{\chi}^0}]_{31})\{(s_\alpha\mathcal{N}_{13} + c_\alpha\mathcal{N}_{14})(s_W\mathcal{N}_{31} - c_W\mathcal{N}_{32}) + (s_W\mathcal{N}_{11} - c_W\mathcal{N}_{12})(s_\alpha\mathcal{N}_{33} + c_\alpha\mathcal{N}_{34})\} + ([\delta\mathbf{Z}^R_{\tilde{\chi}^0}]_{14} + [\delta\mathbf{Z}^R_{\tilde{\chi}^0}]_{41})\{(s_\alpha\mathcal{N}_{13} + c_\alpha\mathcal{N}_{14})(s_W\mathcal{N}_{41} - c_W\mathcal{N}_{42}) + (s_W\mathcal{N}_{11} - c_W\mathcal{N}_{12})(s_\alpha\mathcal{N}_{43} + c_\alpha\mathcal{N}_{44})\}\}\Bigg]. \tag{51}$$

Similarly, the counterterm for the heavy Higgs can be obtained by the replacements $s_\alpha \to c_\alpha$, $c_\alpha \to -s_\alpha$, $\delta Z_{hh} \to \delta Z_{HH}$, and $\delta Z_{hH} \to -\delta Z_{hH}$.

In the above, $\delta\mathbf{Z}^{L,R}_{\tilde{\chi}^0}$ involves renormalized self-energies and counterterms of the mass matrices of the physical states [138,140]. Similarly, δZ_{hH}, δZ_{hh}, and δZ_{HH} come from the renormalization of the neutral Higgs sector,

$$M_{h_i} \to M_{h_i} + \delta M_{h_i}, \tag{52}$$

$$\begin{pmatrix} h \\ H \end{pmatrix} \to \begin{pmatrix} 1 + \frac{1}{2}\delta Z_{hh} & \frac{1}{2}\delta Z_{hH} \\ \frac{1}{2}\delta Z_{Hh} & 1 + \frac{1}{2}\delta Z_{HH} \end{pmatrix}\begin{pmatrix} h \\ H \end{pmatrix}. \tag{53}$$

The other terms in the counterterm vertices are already present in the renormalization of the SM. Here, we refer to [133,145] for the relevant expressions. For instance, the renormalization constants, e.g., $\delta Z_e, \delta s_W$, are fixed by the on-shell conditions. Thus, as a default option in FORMCALC, we use the fine-structure constant $\alpha = \alpha(0) = 1/137.0359996$ defined at the Thomson limit.[5] Similarly, the on shell definition of s_W has been fixed as, $s_W^2 = 1 - \frac{M_W^2}{M_Z^2}$. Though M_W is normally computed using the fine-structure constant in the Thomson limit $\alpha(0)$, the Fermi constant G_μ, and mass of the Z boson, here we stick to $M_W = 80.3484$ in the analysis. This is within the $\sim 1\sigma$ variation if W boson mass measurements are performed by the ATLAS, LHCb, and D0 experiments, excluding the recent CDF results; $M_W = 80.3692 \pm 0.0133$ GeV [149]. The relatively large theoretical uncertainty arises due to parton distribution functions.[6]

Finally, we club the vertex corrections and counterterms as $\Gamma_{\tilde{\chi}^0_1\tilde{\chi}^0_1 h_i} + \delta\Gamma_{\tilde{\chi}^0_1\tilde{\chi}^0_1 h_i}$ to obtain the UV-finite amplitude where $\Gamma_{\tilde{\chi}^0_1\tilde{\chi}^0_1 h_i}$ and $\delta\Gamma_{\tilde{\chi}^0_1\tilde{\chi}^0_1 h_i}$ are defined in Eq. (25) and Eq. (49), respectively. As we will see, to get the UV-finite result, we have to use tree-level masses for the physical states inside the loop.

V. PRECISION MEASUREMENTS AND CONSTRAINTS FROM DIRECT SEARCHES

Here, we summarize different avenues of precision and collider phenomenology, which can be marked along with the SI-DD of the neutralino DM in different parts of the MSSM parameter space. We consider 3 GeV theoretical uncertainty in calculating SUSY Higgs mass leads to the following range [150] for the SM-like Higgs mass in the MSSM:

$$122\,\text{GeV} < m_h < 128\ \text{GeV} \tag{54}$$

Otherwise, we respect the constraints originating from the B-physics measurements[7] at 2σ variations, e.g., $3.02 \times 10^{-4} < \text{BR}(b \to s\gamma) < 3.62 \times 10^{-4}$ [151], $2.23 \times 10^{-9} < \text{BR}(B_s \to \mu^+\mu^-) < 3.63 \times 10^{-9}$ [152]. We recall that our primary interest is to observe the role of the renormalized $\tilde{\chi}^0_1\tilde{\chi}^0_1 h_i$ vertex in the SI-DD where δa_μ can be satisfied using SUSY contributions. Assuming the $\tilde{\chi}^0_1$ to be the only source for DM, we note the acceptable value of the relic abundance data [25,26],

[5]We may recall that the renormalization of electric charge can be written as $e^{\text{bare}} \to e(0)(1 + \delta Z_e^{(0)}) = e(M_Z^2)(1 + \delta Z_e^{e(M_Z^2)}) +$ higher orders, with $e(M_Z^2) = e(0)/(1 - \frac{1}{2}\Delta\alpha)$ and $\delta Z_e^{e(M_Z^2)} = \delta Z_e^{(0)} - \frac{1}{2}\Delta\alpha$ where $\Delta\alpha$ is a finite quantity involving the contributions from the e, μ, τ leptons and the light quarks (i.e., all except t) [139,146–148]. On the contrary, if one uses the "running on shell" value of α, i.e., $\alpha(M_Z^2) = 1/128.93$ or the running $\overline{\text{MS}}$ value $\hat{\alpha}(M_Z) = 1/127.932$ (which usually spectrum-generator like SPHENO considers), then the definition of $\delta Z_e^{e(M_Z^2)}$ has to be adopted. To this end, FORMCALC calculates the charge renormalization constant at the Thomson limit, i.e., $\delta Z_e^{(0)}$ [141], so we always use $\alpha(0)$ or $e(0)$.

[6]In the former calculation, higher-order corrections involving the standard model and the MSSM are needed. Thus, if we compute the M_W instead, the resultant change in the SI-DD cross section is $\lesssim 1\%$.

[7]B-physics constraints are satisfied using SPHENO-4.0.4 that uses the model file for the MSSM from SARAH where the input mass parameters for the SUSY models are defined in $\overline{\text{DR}}$-scheme.

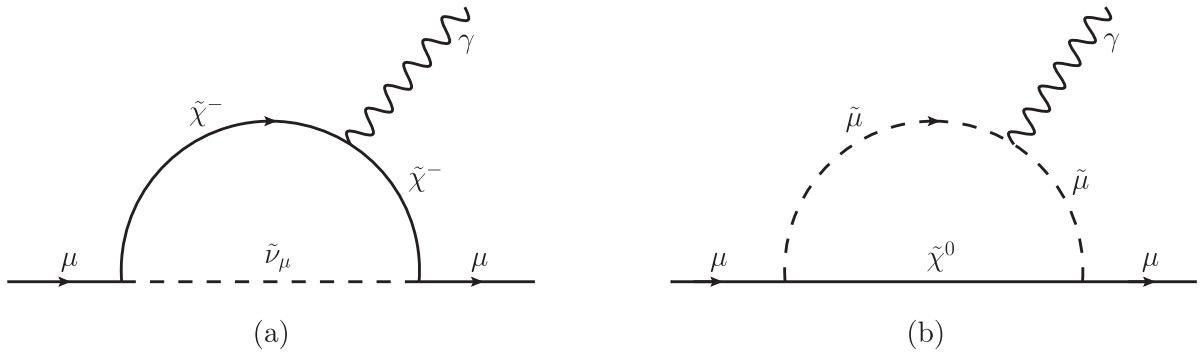

FIG. 3. One-loop contributions to a_μ in MSSM.

$$\Omega_{\rm DM}h^2 = 0.1198 \pm 0.0012. \tag{55}$$

However, as noted in Sec. I, the constraint Eq. (55) is not always endorsed as a necessary condition, especially for understanding the parametric dependence to highlight the region of higher NLO corrections. It is well known that lighter EW spectra with masses not far away from a few hundred GeV are preferred for compliance with δa_μ. The direct search constraints from LHC or LEP can be potentially important for consideration. As mentioned, we set squarks and gluino masses at ≥ 4 TeV to cope with the LHC constraints [49,50]. Thus, it is instructive to lay down a brief discussion of the recent results on the anomalous magnetic moment of the muon and the status of the LHC searches on the MSSM parameter space. It may be added here that the LHC constraints on SUSY searches are finally verified using SMODELS-2.3.0 [153–156].

A. Anomalus magnetic moment of muon (δa_μ) in the MSSM

The recent a_μ measurement by FNAL [54,157] has confirmed the earlier result by the E821 experiment at Brookhaven, yielding the experimental average $a_\mu^{\rm EXP} = 116592061(41) \times 10^{-11}$ which leads to a 4.2σ discrepancy [54] compared to the SM value $a_\mu^{\rm SM} = (116591810 \pm 43) \times 10^{-11}$ [55], which is mainly based on the Refs. [56–75],

$$\delta a_\mu = a_\mu^{\rm EXP} - a_\mu^{\rm SM} = 251 \pm 59 \times 10^{-11}. \tag{56}$$

The E989 experiment at Fermilab recently released an update regarding the measurement of a_μ from Run-2 and Run-3. The new combined value yields a deviation of[8]

$$\delta a_\mu^{\rm New} = (249 \pm 48) \times 10^{-11}, \tag{57}$$

which leads to a 5.1σ discrepancy. However, $\delta a_\mu^{\rm New}$ quoted in Eq. (57) is subject to SM theory prediction, mainly the leading-order hadronic vacuum polarization (HVP) contributions. Here, we stick to [55] where dispersive techniques are used to extract the leading-order HVP contribution from the $e^+e^- \to$ hadrons data. Instead, if the lattice-QCD result for HVP by BMW Collaboration is used, $\delta a_\mu^{\rm New}$ reduces to 1.6σ, leading to 2.1σ tension with the e^+e^- determination of the HVP contribution. In this regard, Ref. [158] discusses how windows in Euclidean time can help to reduce the potential conflicts between evaluations of the HVP contribution to the $(g-2)_\mu$ in lattice-QCD[9] and from $e^+e^- \to$ hadrons cross section data. Along the same line, Ref. [162] also manifested the tension between the lattice QCD approach and the traditional data-driven approach, while for the latter, the recent CMD-3 result was not used. Recently, Ref. [163] calculated the $(g-2)_\mu$ using the data-driven approach. They measured the cross section of the dominant channel $e^+e^- \to \pi^+\pi^-$ using the CMD-3 detector at a center-of-mass energy below 1 GeV, though the result seems to be incompatible with previous determinations [164–168].

In the MSSM, the one-loop contributions to the anomalous magnetic moment of muon or a_μ, as shown in Fig. 3, are mainly mediated by $\tilde{\chi}^- - \tilde{\nu}_\mu$ and $\tilde{\mu} - \tilde{\chi}^0$ [52,169–186].

The $(g-2)_\mu$ prior to the Fermilab Run-1 result are studied in the Refs. [187–189]. In the aftermath of Fermilab Run-1, the $(g-2)_\mu$ was studied in the Refs. [190–195].

The contributions can be written as [173,175]

$$\delta a_\mu^{\tilde{\chi}^0} = \frac{m_\mu}{16\pi^2} \sum_{\ell=1}^{4} \sum_{m=1}^{2} \left[-\frac{m_\mu}{12 m_{\tilde{\mu}_m}^2} (|n_{\ell m}^L|^2 + |n_{\ell m}^R|^2) \mathcal{F}_1^{\mathcal{N}}(x_{\ell m}) + \frac{m_{\tilde{\chi}_\ell^0}}{3 m_{\tilde{\mu}_m}^2} {\rm Re}[n_{\ell m}^L n_{\ell m}^R] \mathcal{F}_2^{\mathcal{N}}(x_{\ell m}) \right], \tag{58}$$

[8]The value of $(g-2)_\mu$ from Run-2 and Run-3 is $a_\mu^{\rm Run-2,3} = (116592055 \pm 24) \times 10^{-11}$. Therefore, the new experimental average becomes $a_\mu^{\rm Exp(New)} = (116592059 \pm 22) \times 10^{-11}$ [76].

[9]References [159–161] also studied recently the window observable for the HVP contribution to $(g-2)_\mu$ from lattice QCD calculations.

$$\delta a_\mu^{\tilde{\chi}^\pm} = \frac{m_\mu}{16\pi^2}\sum_{k=1}^{2}\left[\frac{m_\mu}{12m^2_{\tilde{\nu}_\mu}}(|c_k^L|^2+|c_k^R|^2)\mathcal{F}_1^C(x_k) + \frac{2m_{\tilde{\chi}_k^\pm}}{3m^2_{\tilde{\nu}_\mu}}\mathrm{Re}[c_k^L c_k^R]\mathcal{F}_2^C(x_k)\right], \quad (59)$$

where the summations label the neutralino, smuon, and chargino mass eigenstates, respectively, and

$$n^L_{\ell m} = \frac{1}{\sqrt{2}}(g_1\mathcal{N}_{\ell 1}+g_2\mathcal{N}_{\ell 2})X^*_{m1} - y_\mu \mathcal{N}_{\ell 3}X^*_{m2}, \quad (60)$$

$$n^R_{\ell m} = \sqrt{2}g_1\mathcal{N}_{\ell 1}X_{m2} + y_\mu \mathcal{N}_{\ell 3}X_{m1}, \quad (61)$$

$$c_k^L = -g_2\mathcal{V}_{k1}, \quad (62)$$

$$c_k^R = y_\mu \mathcal{U}_{k2}, \quad (63)$$

with y_μ is the muon Yukawa coupling. The loop functions are given by

$$\mathcal{F}_1^{\mathcal{N}}(x) = \frac{2}{(1-x)^4}[1-6x+3x^2+2x^3-6x^2\ln(x)], \quad (64)$$

$$\mathcal{F}_2^{\mathcal{N}}(x) = \frac{3}{(1-x)^3}[1-x^2+2x\ln(x)], \quad (65)$$

$$\mathcal{F}_1^{C}(x) = \frac{2}{(1-x)^4}[2+3x-6x^2+x^3+6x\ln(x)], \quad (66)$$

$$\mathcal{F}_1^{C}(x) = -\frac{3}{2(1-x)^3}[3-4x+x^2+2\ln(x)], \quad (67)$$

where the definition of the variables $x_{\ell m} = m^2_{\tilde{\chi}^0_\ell}/m^2_{\tilde{\mu}_m}$ and $x_k = m^2_{\tilde{\chi}^\pm_k}/m^2_{\tilde{\nu}_\mu}$ have been used. Since $\delta a_\mu^{\mathrm{SUSY}} > 0$ for $\mu > 0$ and $\delta a_\mu^{\mathrm{SUSY}} < 0$ for $\mu < 0$ [196,197], here, we restrict ourselves to the case where μ is real and positive, i.e., $\mu > 0$ in order to have the positive SUSY contributions to $(g-2)_\mu$. For a light binolike neutralino, i.e., for the scenario $M_1 \ll M_2, \mu$, the loops contain only a light bino and the smuons. In that case, one can write [173],

$$\delta a_\mu^{\mathrm{Bino-like}} = \frac{g_1^2}{48\pi^2}\frac{m_\mu^2 M_1 \mathrm{Re}[\mu\tan\beta - A_\mu^*]}{m^2_{\tilde{\mu}_2}-m^2_{\tilde{\mu}_1}} \times\left[\frac{\mathcal{F}_2^{\mathcal{N}}(x_{11})}{m^2_{\tilde{\mu}_1}} - \frac{\mathcal{F}_2^{\mathcal{N}}(x_{12})}{m^2_{\tilde{\mu}_2}}\right], \quad (68)$$

where $x_{1m} = M_1^2/m^2_{\tilde{\mu}_m}$. For numerical evaluations for flavor constraints including $(g-2)_\mu$, we use SPHENO-4.0.4 [198,199] that uses SARAH-4.14.5 [200,201] for generating the MSSM model files.

It is instructive to note that SPHENO calculates all the one-loop SUSY contributions to $(g-2)_\mu$. But $(g-2)_\mu$ also may receive contributions from the two-loop (mainly Barr-Zee type) diagrams involving fermion/sfermion in the loop [202,203] which in the present case may not offer any significant changes.[10]

B. LHC and LEP bounds on electroweakinos and sleptons

For the searches of charginos/neutralinos and sleptons at $\sqrt{s} = 13$ TeV by ATLAS and CMS we refer the reader [209–216] and [217–221]. Also, the direct production of charginos, neutralinos, and sleptons in the final states with two leptons have been searched by ATLAS at $\sqrt{s} = 8$ TeV [222]. Following the ATLAS searches [213,223], Higgsino-like neutralinos or charginos above the LEP limit can be constrained for a mass difference $\Delta m(\tilde{\chi}^0_2/\tilde{\chi}^\pm_1, \tilde{\chi}^0_1) \geq 2.4$ GeV. Similarly, a lower limit $m_{\tilde{\chi}^\pm_1} \simeq m_{\tilde{\chi}^0_2} \geq 193$ GeV can be set for a mass splitting of 9.3 GeV. Using CMS results $m_{\tilde{\chi}^\pm_1} \simeq 150$ GeV for a mass difference $\sim$3 GeV [221] can be placed. For a recent review of searches for electroweakinos at the LHC, see [224].

Usually, in the Higgsino-like LSP models, a few combinations of electroweak states may be important: $\tilde{\chi}^0_1\tilde{\chi}^0_2, \tilde{\chi}^0_1\tilde{\chi}^\pm_1, \tilde{\chi}^0_2\tilde{\chi}^\pm_1, \tilde{\chi}^+_1\tilde{\chi}^-_1$. The possibility of having a lighter electroweakino in the MSSM without confronting the LHC searches requires a compressed mass spectra; thus it relies on the soft leptons or jets arising in the decays of charginos and neutralinos via off shell EW gauge bosons $\tilde{\chi}^\pm_1 \to W^{(*)} + \tilde{\chi}^0_1$ and $\tilde{\chi}^0_i \to Z^{(*)}/h_{\mathrm{SM}} + \tilde{\chi}^0_1$ (h_{SM} refers to an SM-like Higgs scalar in any BSM model). In the present context, $\tilde{\chi}^0_1$ can be $\tilde{B}$ dominated, whereas relatively heavier neutralinos $\tilde{\chi}^0_2, \tilde{\chi}^0_3$ and $\tilde{\chi}^\pm_1$ may become Higgsino-like. Even a better-compressed scenario can be conceived when a winolike $\tilde{\chi}^0_2$ is lighter than Higgsino-like $\tilde{\chi}^0_3, \tilde{\chi}^0_4$. However, Higgsino-like states cannot be too light since moderate/large gaugino-Higgsino mixings have been excluded via the SI-DD results. For instance, the direct detection of binolike $\tilde{\chi}^0_1$-nucleon cross section set a limit of $\mu \geq 600$ GeV for an LSP mass of 100 GeV (see, e.g., Fig. 10). With this in mind, the presence of lighter sleptons and sneutrinos becomes necessary to satisfy δa_μ. Then Higgsino-like heavier charginos/neutralinos may decay through $\widetilde{\ell}(\ell)\nu(\tilde{\nu})$ or $\widetilde{\ell}\ell, \tilde{\nu}\nu$ or even via winolike neutralino states.

[10]For the two-loop contributions for $(g-2)_\mu$ we refer to `GM2Calc` [203–208]. `GM2Calc` uses the on shell masses for the following parameters:

$$M_1, \quad M_2, \quad \mu, \quad m_{\tilde{\mu}_L}, \quad m_{\tilde{\mu}_R}, \quad (69)$$

where $m_{\tilde{\mu}_L}$ and $m_{\tilde{\mu}_R}$ are the smuon mass parameters. On the other hand, SPHENO, which uses the model file for the MSSM from SARAH, defines the input mass parameters in $\overline{\mathrm{DR}}$-scheme. One may find that `GM2Calc` [203–208] is a more reliable tool for the scenarios where two-loop results can be important.

We summarise here the potentially important final states comprised of l^+l^- ($l \in e,\ \mu,\ \tau$) pair, jets, and missing transverse momentum through pair production of charginos, neutralinos, and sleptons, searched at the ATLAS and CMS Collaborations:

(i) $PP \to \tilde{\chi}_1^\pm \tilde{\chi}_2^0 \to Z\chi_1^0 W^\pm \chi_1^0$ (W and Z bosons can be off shell) are considered in Ref. [211,215,216,218,225]. For on shell vector bosons, Z and W decay to leptonic and leptonic (hadronic) final states, respectively. An ISR jet may lead the required handle to detect the soft leptons above the SM background [211,213]. The lower limits for equal mass $\tilde{\chi}_1^\pm \tilde{\chi}_2^0$ are ∼800 GeV for a massless $\tilde{\chi}_1^0$ [225,226], for decaying with 100% BR in the gauge boson final states. The second lightest neutralino may decay through $h_{\rm SM}$, $\tilde{\chi}_2^0 \to h_{\rm SM} + \tilde{\chi}_1^0$ with 100% BR, is considered in Ref. [214,216,218]. For the $Wh_{\rm SM}$ mediated signals, and, $\Delta m(\tilde{\chi}_2^0, \tilde{\chi}_1^0) \geq m_{h_{\rm SM}}$ minimum $\tilde{\chi}_1^\pm \tilde{\chi}_2^0$ mass set at 190 GeV [216]. Additionally, pair production of charginos followed by its decay to $\widetilde{\ell}(\ell)\nu(\tilde{\nu})$ was considered in Ref. [212].

(ii) In the parameter space of our concern, all the electroweakinos may be below the TeV scale. Thus, pair production of heavier electroweakinos may be important, especially if each of them decays into a lighter electroweakino and an on shell W, Z, and SM-like Higgs boson [227].

(iii) $PP \to \widetilde{\ell}\widetilde{\ell} \to \ell\tilde{\chi}_1^0 \ell\tilde{\chi}_1^0$: Direct pair production of sleptons with $\tilde{l}$ refers mainly $\tilde{e}, \tilde{\mu}$ with each decaying into a charged lepton and $\tilde{\chi}_1^0$, have been searched at [209,212,213,219,228]. Usually, for a lighter $\tilde{e}$ and $\tilde{\mu}$ with masses ≤ 150 GeV, the mass splitting $\Delta m(\widetilde{\ell}, \tilde{\chi}_1^0) \leq 50$ GeV is desired to have an acceptable parameter space point. We always keep track of $\Delta m(\widetilde{\ell}, m_{\tilde{\chi}_1^0})$ and consider $m_{\widetilde{\ell}} \geq 100$ GeV. For relatively heavier sleptons, $m_{\widetilde{\ell}}$-$m_{\tilde{\chi}_1^0}$ plane is depicted in Refs. [219,228].

(iv) Charginos/neutralinos can potentially decay into sleptons, which then decay into leptons, see, e.g., [209]. The mass limits for $\tilde{\chi}_2^0, \tilde{\chi}_1^\pm$ can be excluded up to 1.1 TeV for neutralino masses less than 550 GeV. These channels are important if the respective BRs are 100%. We always keep track of these constraints and find them to be not very important in most of the parameter space.

The aforesaid potentially important searches related to sleptons and EW particles are already included in the recent SMODELS-2.3.0. This includes the new ATLAS and CMS results relevant in the present context, [212,225–229].

VI. METHODOLOGY TO IMPLEMENT ONE-LOOP $\tilde{\chi}_1^0\tilde{\chi}_1^0 h_i$ VERTEX TO MICROMEGAS

We list here the necessary steps followed to evaluate the one-loop renormalized $\tilde{\chi}_1^0\tilde{\chi}_1^0 h_i$ vertex numerically, hence the SI-DD of the LSP. We use FEYNARTS-3.11 [141,230–232], FORMCALC-9.9 [131,141], and LOOPTOOLS-2.16 [131] at different stages as discussed below:

(i) FEYNARTS contains the model files MSSM.mod and MSSMCT.mod in which all the Feynman rules are implemented. We generate all the relevant one-loop diagrams for the $\tilde{\chi}_1^0\tilde{\chi}_1^0 h_i$ (where $h_i = h,\ H$) vertex using FEYNARTS.

(ii) We choose the Feynman gauge for computing the loops, which is also the default choice of FEYNARTS. We include all the diagrams, including Goldstone bosons, to get the gauge-invariant result. There are 234 diagrams for the h-mediated or the H-mediated processes for consideration.

(iii) The total amplitude for all the one-loop diagrams, as evaluated by FEYNARTS, leaves the momentum integrals unevaluated. FORMCALC evaluates all the momentum integrals and writes the amplitude in a simplified form through its internal abbreviation functions.

(iv) The vertex correction parts can be cast as $\Gamma_{\tilde{\chi}_1^0\tilde{\chi}_1^0 h_i} = C_L^{\rm 1L}\mathbf{P_L} + C_R^{\rm 1L}\mathbf{P_R}$, where $\mathbf{P_L}$ and $\mathbf{P_R}$ are left- and right-handed projection operators. We extract the $C_{L,R}^{\rm 1L}$-parts and convert it to `Fortran` codes using routines in FORMCALC.

(v) We use the spectrum calculator SPHENO-4.0.4 [198,199] for numerical evaluations. The model files for the MSSM are generated by SARAH-4.14.5 [200,201]. Then SM and MSSM inputs and MSSM outputs are fed to our code that calculates $C_L^{\rm 1L}$ and $C_R^{\rm 1L}$. At this stage, LOOPTOOLS has been used to evaluate the Passarino-Veltman scalar integrals.

(vi) The loop-corrected $\tilde{\chi}_1^0\tilde{\chi}_1^0 h_i$ vertex contain UV divergencies, unless $\tilde{\chi}_1^0$ is a pure state. The renormalization of $\tilde{\chi}_1^0\tilde{\chi}_1^0 h_i$ vertex is done by using FEYNARTS, FORMCALC, and LOOPTOOLS. We generate the counterterm diagrams for the $\tilde{\chi}_1^0\tilde{\chi}_1^0 h_i$ vertex and create the amplitudes using FEYNARTS. As said before, the relevant expressions may be found in Refs. [132–140]. Thereafter, we choose an appropriate renormalization scheme for our scenarios. Since we focus on the bino-Higgsino-like and bino-wino-Higgsino-like mixed neutralino scenarios, dominated by $\tilde{B}$ component, the suitable scheme is `CCN[1]` which is also the default choice in FORMCALC. Using FORMCALC and adopting `CCN[1]` scheme, we evaluate all the relevant renormalization constants that are contained in the amplitude of the vertex counterterms. The latter has the structure $\delta C_L \mathbf{P_L} + \delta C_R \mathbf{P_R}$ which is the same as that of the vertex with δC_L and δC_R refer to the amplitudes of the vertex counterterms. This leads to the final structure of the corrected $\tilde{\chi}_1^0\tilde{\chi}_1^0 h_i$ vertex as $(C_L^{\rm 1L} + \delta C_L)\mathbf{P_L} + (C_R^{\rm 1L} + \delta C_R)\mathbf{P_R}$.

(vii) The corresponding `Fortran` code is used to check the UV finiteness of our loop-corrected vertices.

There is a parameter "Δ" which is equivalent to $\frac{2}{\epsilon} - \gamma + \log(4\pi)$ and LOOPTOOLS takes its default value to be zero. The UV finiteness requires the final result not to depend on the parameter "Δ" up to a certain numerical precision. So we vary the parameter "Δ" up to 10^7, and we find that the total corrections (i.e., $C_L^{1L} + \delta C_L$ and $C_R^{1L} + \delta C_R$) do not change. This manifests that $(C_{L,R}^{1L} + \delta C_{L,R})$ is UV-finite. Note that we use tree-level masses for all the particles appearing in the loop to get the UV-finite result.

(viii) We endow the renormalized vertices $\tilde{\chi}_1^0\tilde{\chi}_1^0 h$ and $\tilde{\chi}_1^0\tilde{\chi}_1^0 H$ to MICROMEGAS-5.0.4 [124,233–235] to calculate the DM-related observables, e.g., SI-DD cross section and the relic density. Both off shell Higgs states (h, H) assume loop corrected masses. A necessary cross-check at this point is to verify the $B_{\tilde{H}}, B_{\tilde{W}\tilde{H}}$ scenarios under the recent LHC constraints. With the latest SMODELS-2.3.0 [153–156] we delineate the parameter space, which is still allowed under the collider searches.

VII. NUMERICAL RESULTS

Within this section, we present the numerical outcomes, demonstrating the impact of the dark matter direct detection cross section on the MSSM parameter space induced by the one-loop corrections to the $\tilde{\chi}_1^0\tilde{\chi}_1^0 h$ and $\tilde{\chi}_1^0\tilde{\chi}_1^0 H$ vertices. Specifically, we are interested in assessing numerically (I) the relative rise in the one-loop renormalized $\tilde{\chi}_1^0\tilde{\chi}_1^0 h_i$ vertex to its LO value, (II) the updated SI-DD cross section $\sigma_{\rm SI}^{\rm NLO}$ for LSP mass $m_{\tilde{\chi}_1^0}$ and (III) the resultant and revised contours, depicting the lowest band of μ with varying M_1 based upon the recent LUX-ZEPLIN (LZ) experimental limits on $\tilde{\chi}_1^0$-nucleon cross section.

We begin with highlighting the parts of the parameter space in the electroweak MSSM that satisfy δa_μ or other B-physics observables. We choose $\tan\beta = 30$, 10 for both $\tilde{B}_{\tilde{H}}$ and $\tilde{B}_{\tilde{W}\tilde{H}}$ cases, and additionally, the large $\tan\beta$ (=50) limit in the $\tilde{B}_{\tilde{W}\tilde{H}}$ scenario for numerical presentations. The DM constraints for $\tilde{\chi}_1^0$ or a critical checking of the validity of each parameter space point under SUSY searches is partially endorsed as a necessary parameter space criterion. While studying the parametric dependence to delineate the effects of one-loop calculations in (I) and (II), relic abundance or limits from SUSY searches can be observed to be relaxed. However, in predicting M_1-μ plane in (III) or the bench-mark points (BMPs) in Table I, relic constraint [vide Eq. (55)] and the limits from SMODELS-2.3.0 are always respected.

A. $\tilde{B}_{\tilde{H}}$ DM and $\sigma_{\rm SI}^{\rm NLO}$

Here, we perform a scan over the relevant parameters (all masses are in GeV):

$$50 \le M_1 \le 300, \qquad 400 \le \mu \le 1000,$$
$$100 \le m_{\tilde{\mu}_L,\tilde{\mu}_R} \le 350, \qquad 100 \le m_{\tilde{e}_L,\tilde{e}_R} \le 350. \tag{70}$$

We set $\mu \ge 400$ GeV for an efficient parametric scan. For our choice of M_1, the lower values of μ are disfavored, even from the LO SI-DD results. It will be further discussed when we elaborate on our results in Fig. 10. The wino is almost decoupled with $M_2 = 1.5$ TeV; consequently, the neutralino is composed of a dominantly winolike state and Higgsino. Also, lighter sleptons ($\tilde{e}$ and $\tilde{\mu}$) are preferred to comply with the anomalous magnetic moment of muon δa_μ. Relatively heavier staus are considered so as to satisfy the LHC constraints easily. Additionally, all the points satisfy the constraints from B-physics mentioned earlier. The LO $\tilde{\chi}_1^0$-nucleon cross section is related to gaugino-Higgsino mixings induced by the tree-level $\tilde{\chi}_1^0\tilde{\chi}_1^0 h_i$ vertex, noted it as $C_{L,R}^{\rm LO}$ in Eq. (4). Similarly, $C_{L,R}^{\rm NLO}$, the NLO vertex

TABLE I. A few exemplary points presented where $\sigma_{\rm SI}^{\rm NLO}$ excludes a parameter space point, which otherwise is allowed when one considers $\sigma_{\rm SI}^{\rm LO}$. Here, all the mass parameters are in GeV, and the cross sections are in pb. For BMP-I, the bino, wino, and Higgsino compositions are $\mathcal{N}_{11} = 0.9973$, $\mathcal{N}_{12} = -9.9266 \times 10^{-4}$, $\mathcal{N}_{13} = 7.2147 \times 10^{-2}$, and $\mathcal{N}_{14} = -1.3909 \times 10^{-2}$. Similarly, for BMP-II, $\mathcal{N}_{11} = -0.9975$, $\mathcal{N}_{12} = 1.7352 \times 10^{-2}$, $\mathcal{N}_{13} = -6.6141 \times 10^{-2}$, and $\mathcal{N}_{14} = 1.9271 \times 10^{-2}$.

$\tilde{B}_{\tilde{H}}$ LSP										
BMPs	$\tan\beta$	μ	M_1	M_2	M_A	M_H	$m_{\tilde{\mu}_L}$	$m_{\tilde{\mu}_R}$	$m_{\tilde{e}_L}$	$m_{\tilde{e}_R}$
I	30	603	100	1500	2800	2268	178	135	177	131
BMPs	$m_{\tilde{\chi}_1^0}$	$m_{\tilde{\chi}_1^\pm}, m_{\tilde{\chi}_2^0}$	δa_μ	Ωh^2	$C_{L,R}^{\rm LO}(h)$	$C_{L,R}^{\rm NLO}(h)$	$C_{L,R}^{\rm LO}(H)$	$C_{L,R}^{\rm NLO}(H)$	$\sigma_{\rm SI}^{\rm LO}$	$\sigma_{\rm SI}^{\rm NLO}$
I	99	624	2.12×10^{-9}	0.118	0.00583	0.00622	0.02515	0.02625	2.760×10^{-11}	3.130×10^{-11}
$\tilde{B}_{\tilde{W}\tilde{H}}$ LSP										
BMPs	$\tan\beta$	μ	M_1	M_2	M_A	M_H	$m_{\tilde{\mu}_L}$	$m_{\tilde{\mu}_R}$	$m_{\tilde{e}_L}$	$m_{\tilde{e}_R}$
II	30	710	190	265	3000	2392	344	248	254	204
BMPs	$m_{\tilde{\chi}_1^0}$	$m_{\tilde{\chi}_1^\pm}, m_{\tilde{\chi}_2^0}$	δa_μ	Ωh^2	$C_{L,R}^{\rm LO}(h)$	$C_{L,R}^{\rm NLO}(h)$	$C_{L,R}^{\rm LO}(H)$	$C_{L,R}^{\rm NLO}(H)$	$\sigma_{\rm SI}^{\rm LO}$	$\sigma_{\rm SI}^{\rm NLO}$
II	189	282	3.54×10^{-9}	0.119	0.00812	0.00858	0.02433	0.02519	4.709×10^{-11}	5.241×10^{-11}

includes $C_{L,R}^{\rm LO}$, one-loop vertex corrections $C_{L,R}^{\rm 1L}$, and contributions from the counterterms $\delta C_{L,R}$ as

$$C_{L,R}^{\rm NLO} = C_{L,R}^{\rm LO} + C_{L,R}^{\rm 1L} + \delta C_{L,R}. \tag{71}$$

With the set of parameters, stated in Eq. (70), we calculate $C_{L,R}^{\rm LO}$ and $C_{L,R}^{\rm NLO}$. The latter is subsequently fed to MICROMEGAS-5.0.4 for numerical evaluations of $\sigma_{\rm SI}^{\rm NLO}$.

Since we are mainly interested in the relative rise of $C_{L,R}^{\rm NLO}$ over its LO value, a quantity of our interest could be the ratio of their numerical values, $\frac{C_{L,R}^{\rm NLO}}{C_{L,R}^{\rm LO}}$. With this in mind, we plot $\frac{C_{L,R}^{\rm NLO}}{C_{L,R}^{\rm LO}}$, defined henceforth as $\mathcal{R}$, with the mass of LSP for the SM-like Higgs scalar [Figs. 4(a) and 4(b)] and the same for the heavier Higgs (4c and 4d). We recall here that both Higgs scalars interfere in the evaluation of $\sigma_{\rm SI}^{\rm NLO}$. The variations are shown for two sets of $(\tan\beta, M_A) \equiv (30, 2.8), (10, 1.7)$ where the masses of CP-odd Higgs are in TeV. Fewer points are obtained for $\tan\beta = 10$ satisfying the deviation in $(g-2)_\mu$ and other phenomenological constraints. The reason is that $(g-2)_\mu$ depends on the muon Yukawa coupling y_μ, which is inversely proportional to $\cos\beta$, $y_\mu \propto \frac{1}{\cos\beta} \sim \tan\beta$ (for $\tan\beta \geq 5$). It is also evident from Eq. (68). In the case of heavier LSP mass with relatively heavier $\tilde{\chi}_2^0, \tilde{\chi}_3^0$, and $\tilde{\chi}_1^\pm$, the larger value of $\tan\beta$ is favored to satisfy δa_μ. We may verify it numerically

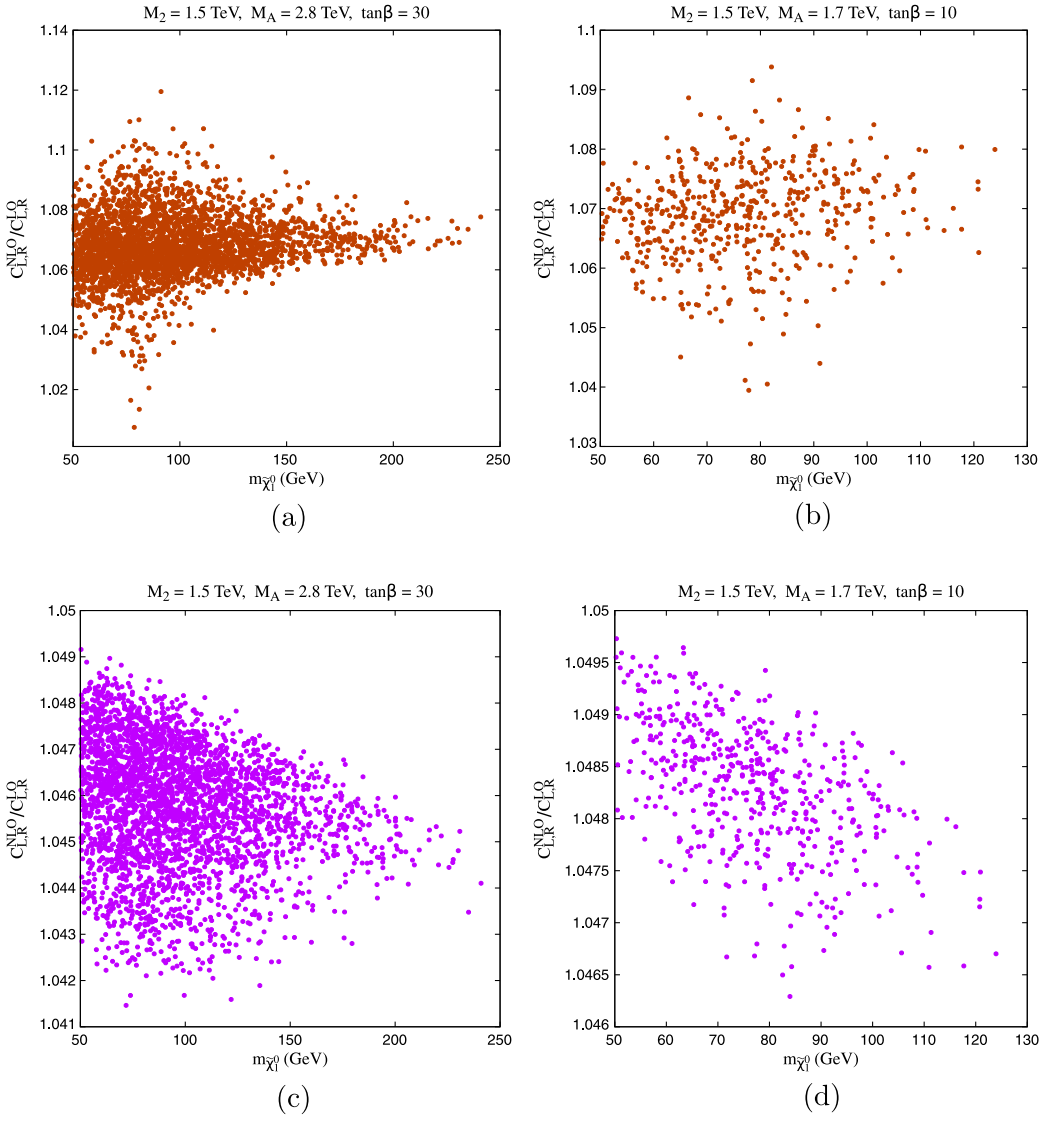

FIG. 4. (a) and (b) show the variations of $\frac{C_{L,R}^{\rm NLO}}{C_{L,R}^{\rm LO}}$ ($\equiv\mathcal{R}$) with the mass of LSP for the SM-like Higgs scalar whereas (c) and (d) show the same for the heavier Higgs state. The choice of parameters is discussed in the text. While $(g-2)_\mu$ and the B-physics constraints are always satisfied, the cosmological relic abundance data [see Eq. (55)] and the SI-DD bounds are not strictly endorsed. It is apparent that as large as ∼12% rise in $\mathcal{R}_h$ and that of ∼5% in $\mathcal{R}_H$ can be observed after including the one-loop radiative corrections along with the counterterm results with the LO results.

from Fig. 4. For a moderate $\tan\beta$ $(= 30)$, one finds a relatively heavier LSP region ($\sim$250 GeV) can be reached that can accommodate the $(g-2)_\mu$ compared to the lower value of $\tan\beta(= 10)$ (which can reach up to the LSP mass of $\sim$130 GeV). It is also apparent from Fig. 4 that an enhancement in $\mathcal{R}$ up to $\mathcal{R}_h = 12\%$ and $\mathcal{R}_H = 5\%$ can be obtained to $\tilde{\chi}_1^0\tilde{\chi}_1^0 h$ and $\tilde{\chi}_1^0\tilde{\chi}_1^0 H$ couplings respectively after considering the NLO results via Eq. (71). The maximum value of $\mathcal{R}_{h,H}$ refers to the scenarios where leading order $C_{L,R}^{\rm LO}$ or the bino-Higgsino mixing hits the minimum value.

The relatively subdued effect in $\mathcal{R}_H$, related to heavier CP-even Higgs scalar, is due to its higher LO value. It can be noted from Eq. (9) and Eq. (10). First, μ assumes higher values than M_1, and then the Higgs mixing angle is $\ll 1$. So, for the tree-level couplings associated with the light Higgs boson, the bino mass term dominates in Eq. (9) while for H boson, the first term within the bracket of Eq. (10) contributes mainly. Thus, the LO couplings are higher for H boson. We show its numerical values, in Fig. 5 for a representative choice of input parameters, $M_2 = 1.5$ TeV, $M_A = 2.8$ TeV. Similarly, we assume $\tan\beta = 30$ for the plot. The green points show $C_{L,R}^{\rm LO}$ for H scalar while red regions present the same for h boson for the same range of parameters, as stated earlier.

Following the relative dominance of h scalar in the $C_{L,R}^{\rm NLO}$, we now turn our attention to quantifying the relative increase of $\mathcal{R}_{h,H}$ in the χ_1^0-nucleon(p) cross section, through $\frac{\sigma_{\rm SI}^{\rm NLO}}{\sigma_{\rm SI}^{\rm LO}}$ [see Figs. 6(a) and 6(b)]. We define the ratio as $\mathcal{R}^\sigma$ for simplicity.

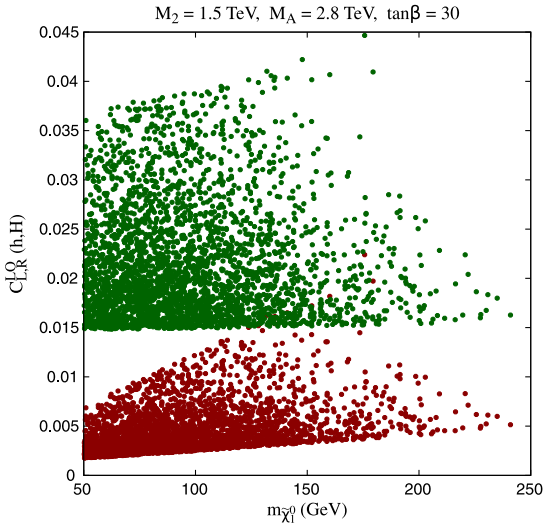

FIG. 5. Variations of the LO or tree-level couplings of $\tilde{\chi}_1^0\tilde{\chi}_1^0 h$ and $\tilde{\chi}_1^0\tilde{\chi}_1^0 H$ vertices with $m_{\tilde{\chi}_1^0}$. The points with larger values of the coupling (green) correspond to the $\tilde{\chi}_1^0\tilde{\chi}_1^0 H$ vertex, and the points with lower values of the coupling (red) correspond to the $\tilde{\chi}_1^0\tilde{\chi}_1^0 h$ vertex. As in Fig. 4, $(g-2)_\mu$ and the B-physics constraints are always satisfied, the cosmological relic abundance data and the SI-DD bounds are relaxed.

The parameters are the same as in Eq. (70). It is evident from Figs. 6(a) and 6(b) that we get an enhancement in $\mathcal{R}^\sigma$ up to $\sim$20% in the SI-DD cross sections after including the one-loop renormalized vertices. In a simple scenario, with either h or H presents in the spectra, the rise in $\sigma_{\rm SI}^{\rm NLO}$ can directly be correlated to the variations in $\tilde{\chi}_1^0\tilde{\chi}_1^0 h$ or $\tilde{\chi}_1^0\tilde{\chi}_1^0 H$ vertex $\sigma_{\rm SI}^{\rm NLO} = \sigma_{\rm SI}^{\rm LO}\frac{(C_{L,R}^{\rm NLO})^2}{(C_{L,R}^{\rm LO})^2} = \sigma_{\rm SI}^{\rm LO}[1 + \frac{2C_{L,R}^{\rm 1L}}{C_{L,R}^{\rm LO}} + \frac{2\delta C_{L,R}}{C_{L,R}^{\rm LO}}]$. When more than one scalar is present, both of the CP-even scalar bosons will interfere and the overall rise in the $\mathcal{R}^\sigma$ can not be apprehended easily.

Finally, we present the NLO cross section $\sigma_{\rm SI}^{\rm NLO}$ with the mass of LSP [Fig. 6(c)] for $\tan\beta = 30$ only. At this stage, it is customary to check the validity of the parameter space under SUSY searches. While the green regions depict part of the MSSM parameter space that otherwise satisfies B-physics constraints and $(g-2)_\mu$, the red points in Fig. 6(c) are additionally consistent with SUSY searches. As noted, the SUSY searches are validated with SMODELS-2.3.0. Even with the one-loop corrected SI-DD, $\sigma_{\rm SI}^{\rm NLO}$, some parts of the parameter space are still not excluded by the latest LZ data. It may be noted here that the exclusion limits from LUX, XENON-1T or LZ are shown assuming the central values only.

B. $\tilde{B}_{\tilde{W}\tilde{H}}$ DM and $\sigma_{\rm SI}^{\rm NLO}$

Having analyzed the $\tilde{B}_{\tilde{H}}$ DM, we now present the numerical results when the neutralino is composed of a dominantly bino, Higgsinos, and a relatively larger component of wino, which already referred to as $\tilde{B}_{\tilde{W}\tilde{H}}$ scenario. Specifically, we consider $M_1 < M_2 \lesssim \mu$ among the EW inputs with a numerical scan over the following ranges of the parameters:

$$50 \le M_1 \le 300, \quad 150 \le M_2 \le 600, \quad 400 \le \mu \le 1000,$$
$$100 \le m_{\tilde{\mu}_L,\tilde{\mu}_R} \le 350, \quad 100 \le m_{\tilde{e}_L,\tilde{e}_R} \le 350. \tag{72}$$

In the above, all the masses are in GeV. The ranges of the parameters are the same as in $\tilde{B}_{\tilde{H}}$ case except that, here, we have taken the lighter wino with $M_2 \in [150, 600]$ GeV to raise the wino composition in $\tilde{\chi}_1^0$ [see Eq. (72)] compared to $\tilde{B}_{\tilde{H}}$ scenario. As for the $\tilde{B}_{\tilde{H}}$ DM, the relative rise in $C_{L,R}^{\rm NLO}$ compared to $C_{L,R}^{\rm LO}$, quantified as $\frac{C_{L,R}^{\rm NLO}}{C_{L,R}^{\rm LO}}$ (or $\mathcal{R}$, for the sake of brevity) is shown with $m_{\tilde{\chi}_1^0}$ for the SM-like Higgs scalar [Figs. 7(a) and 7(b)] and the heavier Higgs [Figs. 7(c) and 7(d)]. As before, we primarily consider $\tan\beta = 30, 10$ with two different values of $M_A = 3, 1.7$ TeV. Additionally, we consider $\tan\beta = 50$ with $M_A = 3$ TeV to reach the larger mass region of the LSP. In Figs. 7(a) and (b) ($\tan\beta = 30$, 10), we can achieve a maximum value for $\mathcal{R}_h$, $\sim$9%. The relative increase $\mathcal{R}_H$ is much smaller $\sim$4.5% irrespective of the value of $\tan\beta$ which follows from the fact that $\tilde{\chi}_1^0\tilde{\chi}_1^0 H$

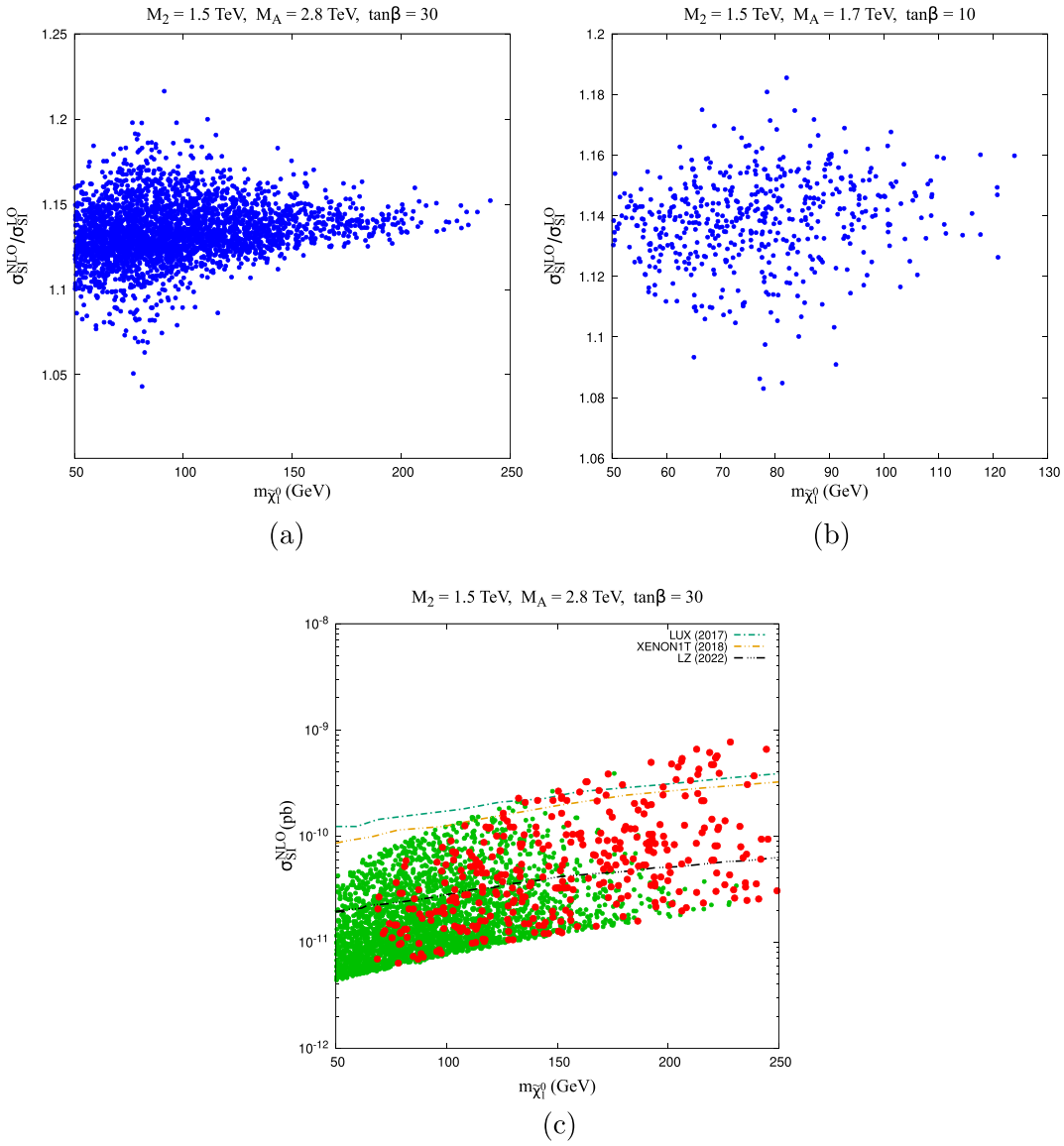

FIG. 6. (a) and (b) represent the variations of $\frac{\sigma_{\rm SI}^{\rm NLO}}{\sigma_{\rm SI}^{\rm LO}}$ or $\mathcal{R}^{\sigma}$ with the mass of LSP, while the variation of $\sigma_{\rm SI}^{\rm NLO}$ with $m_{\tilde{\chi}_1^0}$ is shown in (c) for $\tan\beta = 30$. The red points in (c) are allowed by SMODELS-2.3.0. Note that in this case, the bino fraction in $\tilde{\chi}_1^0$ is $\mathcal{N}_{11}^2 \geq 97\%$. It is evident from (a) and (b) that we get an enhancement up to ∼20% in $\mathcal{R}^{\sigma}$ after including the one-loop renormalized vertices.

takes higher value at the LO. So the ratio $\mathcal{R}_H$ resides on the lower side.

As in the $\tilde{B}_{\tilde{H}}$ case, we may again observe that $\tan\beta = 30$ helps to reach larger values of LSP masses (up to 300 GeV). Since the rise in $m_{\tilde{\chi}_1^0}$, one has to raise the masses of $\tilde{\chi}_1^{\pm}$, a larger $\tan\beta$ would be necessary [see e.g., Eq. (68)]. Moreover, unlike the previous scenario, a light winolike chargino also helps to enhance the BSM contributions to $(g-2)_{\mu}$. So, in contrast to Fig. 4, one can even go to larger masses for the LSP and Higgsino-like states. Along the same line, it may be interesting to see how far we can reach in the LSP mass at a large $\tan\beta$ value (e.g., $\tan\beta = 50$).

Thus, we contemplate a scenario for large $\tan\beta$ (= 50). Here, heavier chargino and neutralino masses (∼600 GeV) can be reached in compliance with $(g-2)_{\mu}$.[11] As before, we compute the EW corrections to the $\tilde{\chi}_1^0\tilde{\chi}_1^0 h_i$ coupling and the corresponding SI-DD cross section. The ranges of the parameters we consider in this scenario are the following:

$$50 \leq M_1 \leq 600, \quad 150 \leq M_2 \leq 1000, \quad 400 \leq \mu \leq 1500,$$
$$100 \leq m_{\tilde{\mu}_L,\tilde{\mu}_R} \leq 650, \quad 100 \leq m_{\tilde{e}_L,\tilde{e}_R} \leq 650. \tag{73}$$

[11]The higher LSP region of masses up to ∼600 GeV can be reached with the large value of $\tan\beta$. The region of the allowed parameter space is mentioned in https://atlas.web.cern.ch/Atlas/GROUPS/PHYSICS/PUBNOTES/ATL-PHYS-PUB-2023-025/fig16.png.

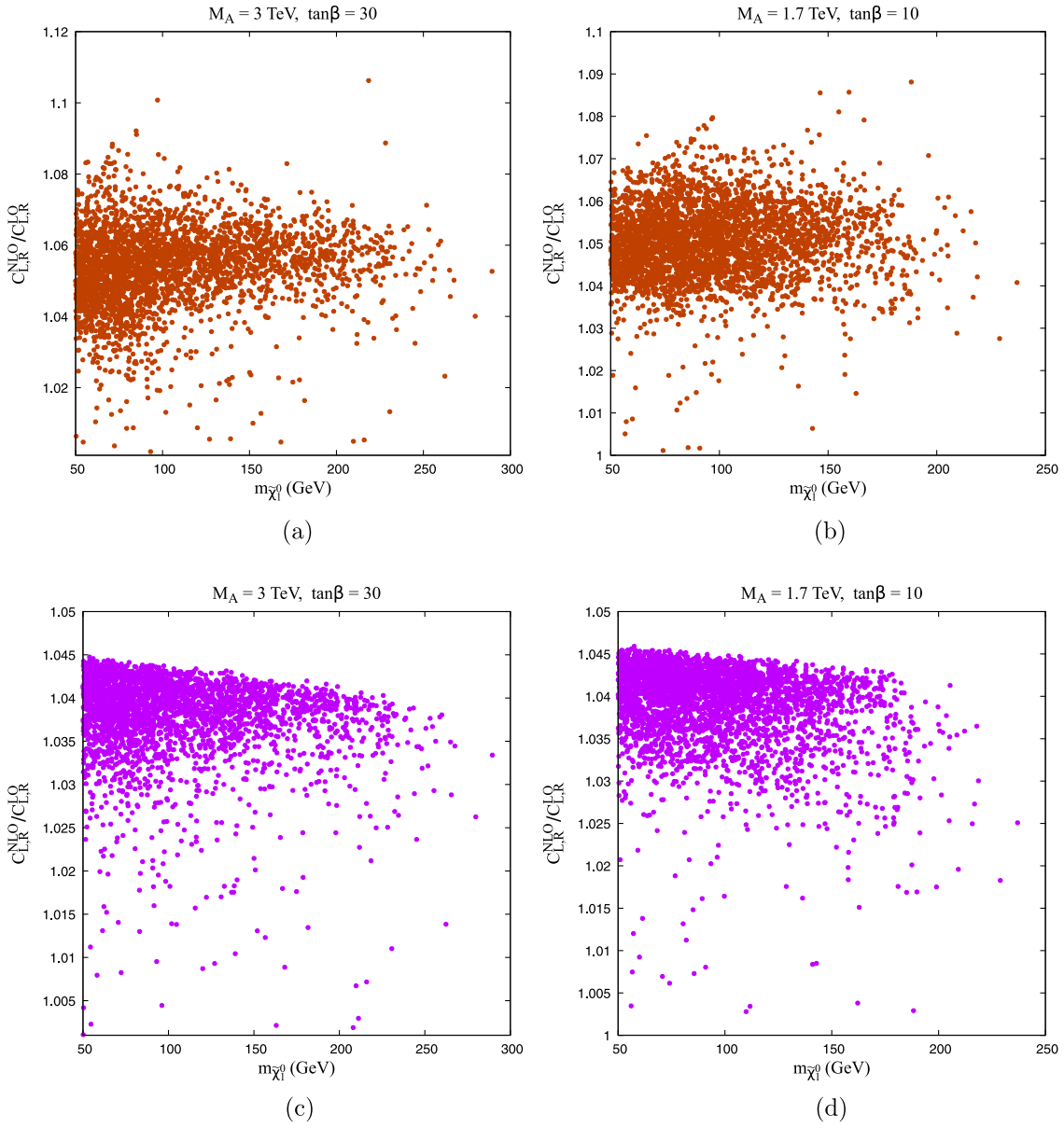

FIG. 7. (a) and (b) show the variations of $\mathcal{R} = \frac{C^{\rm NLO}_{L,R}}{C^{\rm LO}_{L,R}}$ with the mass of LSP for the SM-like Higgs scalar whereas (c) and (d) show the same for the heavier Higgs. These are the same as the $\tilde{B}_{\tilde{H}}$ case except that, here, we have taken the lighter wino with $M_2 \in [150, 600]$ GeV [see Eq. (72)]. As before, $(g-2)_\mu$ and the B-physics constraints are always satisfied; the cosmological relic abundance data and SI-DD constraints are not strictly endorsed.

where all the masses are in GeV. From Fig. 8, we obtain up to ∼13% NLO corrections to the $\tilde{\chi}^0_1\tilde{\chi}^0_1 h$ coupling and that of ∼4.3% corrections to the $\tilde{\chi}^0_1\tilde{\chi}^0_1 H$ coupling.

The resultant change in the SI-DD cross section $\mathcal{R}^\sigma = \frac{\sigma^{\rm NLO}_{\rm SI}}{\sigma^{\rm LO}_{\rm SI}}$ with the mass of LSP for $\tan\beta = 30$, 10, and the large $\tan\beta = 50$, and the variations of $\sigma^{\rm NLO}_{\rm SI}$ with the same for $\tan\beta = 30$ are shown in Fig. 9. As can be seen, $\mathcal{R}^\sigma$ reads ∼20% corrections for our choices of the $\tan\beta$. Additionally, a large part of the parameter space still satisfies the stringent LZ limits. As before, the red points in Fig. 9(c) satisfy the SUSY search limits verified by SMODELS-2.3.0.

With the knowledge gathered from the previous exercise, we may anticipate that for higher values of $\sigma^{\rm NLO}_{\rm SI}$, the MSSM parameter space will be curbed further. As a result, a more stringent bound on the gaugino-Higgsino mixing parameter may be derived. Following the fact that their mass parameters drive the mixing, we observe a rise in the lowest band of the Higgsino mass μ for a given value of M_1, as depicted in Figs. 10(a)–10(c). For the experimental input, we use the 90% confidence limit of LZ in Fig. 10(a), 2σ upper bound ($+2\sigma$) of LZ in Fig. 10(b), and 90% confidence limit of XENON-1T in Fig. 10(c) on the $\sigma_{\tilde{\chi}^0_1-p}$ cross section. We stick to a fixed value of $\tan\beta = 30$ for

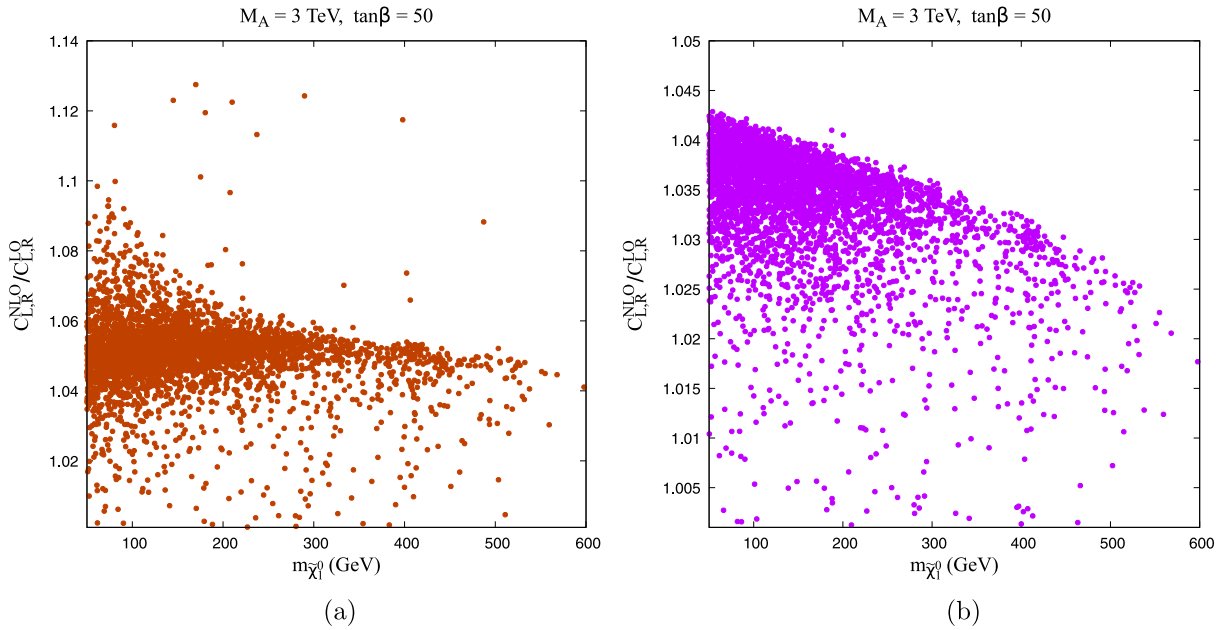

FIG. 8. (a) and (b) represent the variations of $\frac{C^{\rm NLO}_{L,R}}{C^{\rm LO}_{L,R}}$ with the mass of LSP for $\tan\beta = 50$. In this scenario, the LSP has a wino fraction of $\mathcal{N}^2_{11} \geq 85\%$. Here, we obtain ∼13% corrections in the $\tilde{\chi}^0_1\tilde{\chi}^0_1 h$ coupling, and ∼4.3% corrections in the $\tilde{\chi}^0_1\tilde{\chi}^0_1 H$ coupling. As before, $(g-2)_\mu$ and the B-physics constraints are always respected; the cosmological relic abundance data and SI-DD bounds are not considered.

simplicity. Similarly, $M_2 = 1.5$ TeV and $M_A = 2.8$ TeV are assumed. Thus, it leads to $\tilde{B}_{\tilde{H}}$ DM scenario. In Figs. 10(a)–10(c), we observe two contours in the M_1-μ plane, showing the lowest value of the parameters allowed from the SI-DD cross section if one uses (I) $C^{\rm LO}_{L,R}$ and (II) $C^{\rm NLO}_{L,R}$ in the calculations. As before, the B-physics constraints, $(g-2)_\mu$, and the LHC searches on the SUSY parameters are always respected. Moreover, the observed relic density [vide Eq. (55)] is strictly adhered to.

In Fig. 10(a), with the LO of $\tilde{\chi}^0_1\tilde{\chi}^0_1 h_i$ vertex, we find $\mu \geq 550$ GeV for $M_1 = 60$ GeV. After including the NLO corrections [vide Eq. (71)], the lower limit becomes $\mu \geq 575$ for the same value of M_1. Similarly, for $M_1 = 240$ GeV, the μ value shifts from 732 GeV to 758 GeV upon including the NLO corrections. Therefore, μ shifts upward by ∼25 GeV in this case. Similarly, in Figs. 10(b) and 10(c), μ shifts upward by ∼20 GeV. The underlying reason for the relatively lower shift in Figs. 10(b) and 10(c) depends on the fact that the maximum value for the wino-Higgsino mixing at the LO in the first case [i.e., Fig. 10(a)] is relatively smaller than the latter cases, which suppresses the LO value of the $\tilde{\chi}^0_1\tilde{\chi}^0_1 h(H)$. Therefore, the NLO corrections in the first case are larger, and a relatively higher shift in the μ value is obtained. Overall, the lower bound in μ shifts upward, leading to more stringent limits in the M_1-μ plane when the NLO corrections are included. Typically, one may extend the contours for lower or higher values of M_1. But, then $(g-2)_\mu$ and SMODELS-2.3.0 are somewhat restrictive on the MSSM parameter space.

We now examine the allowed parameter space through a few BMPs that, as before, satisfy all the necessary B-physics constraints, DD bounds on DM, δa_μ, and the present SUSY search.[12] We mainly present a few BMPs, which are allowed by the SI-DD cross section based on $C^{\rm LO}_{L,R}$, but become excluded when NLO corrected $\chi^0_1\chi^0_1 h_i$ vertex is considered instead. For BMP-I in Table I, where the LSP is $\tilde{B}_{\tilde{H}}$, having $m_{\tilde{\chi}^0_1} = 99$ GeV, we get 6.7% rise to $\tilde{\chi}^0_1\tilde{\chi}^0_1 h$ vertex and 4.4% rise to $\tilde{\chi}^0_1\tilde{\chi}^0_1 H$ vertex following the inclusion of the NLO corrections. Finally, we obtain an overall 13.4% enhancement to the SI-DD cross section. The LO cross section for this BMP is 2.760×10^{-11} pb, which resides below the central line of LZ (the LZ limit is 2.9×10^{-11} pb for this point), thus, allowed by the DD bound. After including the NLO corrections, the DD cross section becomes 3.130×10^{-11} pb, which is ruled out by the DD limit of LZ.

In another example, we consider the BMP-II[13] where $m_{\tilde{\chi}^0_1} = 189$ GeV, we obtain 5.7% and 3.5% rise to $\mathcal{R}_h$ and

[12]The first BMP is allowed by the condition $\Delta m(\tilde{\ell}, \tilde{\chi}^0_1) \leq 50$ GeV for $\tilde{e}$ and $\tilde{\mu}$ masses ≤ 150 GeV (see Sec. V B for details) whereas the second BMP is allowed as mentioned in https://atlas.web.cern.ch/Atlas/GROUPS/PHYSICS/PUBNOTES/ATL-PHYS-PUB-2023-025/fig16.png.

[13]Here, charginos/neutralinos can decay into selectrons with a non-negligible BR. However, the BRs of the decays $\tilde{\chi}^\pm_1, \tilde{\chi}^0_2$ to $\tilde{\nu}_e e$, $\tilde{\ell}_{eL} e_L$ can be made insignificant by slightly pushing the selectron masses, which does not cause any change in the rest of the analysis.

$\mathcal{R}_H$ respectively and 11.3% corrections to the DD cross-section. In this case, the LO cross section is 4.709×10^{-11} pb, again below the central line of LZ (the LZ limit is 5.0×10^{-11} pb for this point), hence allowed by the SI-DD searches. After incorporating the NLO corrections, we obtain the SI-DD cross-section 5.241×10^{-11} pb, which is now above the LZ line and hence excluded by the SI-DD search of LZ.

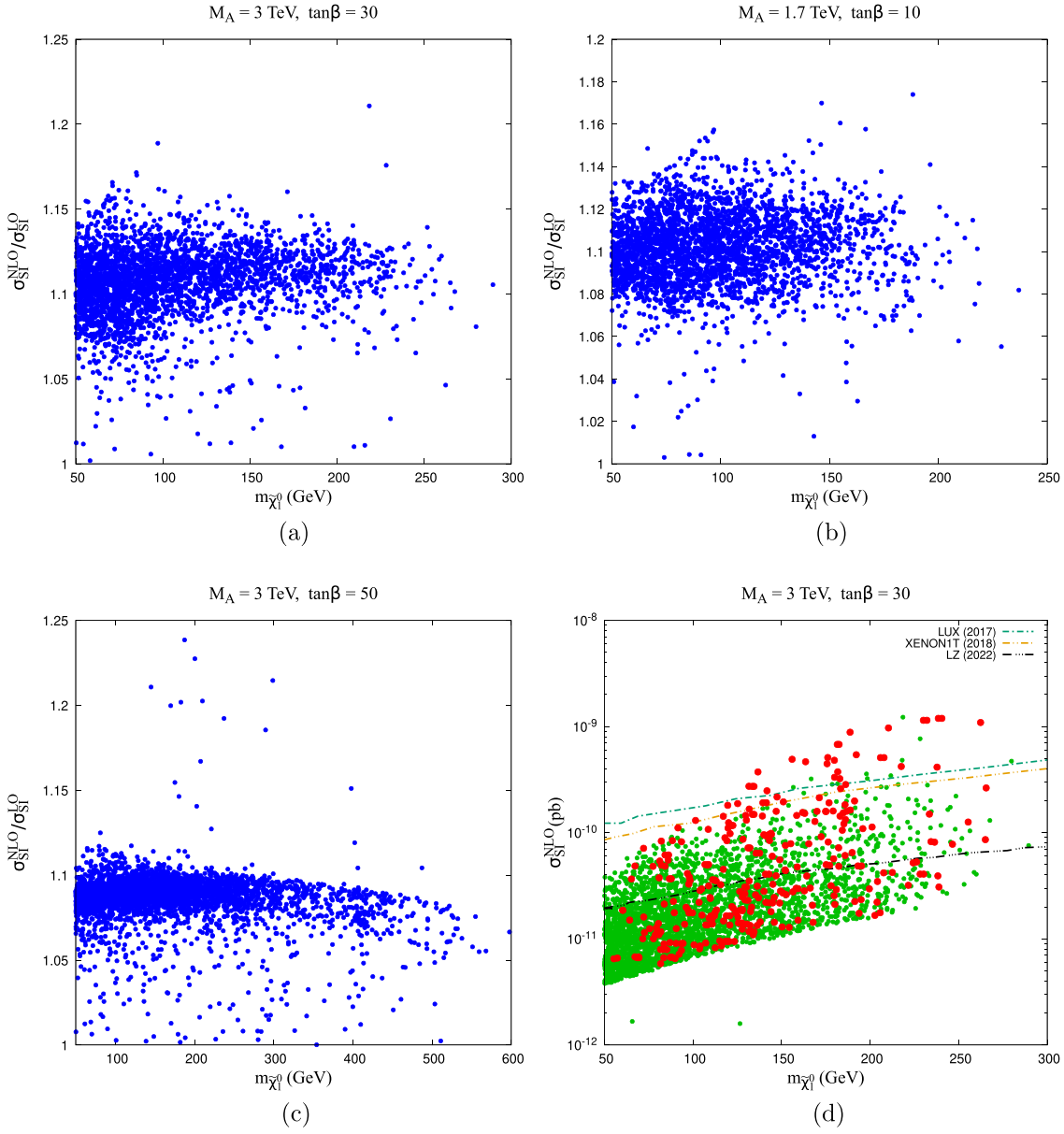

FIG. 9. (a), (b), and (c) represent the variations of $\frac{\sigma_{\mathrm{SI}}^{\mathrm{NLO}}}{\sigma_{\mathrm{SI}}^{\mathrm{LO}}}$ with the mass of LSP, and (d) $\sigma_{\mathrm{SI}}^{\mathrm{NLO}}$ with the same for $\tan\beta = 30$. In (d), the red points satisfy the present SUSY search constraints, verified by SMODELS-2.3.0. Here, the LSP has a bino fraction of $\mathcal{N}_{11}^2 \geq 97\%$. Note that we get ∼20% corrections in the cross sections for $\tan\beta = 30$, 50 and ∼18% for $\tan\beta = 10$.

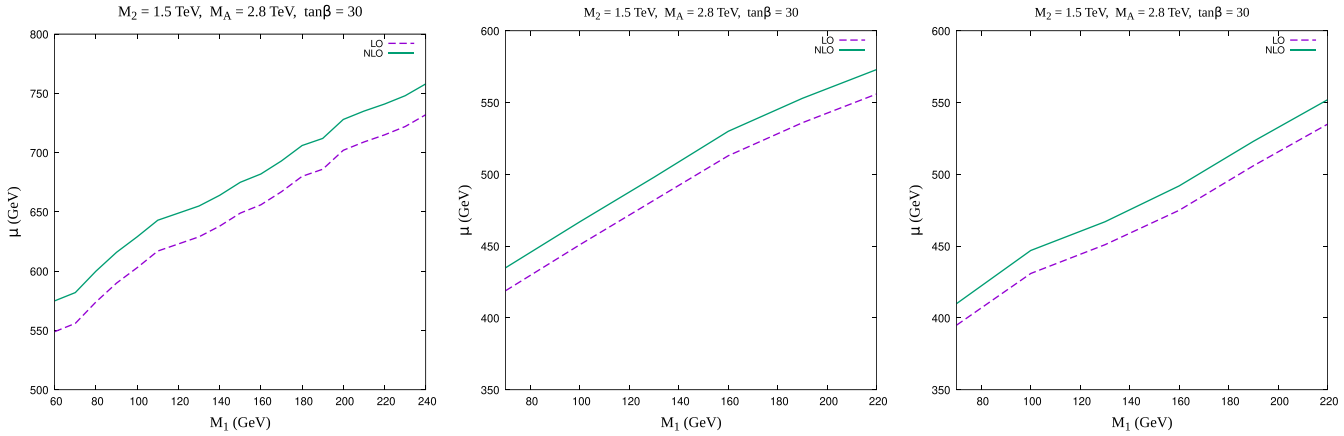

FIG. 10. Contours depicting the lowest values of μ for a given M_1, computed from $C_{L,R}^{\mathrm{LO}}$ and $C_{L,R}^{\mathrm{NLO}}$ for the $\chi_1^0\chi_1^0 h_i$ coupling using (a) 90% confidence limit of LZ, (b) 2σ upper bound ($+2\sigma$) of LZ, and (c) 90% confidence limit of $XENON-1T(2018)$. Overall, the lower bound in μ shifts upward, leading to more stringent limits in the M_1-μ plane if the NLO corrections are included. The B-physics constraints, δa_μ, the cosmological relic abundance data, and the constraints following SMODELS-2.3.0 are always respected.

VIII. CONCLUSIONS

A dominantly binolike $\tilde{\chi}_1^0$, but having (i) a minimal Higgsino component and (ii) a minimal wino-Higgsino component in the MSSM can accommodate $(g-2)_\mu$, the recent SUSY search constraints, and the LO DM-nucleon scattering cross section for the DM searches. Defining them as $\tilde{B}_{\tilde{H}}$ and $\tilde{B}_{\tilde{W}\tilde{H}}$, we have computed the NLO corrections to the LSP-Higgs interaction vertices, mainly focusing on the electroweak particles only. There are a total of 234 diagrams for the $\tilde{\chi}_1^0\tilde{\chi}_1^0 h$ vertex corrections and 234 for the $\tilde{\chi}_1^0\tilde{\chi}_1^0 H$ vertex corrections at the particle level. We have assembled all the diagrams by six topologies and presented the analytical expressions for each topology. To get the UV-finite result, we have included the vertex counterterms. For the $\tilde{B}_{\tilde{H}}$ LSP, including NLO corrections, we have obtained up to 12% and 5% enhancement to the $\tilde{\chi}_1^0\tilde{\chi}_1^0 h$ and $\tilde{\chi}_1^0\tilde{\chi}_1^0 H$ couplings, respectively, which in turn leads to an enhancement up to 20% to the SI-DD cross section. Similarly, for the $\tilde{B}_{\tilde{W}\tilde{H}}$ LSP, we have obtained up to 20% enhancement to the SI-DD cross section. Through the detailed numerical studies, we have shown that the relative enhancement has only a mild dependence over $\tan\beta$. With the improved corrections, the MSSM parameter space is further squeezed, though somewhat moderately. Finally, we reanalyze the exclusion limits in the M_1-μ plane computed from the SI-DD cross section for the $\tilde{B}_{\tilde{H}}$ LSP, using leading-order and NLO corrected couplings. Here, $\tan\beta = 30$ is assumed for the presentation. Overall, a rise of about ~25 GeV in the Higgsino mass parameter can be observed for $M_1 \in [60, 240]$ GeV after incorporating the NLO corrections if one uses the 90% confidence limit of the LZ results on the SI-DD cross section. For other values of $\tan\beta$, a similar shift in the μ parameter can easily be anticipated. Moreover, a higher value of $\tan\beta(=50)$ is favored to satisfy the $(g-2)_\mu$ for a heavier LSP (with mass ~600 GeV). However, even here, the relative rise in the NLO coupling or cross section is of the same size, which leads to a similar rise in the μ parameter in the M_1-μ plane.

ACKNOWLEDGMENTS

Our computations were supported in part by SAMKHYA: the High-Performance Computing Facility provided by the Institute of Physics (IoP), Bhubaneswar, India. The authors thank B. De for his contributions in the early stages of his work. We acknowledge C. Schappacher, A. Pukhov, and S. Heinemeyer for their valuable discussions. A. C. also acknowledges the local hospitality at IoP, Bhubaneswar, during the meeting IMHEP-19 and IMHEP-22, where some parts of the work were done. A. C. and S. A. P. also acknowledge the hospitality at IoP, Bhubaneswar, during a visit. S. B. acknowledges the local hospitality at SNIoE, Greater Noida, during the meeting at WPAC-2023, where this work was finalized. The authors also acknowledge the support received from the SERB project.

APPENDIX A: COUPLINGS

For the sake of completeness, here we present all the vertex factors following Ref. [107] that appeared in the triangular topologies presented in Sec. IV A.

Topology-1(a):

(1) $h_i = h/H$, $F = \tilde{\chi}_\ell^0$, and $S = S' = h$.

$$\xi_{LL} = \lambda_{h_i hh}\mathcal{G}^L_{\tilde{\chi}_1^0\tilde{\chi}_\ell^0 h}\mathcal{G}^{R*}_{\tilde{\chi}_1^0\tilde{\chi}_\ell^0 h},$$
$$\xi_{LR} = \lambda_{h_i hh}\mathcal{G}^L_{\tilde{\chi}_1^0\tilde{\chi}_\ell^0 h}\mathcal{G}^{L*}_{\tilde{\chi}_1^0\tilde{\chi}_\ell^0 h}, \tag{A1}$$

$$\xi_{RL} = \lambda_{h_i hh}\mathcal{G}^{R}_{\tilde{\chi}^0_1\tilde{\chi}^0_\ell h}\mathcal{G}^{R*}_{\tilde{\chi}^0_1\tilde{\chi}^0_\ell h},$$
$$\xi_{RR} = \lambda_{h_i hh}\mathcal{G}^{R}_{\tilde{\chi}^0_1\tilde{\chi}^0_\ell h}\mathcal{G}^{L*}_{\tilde{\chi}^0_1\tilde{\chi}^0_\ell h}, \tag{A2}$$

where $\ell = 1, \ldots, 4$; $\lambda_{h_i h_i h_i} = -3\frac{g_2 M_Z}{2c_W}B_{h_i}$, with

$$B_{h_i} = \begin{cases} c_{2\alpha}s_{\beta+\alpha}; & h_i = h \\ c_{2\alpha}c_{\beta+\alpha}; & h_i = H \end{cases},$$

$$\mathcal{G}^{L}_{\tilde{\chi}^0_1\tilde{\chi}^0_\ell h_i} = \begin{cases} g_2(Q''^{*}_{\ell 1}s_\alpha + S''^{*}_{\ell 1}c_\alpha); & h_i = h \\ g_2(-Q''^{*}_{\ell 1}c_\alpha + S''^{*}_{\ell 1}s_\alpha); & h_i = H \end{cases},$$

$$\mathcal{G}^{R}_{\tilde{\chi}^0_1\tilde{\chi}^0_\ell h_i} = \begin{cases} g_2(Q''_{1\ell}s_\alpha + S''_{1\ell}c_\alpha); & h_i = h \\ g_2(-Q''_{1\ell}c_\alpha + S''_{1\ell}s_\alpha); & h_i = H \end{cases}.$$

(2) $h_i = h/H$, $F = \tilde{\chi}^0_\ell$, and $S = h$, $S' = H$ or $S = H$, $S' = h$.

$$\xi_{LL} = \lambda_{h_i hH}\mathcal{G}^{L}_{\tilde{\chi}^0_1\tilde{\chi}^0_\ell H}\mathcal{G}^{R*}_{\tilde{\chi}^0_1\tilde{\chi}^0_\ell h},$$
$$\xi_{LR} = \lambda_{h_i hH}\mathcal{G}^{L}_{\tilde{\chi}^0_1\tilde{\chi}^0_\ell H}\mathcal{G}^{L*}_{\tilde{\chi}^0_1\tilde{\chi}^0_\ell h}, \tag{A3}$$

$$\xi_{RL} = \lambda_{h_i hH}\mathcal{G}^{R}_{\tilde{\chi}^0_1\tilde{\chi}^0_\ell H}\mathcal{G}^{R*}_{\tilde{\chi}^0_1\tilde{\chi}^0_\ell h},$$
$$\xi_{RR} = \lambda_{h_i hH}\mathcal{G}^{R}_{\tilde{\chi}^0_1\tilde{\chi}^0_\ell H}\mathcal{G}^{L*}_{\tilde{\chi}^0_1\tilde{\chi}^0_\ell h}, \tag{A4}$$

where $\lambda_{h_i hH} = \frac{g_2 M_Z}{2c_W}C_{h_i}$, with

$$C_{h_i} = \begin{cases} -2s_{2\alpha}s_{\beta+\alpha} + c_{\beta+\alpha}c_{2\alpha}; & h_i = h \\ 2s_{2\alpha}c_{\beta+\alpha} + s_{\beta+\alpha}c_{2\alpha}; & h_i = H \end{cases}.$$

(3) $h_i = h/H$, $F = \tilde{\chi}^0_\ell$, and $S = S' = H$.

$$\xi_{LL} = \lambda_{h_i HH}\mathcal{G}^{L}_{\tilde{\chi}^0_1\tilde{\chi}^0_\ell H}\mathcal{G}^{R*}_{\tilde{\chi}^0_1\tilde{\chi}^0_\ell H},$$
$$\xi_{LR} = \lambda_{h_i HH}\mathcal{G}^{L}_{\tilde{\chi}^0_1\tilde{\chi}^0_\ell H}\mathcal{G}^{L*}_{\tilde{\chi}^0_1\tilde{\chi}^0_\ell H}, \tag{A5}$$

$$\xi_{RL} = \lambda_{h_i HH}\mathcal{G}^{R}_{\tilde{\chi}^0_1\tilde{\chi}^0_\ell H}\mathcal{G}^{R*}_{\tilde{\chi}^0_1\tilde{\chi}^0_\ell H},$$
$$\xi_{RR} = \lambda_{h_i HH}\mathcal{G}^{R}_{\tilde{\chi}^0_1\tilde{\chi}^0_\ell H}\mathcal{G}^{L*}_{\tilde{\chi}^0_1\tilde{\chi}^0_\ell H}, \tag{A6}$$

(4) $h_i = h/H$, $F = \tilde{\chi}^0_\ell$, and $S = S' = A$.

$$\xi_{LL} = \lambda_{h_i AA}\mathcal{G}^{L}_{\tilde{\chi}^0_1\tilde{\chi}^0_\ell A}\mathcal{G}^{R*}_{\tilde{\chi}^0_1\tilde{\chi}^0_\ell A},$$
$$\xi_{LR} = \lambda_{h_i AA}\mathcal{G}^{L}_{\tilde{\chi}^0_1\tilde{\chi}^0_\ell A}\mathcal{G}^{L*}_{\tilde{\chi}^0_1\tilde{\chi}^0_\ell A}, \tag{A7}$$

$$\xi_{RL} = \lambda_{h_i AA}\mathcal{G}^{R}_{\tilde{\chi}^0_1\tilde{\chi}^0_\ell A}\mathcal{G}^{R*}_{\tilde{\chi}^0_1\tilde{\chi}^0_\ell A},$$
$$\xi_{RR} = \lambda_{h_i AA}\mathcal{G}^{R}_{\tilde{\chi}^0_1\tilde{\chi}^0_\ell A}\mathcal{G}^{L*}_{\tilde{\chi}^0_1\tilde{\chi}^0_\ell A}, \tag{A8}$$

where $\lambda_{h_i AA} = -\frac{g_2 M_Z}{2c_W}c_{2\beta}D_{h_i}$, with

$$D_{h_i} = \begin{cases} s_{\beta+\alpha}; & h_i = h \\ -c_{\beta+\alpha}; & h_i = H \end{cases},$$

$\mathcal{G}^{L}_{\tilde{\chi}^0_1\tilde{\chi}^0_\ell A} = i(Q''^{*}_{\ell 1}s_\beta - S''^{*}_{\ell 1}c_\beta)$, and $\mathcal{G}^{R}_{\tilde{\chi}^0_1\tilde{\chi}^0_\ell A} = i(-Q''_{1\ell}s_\beta + S''_{1\ell}c_\beta)$.

(5) $h_i = h/H$, $F = \tilde{\chi}^0_\ell$, and $S = A$, $S' = G$ or $S = G$, $S' = A$.

$$\xi_{LL} = \lambda_{h_i AG}\mathcal{G}^{L}_{\tilde{\chi}^0_1\tilde{\chi}^0_\ell G}\mathcal{G}^{R*}_{\tilde{\chi}^0_1\tilde{\chi}^0_\ell A},$$
$$\xi_{LR} = \lambda_{h_i AG}\mathcal{G}^{L}_{\tilde{\chi}^0_1\tilde{\chi}^0_\ell G}\mathcal{G}^{L*}_{\tilde{\chi}^0_1\tilde{\chi}^0_\ell A}, \tag{A9}$$

$$\xi_{RL} = \lambda_{h_i AG}\mathcal{G}^{R}_{\tilde{\chi}^0_1\tilde{\chi}^0_\ell G}\mathcal{G}^{R*}_{\tilde{\chi}^0_1\tilde{\chi}^0_\ell A},$$
$$\xi_{RR} = \lambda_{h_i AG}\mathcal{G}^{R}_{\tilde{\chi}^0_1\tilde{\chi}^0_\ell G}\mathcal{G}^{L*}_{\tilde{\chi}^0_1\tilde{\chi}^0_\ell A}, \tag{A10}$$

where $\lambda_{h_i AG} = -\frac{g_2 M_Z}{2c_W}s_{2\beta}D_{h_i}$, $\mathcal{G}^{L}_{\tilde{\chi}^0_1\tilde{\chi}^0_\ell G} = ig_2(-Q''^{*}_{\ell 1}c_\beta - S''^{*}_{\ell 1}s_\beta)$, and $\mathcal{G}^{R}_{\tilde{\chi}^0_1\tilde{\chi}^0_\ell G} = ig_2(Q''_{1\ell}c_\beta + S''_{1\ell}s_\beta)$.

(6) $h_i = h/H$, $F = \tilde{\chi}^0_\ell$, and $S = S' = G$.

$$\xi_{LL} = \lambda_{h_i GG}\mathcal{G}^{L}_{\tilde{\chi}^0_1\tilde{\chi}^0_\ell G}\mathcal{G}^{R*}_{\tilde{\chi}^0_1\tilde{\chi}^0_\ell G},$$
$$\xi_{LR} = \lambda_{h_i GG}\mathcal{G}^{L}_{\tilde{\chi}^0_1\tilde{\chi}^0_\ell G}\mathcal{G}^{L*}_{\tilde{\chi}^0_1\tilde{\chi}^0_\ell G}, \tag{A11}$$

$$\xi_{RL} = \lambda_{h_i GG}\mathcal{G}^{R}_{\tilde{\chi}^0_1\tilde{\chi}^0_\ell G}\mathcal{G}^{R*}_{\tilde{\chi}^0_1\tilde{\chi}^0_\ell G},$$
$$\xi_{RR} = \lambda_{h_i GG}\mathcal{G}^{R}_{\tilde{\chi}^0_1\tilde{\chi}^0_\ell G}\mathcal{G}^{L*}_{\tilde{\chi}^0_1\tilde{\chi}^0_\ell G}, \tag{A12}$$

where $\lambda_{h_i GG} = -\frac{g_2 M_Z}{2c_W}c_{2\beta}D'_{h_i}$, with

$$D'_{h_i} = \begin{cases} -s_{\beta+\alpha}; & h_i = h \\ c_{\beta+\alpha}; & h_i = H \end{cases}.$$

(7) $h_i = h/H$, $F = \tilde{\chi}^{\pm}_\ell$, and $S = S' = H^{\pm}$.

$$\xi_{LL} = \lambda_{h_i H^{\pm}H^{\pm}}\mathcal{G}^{L}_{\tilde{\chi}^0_1\tilde{\chi}^{\pm}_\ell H^{\pm}}\mathcal{G}^{R*}_{\tilde{\chi}^0_1\tilde{\chi}^{\pm}_\ell H^{\pm}},$$
$$\xi_{LR} = \lambda_{h_i H^{\pm}H^{\pm}}\mathcal{G}^{L}_{\tilde{\chi}^0_1\tilde{\chi}^{\pm}_\ell H^{\pm}}\mathcal{G}^{L*}_{\tilde{\chi}^0_1\tilde{\chi}^{\pm}_\ell H^{\pm}}, \tag{A13}$$

$$\xi_{RL} = \lambda_{h_i H^{\pm}H^{\pm}}\mathcal{G}^{R}_{\tilde{\chi}^0_1\tilde{\chi}^{\pm}_\ell H^{\pm}}\mathcal{G}^{R*}_{\tilde{\chi}^0_1\tilde{\chi}^{\pm}_\ell H^{\pm}},$$
$$\xi_{RR} = \lambda_{h_i H^{\pm}H^{\pm}}\mathcal{G}^{R}_{\tilde{\chi}^0_1\tilde{\chi}^{\pm}_\ell H^{\pm}}\mathcal{G}^{L*}_{\tilde{\chi}^0_1\tilde{\chi}^{\pm}_\ell H^{\pm}}, \tag{A14}$$

where, $\lambda_{h_i H^{\pm}H^{\pm}} = -g_2 A_{h_i}$, with

$$A_{h_i} = \begin{cases} M_W s_{\beta-\alpha} + \frac{M_Z}{2c_W}c_{2\beta}s_{\beta+\alpha}; & h_i = h \\ M_W c_{\beta-\alpha} - \frac{M_Z}{2c_W}c_{2\beta}c_{\beta+\alpha}; & h_i = H \end{cases},$$

$\mathcal{G}^{L}_{\tilde{\chi}^0_1\tilde{\chi}^{\pm}_\ell H^{\pm}} = -g_2 Q'^{L}_{1\ell}$, and $\mathcal{G}^{R}_{\tilde{\chi}^0_1\tilde{\chi}^{\pm}_\ell H^{\pm}} = -g_2 Q'^{R}_{1\ell}$.

(8) $h_i = h/H$, $F = \tilde{\chi}^{\pm}_\ell$, and $S = H^{\pm}$, $S' = G^{\pm}$ or $S = G^{\pm}$, $S' = H^{\pm}$.

$$\xi_{LL} = \lambda_{h_i H^\pm G^\pm} \mathcal{G}^L_{\tilde{\chi}^0_1 \tilde{\chi}^\pm_\ell G^\pm} \mathcal{G}^{R*}_{\tilde{\chi}^0_1 \tilde{\chi}^\pm_\ell H^\pm},$$
$$\xi_{LR} = \lambda_{h_i H^\pm G^\pm} \mathcal{G}^L_{\tilde{\chi}^0_1 \tilde{\chi}^\pm_\ell G^\pm} \mathcal{G}^{L*}_{\tilde{\chi}^0_1 \tilde{\chi}^\pm_\ell H^\pm}, \quad \text{(A15)}$$

$$\xi_{RL} = \lambda_{h_i H^\pm G^\pm} \mathcal{G}^R_{\tilde{\chi}^0_1 \tilde{\chi}^\pm_\ell G^\pm} \mathcal{G}^{R*}_{\tilde{\chi}^0_1 \tilde{\chi}^\pm_\ell H^\pm},$$
$$\xi_{RR} = \lambda_{h_i H^\pm G^\pm} \mathcal{G}^R_{\tilde{\chi}^0_1 \tilde{\chi}^\pm_\ell G^\pm} \mathcal{G}^{L*}_{\tilde{\chi}^0_1 \tilde{\chi}^\pm_\ell H^\pm}, \quad \text{(A16)}$$

where $\lambda_{h_i H^\pm G^\pm} = -\frac{g_2 M_W}{2} A'_{h_i}$, with

$$A'_{h_i} = \begin{cases} \frac{s_{2\beta} s_{\beta+\alpha}}{c_W^2} - c_{\beta-\alpha}; & h_i = h \\ -\frac{s_{2\beta} c_{\beta+\alpha}}{c_W^2} - s_{\beta-\alpha}; & h_i = H \end{cases},$$

$\mathcal{G}^L_{\tilde{\chi}^0_1 \tilde{\chi}^\pm_\ell G^\pm} = -g_2 t_\beta Q'^L_{1\ell}$, and $\mathcal{G}^R_{\tilde{\chi}^0_1 \tilde{\chi}^\pm_\ell G^\pm} = \frac{g_2}{t_\beta} Q'^R_{1\ell}$.

(9) $h_i = h/H$, $F = \tilde{\chi}^\pm_\ell$, and $S = S' = G^\pm$.

$$\xi_{LL} = \lambda_{h_i G^\pm G^\pm} \mathcal{G}^L_{\tilde{\chi}^0_1 \tilde{\chi}^\pm_\ell G^\pm} \mathcal{G}^{R*}_{\tilde{\chi}^0_1 \tilde{\chi}^\pm_\ell G^\pm},$$
$$\xi_{LR} = \lambda_{h_i G^\pm G^\pm} \mathcal{G}^L_{\tilde{\chi}^0_1 \tilde{\chi}^\pm_\ell G^\pm} \mathcal{G}^{L*}_{\tilde{\chi}^0_1 \tilde{\chi}^\pm_\ell G^\pm}, \quad \text{(A17)}$$

$$\xi_{RL} = \lambda_{h_i G^\pm G^\pm} \mathcal{G}^R_{\tilde{\chi}^0_1 \tilde{\chi}^\pm_\ell G^\pm} \mathcal{G}^{R*}_{\tilde{\chi}^0_1 \tilde{\chi}^\pm_\ell G^\pm},$$
$$\xi_{RR} = \lambda_{h_i G^\pm G^\pm} \mathcal{G}^R_{\tilde{\chi}^0_1 \tilde{\chi}^\pm_\ell G^\pm} \mathcal{G}^{L*}_{\tilde{\chi}^0_1 \tilde{\chi}^\pm_\ell G^\pm}, \quad \text{(A18)}$$

where $\lambda_{h_i G^\pm G^\pm} = -\frac{g_2 M_Z}{2 c_W} c_{2\beta} D'_{h_i}$.

(10) $h_i = h/H$, $F = \nu_n$, $S = \tilde{\nu}_\ell$, $S' = \tilde{\nu}_m$.

$$\xi_{LL} = 0, \qquad \xi_{LR} = \lambda_{h_i \tilde{\nu}_\ell \tilde{\nu}_m} \mathcal{G}^L_{\tilde{\chi}^0_1 \nu_n \tilde{\nu}_\ell} \mathcal{G}^{L*}_{\tilde{\chi}^0_1 \nu_n \tilde{\nu}_m}, \quad \text{(A19)}$$

$$\xi_{RL} = 0, \qquad \xi_{RR} = 0, \quad \text{(A20)}$$

where $\ell, m, n = 1, 2, 3$; $\mathcal{G}^L_{\tilde{\chi}^0_1 \nu_n \tilde{\nu}_m} = G^\nu_{nm1}$,

$$\lambda_{h_i \tilde{\nu}_\ell \tilde{\nu}_m} = \begin{cases} c_g[\tilde{\nu}] s_{\alpha+\beta} \delta_{\ell m}; & h_i = h \\ -c_g[\tilde{\nu}] c_{\alpha+\beta} \delta_{\ell m}; & h_i = H \end{cases},$$

with $c_g[\tilde{\nu}] \equiv \frac{g_2 M_W}{2}(1 + t_W^2)$.

(11) $h_i = h/H$, $F = e_n$, $S = \tilde{e}_\ell$, $S' = \tilde{e}_m$.

$$\xi_{LL} = \lambda_{h_i \tilde{e}_\ell \tilde{e}_m} \mathcal{G}^L_{e_n \tilde{e}_m \tilde{\chi}^0_1} \mathcal{G}^{R*}_{e_n \tilde{e}_\ell \tilde{\chi}^0_1},$$
$$\xi_{LR} = \lambda_{h_i \tilde{e}_\ell \tilde{e}_m} \mathcal{G}^L_{e_n \tilde{e}_m \tilde{\chi}^0_1} \mathcal{G}^{L*}_{e_n \tilde{e}_\ell \tilde{\chi}^0_1}, \quad \text{(A21)}$$

$$\xi_{RL} = \lambda_{h_i \tilde{e}_\ell \tilde{e}_m} \mathcal{G}^R_{e_n \tilde{e}_m \tilde{\chi}^0_1} \mathcal{G}^{R*}_{e_n \tilde{e}_\ell \tilde{\chi}^0_1},$$
$$\xi_{RR} = \lambda_{h_i \tilde{e}_\ell \tilde{e}_m} \mathcal{G}^R_{e_n \tilde{e}_m \tilde{\chi}^0_1} \mathcal{G}^{L*}_{e_n \tilde{e}_\ell \tilde{\chi}^0_1}, \quad \text{(A22)}$$

where $n = 1, 2, 3$; $\ell, m = 1, \ldots, 6$; $\mathcal{G}^L_{e_n \tilde{e}_m \tilde{\chi}^0_1} = G^{e_L}_{nm1}$, $\mathcal{G}^R_{e_n \tilde{e}_m \tilde{\chi}^0_1} = G^{e_R}_{nm1}$, and

$$\lambda_{h_i \tilde{e}_\ell \tilde{e}_m} = \begin{cases} -c_A[\tilde{e}_\ell, \tilde{e}_m] s_\alpha + c_\mu[\tilde{e}_\ell, \tilde{e}_m] c_\alpha + c_g[\tilde{e}_\ell, \tilde{e}_m] s_{\alpha+\beta}; & h_i = h \\ c_A[\tilde{e}_\ell, \tilde{e}_m] c_\alpha + c_\mu[\tilde{e}_\ell, \tilde{e}_m] s_\alpha - c_g[\tilde{e}_\ell, \tilde{e}_m] c_{\alpha+\beta}; & h_i = H \end{cases},$$

where

$$c_A[\tilde{e}_\ell, \tilde{e}_m] \equiv \frac{g_2}{M_W c_\beta} \left\{ -\sum_{i=1}^{3} m^2_{e_i} [W^{\tilde{e}*}_{i\ell} W^{\tilde{e}}_{im} + W^{\tilde{e}*}_{i+3\ell} W^{\tilde{e}}_{i+3m}] + \frac{1}{2} \sum_{i,j=1}^{3} [(\mathbf{m_e A^e}^\dagger)_{ij} W^{\tilde{e}*}_{i\ell} W^{\tilde{e}}_{j+3m} + (\mathbf{m_e A^e})_{ij} W^{\tilde{e}*}_{j+3\ell} W^{\tilde{e}}_{im}] \right\},$$

$$c_\mu[\tilde{e}_\ell, \tilde{e}_m] \equiv \frac{g_2}{2 M_W c_\beta} \sum_{i=1}^{3} m_{e_i} [\mu \widetilde{W^{e*}_{i\ell}} W^{\tilde{e}}_{i+3m} + \mu^* \widetilde{W^{e*}_{i+3\ell}} W^{\tilde{e}}_{im}],$$

$$c_\mu[\tilde{e}_\ell, \tilde{e}_m] \equiv \frac{g_2 M_W}{2} \sum_{i=1}^{3} [\widetilde{W^{e*}_{i\ell}} W^{\tilde{e}}_{im} (t_W^2 - 1) - 2 t_W^2 \widetilde{W^{e*}_{i+3\ell}} W^{\tilde{e}}_{i+3m}].$$

Topology-1(b):

(1) $h_i = h/H$, $S = h/H$, $F = \tilde{\chi}^0_\ell$, $F' = \tilde{\chi}^0_n$.

$$\zeta_{LLL} = \mathcal{G}^L_{\tilde{\chi}^0_1 \tilde{\chi}^0_n h_i} \mathcal{G}^L_{\tilde{\chi}^0_\ell \tilde{\chi}^0_n h_i} \mathcal{G}^{R*}_{\tilde{\chi}^0_1 \tilde{\chi}^0_\ell h_i}, \qquad \zeta_{LLR} = \mathcal{G}^L_{\tilde{\chi}^0_1 \tilde{\chi}^0_n h_i} \mathcal{G}^L_{\tilde{\chi}^0_\ell \tilde{\chi}^0_n h_i} \mathcal{G}^{L*}_{\tilde{\chi}^0_1 \tilde{\chi}^0_\ell h_i},$$
$$\zeta_{LRL} = \mathcal{G}^L_{\tilde{\chi}^0_1 \tilde{\chi}^0_n h_i} \mathcal{G}^R_{\tilde{\chi}^0_\ell \tilde{\chi}^0_n h_i} \mathcal{G}^{R*}_{\tilde{\chi}^0_1 \tilde{\chi}^0_\ell h_i}, \qquad \zeta_{LRR} = \mathcal{G}^L_{\tilde{\chi}^0_1 \tilde{\chi}^0_n h_i} \mathcal{G}^R_{\tilde{\chi}^0_\ell \tilde{\chi}^0_n h_i} \mathcal{G}^{L*}_{\tilde{\chi}^0_1 \tilde{\chi}^0_\ell h_i},$$
$$\zeta_{RLL} = \mathcal{G}^R_{\tilde{\chi}^0_1 \tilde{\chi}^0_n h_i} \mathcal{G}^L_{\tilde{\chi}^0_\ell \tilde{\chi}^0_n h_i} \mathcal{G}^{R*}_{\tilde{\chi}^0_1 \tilde{\chi}^0_\ell h_i}, \qquad \zeta_{RLR} = \mathcal{G}^R_{\tilde{\chi}^0_1 \tilde{\chi}^0_n h_i} \mathcal{G}^L_{\tilde{\chi}^0_\ell \tilde{\chi}^0_n h_i} \mathcal{G}^{L*}_{\tilde{\chi}^0_1 \tilde{\chi}^0_\ell h_i},$$
$$\zeta_{RRL} = \mathcal{G}^R_{\tilde{\chi}^0_1 \tilde{\chi}^0_n h_i} \mathcal{G}^R_{\tilde{\chi}^0_\ell \tilde{\chi}^0_n h_i} \mathcal{G}^{R*}_{\tilde{\chi}^0_1 \tilde{\chi}^0_\ell h_i}, \qquad \zeta_{RRR} = \mathcal{G}^R_{\tilde{\chi}^0_1 \tilde{\chi}^0_n h_i} \mathcal{G}^R_{\tilde{\chi}^0_\ell \tilde{\chi}^0_n h_i} \mathcal{G}^{L*}_{\tilde{\chi}^0_1 \tilde{\chi}^0_\ell h_i},$$

where

$$\mathcal{G}^{L}_{\tilde{\chi}^0_\ell \tilde{\chi}^0_n h_i} = \begin{cases} g_2(Q''^{*}_{\ell n} s_\alpha + S''^{*}_{\ell n} c_\alpha); & h_i = h \\ -g_2(Q''^{*}_{\ell n} c_\alpha - S''^{*}_{\ell n} s_\alpha); & h_i = H \end{cases}$$

and

$$\mathcal{G}^{R}_{\tilde{\chi}^0_\ell \tilde{\chi}^0_n h_i} = \begin{cases} g_2(Q''_{n\ell} s_\alpha + S''_{n\ell} c_\alpha); & h_i = h \\ -g_2(Q''_{n\ell} c_\alpha - S''_{n\ell} s_\alpha); & h_i = H \end{cases}.$$

(2) $h_i = h/H$, $S = A$, $F = \tilde{\chi}^0_\ell$, $F' = \tilde{\chi}^0_n$.

$$\begin{aligned}
\zeta_{LLL} &= \mathcal{G}^{L}_{\tilde{\chi}^0_1 \tilde{\chi}^0_n A} \mathcal{G}^{L}_{\tilde{\chi}^0_\ell \tilde{\chi}^0_n h_i} \mathcal{G}^{R*}_{\tilde{\chi}^0_1 \tilde{\chi}^0_\ell A}, & \zeta_{LLR} &= \mathcal{G}^{L}_{\tilde{\chi}^0_1 \tilde{\chi}^0_n A} \mathcal{G}^{L}_{\tilde{\chi}^0_\ell \tilde{\chi}^0_n h_i} \mathcal{G}^{L*}_{\tilde{\chi}^0_1 \tilde{\chi}^0_\ell A}, \\
\zeta_{LRL} &= \mathcal{G}^{L}_{\tilde{\chi}^0_1 \tilde{\chi}^0_n A} \mathcal{G}^{R}_{\tilde{\chi}^0_\ell \tilde{\chi}^0_n h_i} \mathcal{G}^{R*}_{\tilde{\chi}^0_1 \tilde{\chi}^0_\ell A}, & \zeta_{LRR} &= \mathcal{G}^{L}_{\tilde{\chi}^0_1 \tilde{\chi}^0_n A} \mathcal{G}^{R}_{\tilde{\chi}^0_\ell \tilde{\chi}^0_n h_i} \mathcal{G}^{L*}_{\tilde{\chi}^0_1 \tilde{\chi}^0_\ell A}, \\
\zeta_{RLL} &= \mathcal{G}^{R}_{\tilde{\chi}^0_1 \tilde{\chi}^0_n A} \mathcal{G}^{L}_{\tilde{\chi}^0_\ell \tilde{\chi}^0_n h_i} \mathcal{G}^{R*}_{\tilde{\chi}^0_1 \tilde{\chi}^0_\ell A}, & \zeta_{RLR} &= \mathcal{G}^{R}_{\tilde{\chi}^0_1 \tilde{\chi}^0_n A} \mathcal{G}^{L}_{\tilde{\chi}^0_\ell \tilde{\chi}^0_n h_i} \mathcal{G}^{L*}_{\tilde{\chi}^0_1 \tilde{\chi}^0_\ell A}, \\
\zeta_{RRL} &= \mathcal{G}^{R}_{\tilde{\chi}^0_1 \tilde{\chi}^0_n A} \mathcal{G}^{R}_{\tilde{\chi}^0_\ell \tilde{\chi}^0_n h_i} \mathcal{G}^{R*}_{\tilde{\chi}^0_1 \tilde{\chi}^0_\ell A}, & \zeta_{RRR} &= \mathcal{G}^{R}_{\tilde{\chi}^0_1 \tilde{\chi}^0_n A} \mathcal{G}^{R}_{\tilde{\chi}^0_\ell \tilde{\chi}^0_n h_i} \mathcal{G}^{L*}_{\tilde{\chi}^0_1 \tilde{\chi}^0_\ell A},
\end{aligned}$$

where $\mathcal{G}^{L}_{\tilde{\chi}^0_1 \tilde{\chi}^0_n A} = i(Q''^{*}_{n1} s_\beta - S''^{*}_{n1} c_\beta)$ and $\mathcal{G}^{R}_{\tilde{\chi}^0_1 \tilde{\chi}^0_n A} = i(-Q''_{1n} s_\beta + S''_{1n} c_\beta)$.

(3) $h_i = h/H$, $S = G$, $F = \tilde{\chi}^0_\ell$, $F' = \tilde{\chi}^0_n$.

$$\begin{aligned}
\zeta_{LLL} &= \mathcal{G}^{L}_{\tilde{\chi}^0_1 \tilde{\chi}^0_n G} \mathcal{G}^{L}_{\tilde{\chi}^0_\ell \tilde{\chi}^0_n h_i} \mathcal{G}^{R*}_{\tilde{\chi}^0_1 \tilde{\chi}^0_\ell G}, & \zeta_{LLR} &= \mathcal{G}^{L}_{\tilde{\chi}^0_1 \tilde{\chi}^0_n G} \mathcal{G}^{L}_{\tilde{\chi}^0_\ell \tilde{\chi}^0_n h_i} \mathcal{G}^{L*}_{\tilde{\chi}^0_1 \tilde{\chi}^0_\ell G}, \\
\zeta_{LRL} &= \mathcal{G}^{L}_{\tilde{\chi}^0_1 \tilde{\chi}^0_n G} \mathcal{G}^{R}_{\tilde{\chi}^0_\ell \tilde{\chi}^0_n h_i} \mathcal{G}^{R*}_{\tilde{\chi}^0_1 \tilde{\chi}^0_\ell G}, & \zeta_{LRR} &= \mathcal{G}^{L}_{\tilde{\chi}^0_1 \tilde{\chi}^0_n G} \mathcal{G}^{R}_{\tilde{\chi}^0_\ell \tilde{\chi}^0_n h_i} \mathcal{G}^{L*}_{\tilde{\chi}^0_1 \tilde{\chi}^0_\ell G}, \\
\zeta_{RLL} &= \mathcal{G}^{R}_{\tilde{\chi}^0_1 \tilde{\chi}^0_n G} \mathcal{G}^{L}_{\tilde{\chi}^0_\ell \tilde{\chi}^0_n h_i} \mathcal{G}^{R*}_{\tilde{\chi}^0_1 \tilde{\chi}^0_\ell G}, & \zeta_{RLR} &= \mathcal{G}^{R}_{\tilde{\chi}^0_1 \tilde{\chi}^0_n G} \mathcal{G}^{L}_{\tilde{\chi}^0_\ell \tilde{\chi}^0_n h_i} \mathcal{G}^{L*}_{\tilde{\chi}^0_1 \tilde{\chi}^0_\ell G}, \\
\zeta_{RRL} &= \mathcal{G}^{R}_{\tilde{\chi}^0_1 \tilde{\chi}^0_n G} \mathcal{G}^{R}_{\tilde{\chi}^0_\ell \tilde{\chi}^0_n h_i} \mathcal{G}^{R*}_{\tilde{\chi}^0_1 \tilde{\chi}^0_\ell G}, & \zeta_{RRR} &= \mathcal{G}^{R}_{\tilde{\chi}^0_1 \tilde{\chi}^0_n G} \mathcal{G}^{R}_{\tilde{\chi}^0_\ell \tilde{\chi}^0_n h_i} \mathcal{G}^{L*}_{\tilde{\chi}^0_1 \tilde{\chi}^0_\ell G}.
\end{aligned}$$

(4) $h_i = h/H$, $S = H^\pm$, $F = \tilde{\chi}^\pm_\ell$, $F' = \tilde{\chi}^\pm_n$.

$$\begin{aligned}
\zeta_{LLL} &= \mathcal{G}^{L}_{\tilde{\chi}^0_1 \tilde{\chi}^\pm_n H^\pm} \mathcal{G}^{L}_{\tilde{\chi}^\pm_\ell \tilde{\chi}^\pm_n h_i} \mathcal{G}^{R*}_{\tilde{\chi}^0_1 \tilde{\chi}^\pm_\ell H^\pm}, & \zeta_{LLR} &= \mathcal{G}^{L}_{\tilde{\chi}^0_1 \tilde{\chi}^\pm_n H^\pm} \mathcal{G}^{L}_{\tilde{\chi}^\pm_\ell \tilde{\chi}^\pm_n h_i} \mathcal{G}^{L*}_{\tilde{\chi}^0_1 \tilde{\chi}^\pm_\ell H^\pm}, \\
\zeta_{LRL} &= \mathcal{G}^{L}_{\tilde{\chi}^0_1 \tilde{\chi}^\pm_n H^\pm} \mathcal{G}^{R}_{\tilde{\chi}^\pm_\ell \tilde{\chi}^\pm_n h_i} \mathcal{G}^{R*}_{\tilde{\chi}^0_1 \tilde{\chi}^\pm_\ell H^\pm}, & \zeta_{LRR} &= \mathcal{G}^{L}_{\tilde{\chi}^0_1 \tilde{\chi}^\pm_n H^\pm} \mathcal{G}^{R}_{\tilde{\chi}^\pm_\ell \tilde{\chi}^\pm_n h_i} \mathcal{G}^{L*}_{\tilde{\chi}^0_1 \tilde{\chi}^\pm_\ell H^\pm}, \\
\zeta_{RLL} &= \mathcal{G}^{R}_{\tilde{\chi}^0_1 \tilde{\chi}^\pm_n H^\pm} \mathcal{G}^{L}_{\tilde{\chi}^\pm_\ell \tilde{\chi}^\pm_n h_i} \mathcal{G}^{R*}_{\tilde{\chi}^0_1 \tilde{\chi}^\pm_\ell H^\pm}, & \zeta_{RLR} &= \mathcal{G}^{R}_{\tilde{\chi}^0_1 \tilde{\chi}^\pm_n H^\pm} \mathcal{G}^{L}_{\tilde{\chi}^\pm_\ell \tilde{\chi}^\pm_n h_i} \mathcal{G}^{L*}_{\tilde{\chi}^0_1 \tilde{\chi}^\pm_\ell H^\pm}, \\
\zeta_{RRL} &= \mathcal{G}^{R}_{\tilde{\chi}^0_1 \tilde{\chi}^\pm_n H^\pm} \mathcal{G}^{R}_{\tilde{\chi}^\pm_\ell \tilde{\chi}^\pm_n h_i} \mathcal{G}^{R*}_{\tilde{\chi}^0_1 \tilde{\chi}^\pm_\ell H^\pm}, & \zeta_{RRR} &= \mathcal{G}^{R}_{\tilde{\chi}^0_1 \tilde{\chi}^\pm_n H^\pm} \mathcal{G}^{R}_{\tilde{\chi}^\pm_\ell \tilde{\chi}^\pm_n h_i} \mathcal{G}^{L*}_{\tilde{\chi}^0_1 \tilde{\chi}^\pm_\ell H^\pm}.
\end{aligned}$$

(5) $h_i = h/H$, $S = G^\pm$, $F = \tilde{\chi}^\pm_\ell$, $F' = \tilde{\chi}^\pm_n$.

$$\begin{aligned}
\zeta_{LLL} &= \mathcal{G}^{L}_{\tilde{\chi}^0_1 \tilde{\chi}^\pm_n G^\pm} \mathcal{G}^{L}_{\tilde{\chi}^\pm_\ell \tilde{\chi}^\pm_n h_i} \mathcal{G}^{R*}_{\tilde{\chi}^0_1 \tilde{\chi}^\pm_\ell G^\pm}, & \zeta_{LLR} &= \mathcal{G}^{L}_{\tilde{\chi}^0_1 \tilde{\chi}^\pm_n G^\pm} \mathcal{G}^{L}_{\tilde{\chi}^\pm_\ell \tilde{\chi}^\pm_n h_i} \mathcal{G}^{L*}_{\tilde{\chi}^0_1 \tilde{\chi}^\pm_\ell G^\pm}, \\
\zeta_{LRL} &= \mathcal{G}^{L}_{\tilde{\chi}^0_1 \tilde{\chi}^\pm_n G^\pm} \mathcal{G}^{R}_{\tilde{\chi}^\pm_\ell \tilde{\chi}^\pm_n h_i} \mathcal{G}^{R*}_{\tilde{\chi}^0_1 \tilde{\chi}^\pm_\ell G^\pm}, & \zeta_{LRR} &= \mathcal{G}^{L}_{\tilde{\chi}^0_1 \tilde{\chi}^\pm_n G^\pm} \mathcal{G}^{R}_{\tilde{\chi}^\pm_\ell \tilde{\chi}^\pm_n h_i} \mathcal{G}^{L*}_{\tilde{\chi}^0_1 \tilde{\chi}^\pm_\ell G^\pm}, \\
\zeta_{RLL} &= \mathcal{G}^{R}_{\tilde{\chi}^0_1 \tilde{\chi}^\pm_n G^\pm} \mathcal{G}^{L}_{\tilde{\chi}^\pm_\ell \tilde{\chi}^\pm_n h_i} \mathcal{G}^{R*}_{\tilde{\chi}^0_1 \tilde{\chi}^\pm_\ell G^\pm}, & \zeta_{RLR} &= \mathcal{G}^{R}_{\tilde{\chi}^0_1 \tilde{\chi}^\pm_n G^\pm} \mathcal{G}^{L}_{\tilde{\chi}^\pm_\ell \tilde{\chi}^\pm_n h_i} \mathcal{G}^{L*}_{\tilde{\chi}^0_1 \tilde{\chi}^\pm_\ell G^\pm}, \\
\zeta_{RRL} &= \mathcal{G}^{R}_{\tilde{\chi}^0_1 \tilde{\chi}^\pm_n G^\pm} \mathcal{G}^{R}_{\tilde{\chi}^\pm_\ell \tilde{\chi}^\pm_n h_i} \mathcal{G}^{R*}_{\tilde{\chi}^0_1 \tilde{\chi}^\pm_\ell G^\pm}, & \zeta_{RRR} &= \mathcal{G}^{R}_{\tilde{\chi}^0_1 \tilde{\chi}^\pm_n G^\pm} \mathcal{G}^{R}_{\tilde{\chi}^\pm_\ell \tilde{\chi}^\pm_n h_i} \mathcal{G}^{L*}_{\tilde{\chi}^0_1 \tilde{\chi}^\pm_\ell G^\pm}.
\end{aligned}$$

(6) $h_i = h/H$, $S = \tilde{e}_m$, $F = e_\ell$, $F' = e_n$.

$$\zeta_{LLL} = \mathcal{G}^L_{\tilde{\chi}^0_1 \tilde{e}_m e_n} \mathcal{G}^L_{e_\ell e_n h_i} \mathcal{G}^{R*}_{\tilde{\chi}^0_1 \tilde{e}_m e_\ell}, \qquad \zeta_{LLR} = \mathcal{G}^L_{\tilde{\chi}^0_1 \tilde{e}_m e_n} \mathcal{G}^L_{e_\ell e_n h_i} \mathcal{G}^{L*}_{\tilde{\chi}^0_1 \tilde{e}_m e_\ell},$$
$$\zeta_{LRL} = \mathcal{G}^L_{\tilde{\chi}^0_1 \tilde{e}_m e_n} \mathcal{G}^R_{e_\ell e_n h_i} \mathcal{G}^{R*}_{\tilde{\chi}^0_1 \tilde{e}_m e_\ell}, \qquad \zeta_{LRR} = \mathcal{G}^L_{\tilde{\chi}^0_1 \tilde{e}_m e_n} \mathcal{G}^R_{e_\ell e_n h_i} \mathcal{G}^{L*}_{\tilde{\chi}^0_1 \tilde{e}_m e_\ell},$$
$$\zeta_{RLL} = \mathcal{G}^R_{\tilde{\chi}^0_1 \tilde{e}_m e_n} \mathcal{G}^L_{e_\ell e_n h_i} \mathcal{G}^{R*}_{\tilde{\chi}^0_1 \tilde{e}_m e_\ell}, \qquad \zeta_{RLR} = \mathcal{G}^R_{\tilde{\chi}^0_1 \tilde{e}_m e_n} \mathcal{G}^L_{e_\ell e_n h_i} \mathcal{G}^{L*}_{\tilde{\chi}^0_1 \tilde{e}_m e_\ell},$$
$$\zeta_{RRL} = \mathcal{G}^R_{\tilde{\chi}^0_1 \tilde{e}_m e_n} \mathcal{G}^R_{e_\ell e_n h_i} \mathcal{G}^{R*}_{\tilde{\chi}^0_1 \tilde{e}_m e_\ell}, \qquad \zeta_{RRR} = \mathcal{G}^R_{\tilde{\chi}^0_1 \tilde{e}_m e_n} \mathcal{G}^R_{e_\ell e_n h_i} \mathcal{G}^{L*}_{\tilde{\chi}^0_1 \tilde{e}_m e_\ell},$$

where $\ell, n = 1, 2, 3$; $m = 1, \ldots, 6$; $\mathcal{G}^L_{\tilde{\chi}^0_1 \tilde{e}_m e_n} = G^{e_L}_{nm1}$, $\mathcal{G}^R_{\tilde{\chi}^0_1 \tilde{e}_m e_n} = G^{e_R}_{nm1}$.

Topology-1(c):

(1) $h_i = h/H$, $F = \tilde{\chi}^0_\ell$, $F' = \tilde{\chi}^0_n$, $V = Z$.

$$\Lambda_{LLL} = \mathcal{G}^L_{\tilde{\chi}^0_1 \tilde{\chi}^0_n Z} \mathcal{G}^L_{\tilde{\chi}^0_\ell \tilde{\chi}^0_n h_i} \mathcal{G}^{L*}_{\tilde{\chi}^0_1 \tilde{\chi}^0_\ell Z}, \qquad \Lambda_{LLR} = -\mathcal{G}^L_{\tilde{\chi}^0_1 \tilde{\chi}^0_n Z} \mathcal{G}^L_{\tilde{\chi}^0_\ell \tilde{\chi}^0_n h_i} \mathcal{G}^L_{\tilde{\chi}^0_1 \tilde{\chi}^0_\ell Z},$$
$$\Lambda_{LRL} = \mathcal{G}^L_{\tilde{\chi}^0_1 \tilde{\chi}^0_n Z} \mathcal{G}^R_{\tilde{\chi}^0_\ell \tilde{\chi}^0_n h_i} \mathcal{G}^{L*}_{\tilde{\chi}^0_1 \tilde{\chi}^0_\ell Z}, \qquad \Lambda_{LRR} = -\mathcal{G}^L_{\tilde{\chi}^0_1 \tilde{\chi}^0_n Z} \mathcal{G}^R_{\tilde{\chi}^0_\ell \tilde{\chi}^0_n h_i} \mathcal{G}^L_{\tilde{\chi}^0_1 \tilde{\chi}^0_\ell Z},$$
$$\Lambda_{RLL} = \mathcal{G}^R_{\tilde{\chi}^0_1 \tilde{\chi}^0_n Z} \mathcal{G}^L_{\tilde{\chi}^0_\ell \tilde{\chi}^0_n h_i} \mathcal{G}^{L*}_{\tilde{\chi}^0_1 \tilde{\chi}^0_\ell Z}, \qquad \Lambda_{RLR} = -\mathcal{G}^R_{\tilde{\chi}^0_1 \tilde{\chi}^0_n Z} \mathcal{G}^L_{\tilde{\chi}^0_\ell \tilde{\chi}^0_n h_i} \mathcal{G}^L_{\tilde{\chi}^0_1 \tilde{\chi}^0_\ell Z},$$
$$\Lambda_{RRL} = \mathcal{G}^R_{\tilde{\chi}^0_1 \tilde{\chi}^0_n Z} \mathcal{G}^R_{\tilde{\chi}^0_\ell \tilde{\chi}^0_n h_i} \mathcal{G}^{L*}_{\tilde{\chi}^0_1 \tilde{\chi}^0_\ell Z}, \qquad \Lambda_{RRR} = -\mathcal{G}^R_{\tilde{\chi}^0_1 \tilde{\chi}^0_n Z} \mathcal{G}^R_{\tilde{\chi}^0_\ell \tilde{\chi}^0_n h_i} \mathcal{G}^L_{\tilde{\chi}^0_1 \tilde{\chi}^0_\ell Z},$$

where $\mathcal{G}^L_{\tilde{\chi}^0_\ell \tilde{\chi}^0_n Z} = \frac{g_2}{c_W} N^L_{\ell n}$ and $\mathcal{G}^R_{\tilde{\chi}^0_\ell \tilde{\chi}^0_n Z} = \frac{g_2}{c_W} N^R_{\ell n}$.

(2) $h_i = h/H$, $F = \tilde{\chi}^\pm_\ell$, $F' = \tilde{\chi}^\pm_n$, $V = W^\pm$

$$\Lambda_{LLL} = \mathcal{G}^L_{\tilde{\chi}^0_1 \tilde{\chi}^\pm_n W^\pm} \mathcal{G}^L_{\tilde{\chi}^\pm_\ell \tilde{\chi}^\pm_n h_i} \mathcal{G}^{R*}_{\tilde{\chi}^0_1 \tilde{\chi}^\pm_\ell W^\pm}, \qquad \Lambda_{LLR} = \mathcal{G}^L_{\tilde{\chi}^0_1 \tilde{\chi}^\pm_n W^\pm} \mathcal{G}^L_{\tilde{\chi}^\pm_\ell \tilde{\chi}^\pm_n h_i} \mathcal{G}^{L*}_{\tilde{\chi}^0_1 \tilde{\chi}^\pm_\ell W^\pm},$$
$$\Lambda_{LRL} = \mathcal{G}^L_{\tilde{\chi}^0_1 \tilde{\chi}^\pm_n W^\pm} \mathcal{G}^R_{\tilde{\chi}^\pm_\ell \tilde{\chi}^\pm_n h_i} \mathcal{G}^{R*}_{\tilde{\chi}^0_1 \tilde{\chi}^\pm_\ell W^\pm}, \qquad \Lambda_{LRR} = \mathcal{G}^L_{\tilde{\chi}^0_1 \tilde{\chi}^\pm_n W^\pm} \mathcal{G}^R_{\tilde{\chi}^\pm_\ell \tilde{\chi}^\pm_n h_i} \mathcal{G}^{L*}_{\tilde{\chi}^0_1 \tilde{\chi}^\pm_\ell W^\pm},$$
$$\Lambda_{RLL} = \mathcal{G}^R_{\tilde{\chi}^0_1 \tilde{\chi}^\pm_n W^\pm} \mathcal{G}^L_{\tilde{\chi}^\pm_\ell \tilde{\chi}^\pm_n h_i} \mathcal{G}^{R*}_{\tilde{\chi}^0_1 \tilde{\chi}^\pm_\ell W^\pm}, \qquad \Lambda_{RLR} = \mathcal{G}^R_{\tilde{\chi}^0_1 \tilde{\chi}^\pm_n W^\pm} \mathcal{G}^L_{\tilde{\chi}^\pm_\ell \tilde{\chi}^\pm_n h_i} \mathcal{G}^{L*}_{\tilde{\chi}^0_1 \tilde{\chi}^\pm_\ell W^\pm},$$
$$\Lambda_{RRL} = \mathcal{G}^R_{\tilde{\chi}^0_1 \tilde{\chi}^\pm_n W^\pm} \mathcal{G}^R_{\tilde{\chi}^\pm_\ell \tilde{\chi}^\pm_n h_i} \mathcal{G}^{R*}_{\tilde{\chi}^0_1 \tilde{\chi}^\pm_\ell W^\pm}, \qquad \Lambda_{RRR} = \mathcal{G}^R_{\tilde{\chi}^0_1 \tilde{\chi}^\pm_n W^\pm} \mathcal{G}^R_{\tilde{\chi}^\pm_\ell \tilde{\chi}^\pm_n h_i} \mathcal{G}^{L*}_{\tilde{\chi}^0_1 \tilde{\chi}^\pm_\ell W^\pm},$$

where $\mathcal{G}^L_{\tilde{\chi}^0_\ell \tilde{\chi}^\pm_n W^\pm} = g_2 C^L_{\ell n}$ and $\mathcal{G}^R_{\tilde{\chi}^0_\ell \tilde{\chi}^\pm_n W^\pm} = g_2 C^R_{\ell n}$.

Topology-1(d):

(1) $h_i = h/H$, $F = \tilde{\chi}^0_\ell$, $V = Z$.

$$\eta_{LL} = \mathcal{G}_{ZZh_i} \mathcal{G}^L_{\tilde{\chi}^0_1 \tilde{\chi}^0_\ell Z} \mathcal{G}^{L*}_{\tilde{\chi}^0_1 \tilde{\chi}^0_\ell Z}, \qquad \eta_{LR} = -\mathcal{G}_{ZZh_i} \mathcal{G}^L_{\tilde{\chi}^0_1 \tilde{\chi}^0_\ell Z} \mathcal{G}^L_{\tilde{\chi}^0_1 \tilde{\chi}^0_\ell Z},$$
$$\eta_{RL} = \mathcal{G}_{ZZh_i} \mathcal{G}^R_{\tilde{\chi}^0_1 \tilde{\chi}^0_\ell Z} \mathcal{G}^{L*}_{\tilde{\chi}^0_1 \tilde{\chi}^0_\ell Z}, \qquad \eta_{RR} = -\mathcal{G}_{ZZh_i} \mathcal{G}^R_{\tilde{\chi}^0_1 \tilde{\chi}^0_\ell Z} \mathcal{G}^L_{\tilde{\chi}^0_1 \tilde{\chi}^0_\ell Z},$$

where $\mathcal{G}_{ZZh_i} = g_2 M_Z g^{\mu\nu} Y_{h_i}$, with

$$Y_{h_i} = \begin{cases} \frac{s_{\beta-\alpha}}{c_W}; & h_i = h \\ \frac{c_{\beta-\alpha}}{c_W}; & h_i = H \end{cases}.$$

(2) $h_i = h/H$, $F = \tilde{\chi}^\pm_\ell$, $V = W^\pm$.

$$\eta_{LL} = \mathcal{G}_{W^\pm W^\pm h_i} \mathcal{G}^L_{\tilde{\chi}^0_1 \tilde{\chi}^\pm_\ell W^\pm} \mathcal{G}^{R*}_{\tilde{\chi}^0_1 \tilde{\chi}^\pm_\ell W^\pm}, \qquad \eta_{LR} = \mathcal{G}_{W^\pm W^\pm h_i} \mathcal{G}^L_{\tilde{\chi}^0_1 \tilde{\chi}^\pm_\ell W^\pm} \mathcal{G}^{L*}_{\tilde{\chi}^0_1 \tilde{\chi}^\pm_\ell W^\pm},$$
$$\eta_{RL} = \mathcal{G}_{W^\pm W^\pm h_i} \mathcal{G}^R_{\tilde{\chi}^0_1 \tilde{\chi}^\pm_\ell W^\pm} \mathcal{G}^{R*}_{\tilde{\chi}^0_1 \tilde{\chi}^\pm_\ell W^\pm}, \qquad \eta_{RR} = \mathcal{G}_{W^\pm W^\pm h_i} \mathcal{G}^R_{\tilde{\chi}^0_1 \tilde{\chi}^\pm_\ell W^\pm} \mathcal{G}^{L*}_{\tilde{\chi}^0_1 \tilde{\chi}^\pm_\ell W^\pm},$$

where $\mathcal{G}_{W^\pm W^\pm h_i} = g_2 M_W g^{\mu\nu} Y'_{h_i}$, with

$$Y'_{h_i} = \begin{cases} s_{\beta-\alpha}; & h_i = h \\ c_{\beta-\alpha}; & h_i = H \end{cases}.$$

Topology-1(e):

(1) $h_i = h/H$, $F = \tilde{\chi}^0_\ell$, $S = A$, $V = Z$.

$$\psi_{LL} = \mathcal{G}_{h_iAZ}\mathcal{G}^L_{\tilde{\chi}^0_1\tilde{\chi}^0_\ell Z}\mathcal{G}^{R*}_{\tilde{\chi}^0_1\tilde{\chi}^0_\ell A},$$
$$\psi_{LR} = \mathcal{G}_{h_iAZ}\mathcal{G}^L_{\tilde{\chi}^0_1\tilde{\chi}^0_\ell Z}\mathcal{G}^{L*}_{\tilde{\chi}^0_1\tilde{\chi}^0_\ell A},$$
$$\psi_{RL} = \mathcal{G}_{h_iAZ}\mathcal{G}^R_{\tilde{\chi}^0_1\tilde{\chi}^0_\ell Z}\mathcal{G}^{R*}_{\tilde{\chi}^0_1\tilde{\chi}^0_\ell A},$$
$$\psi_{RR} = \mathcal{G}_{h_iAZ}\mathcal{G}^R_{\tilde{\chi}^0_1\tilde{\chi}^0_\ell Z}\mathcal{G}^{L*}_{\tilde{\chi}^0_1\tilde{\chi}^0_\ell A},$$

where $\mathcal{G}_{h_iAZ} = \frac{g_2}{2c_W}Y''_{h_i}$, with

$$Y''_{h_i} = \begin{cases} c_{\beta-\alpha}; & h_i = h \\ -s_{\beta-\alpha}; & h_i = H \end{cases}.$$

(2) $h_i = h/H$, $F = \tilde{\chi}^0_\ell$, $S = G$, $V = Z$.

$$\psi_{LL} = \mathcal{G}_{h_iGZ}\mathcal{G}^L_{\tilde{\chi}^0_1\tilde{\chi}^0_\ell Z}\mathcal{G}^{R*}_{\tilde{\chi}^0_1\tilde{\chi}^0_\ell G},$$
$$\psi_{LR} = \mathcal{G}_{h_iGZ}\mathcal{G}^L_{\tilde{\chi}^0_1\tilde{\chi}^0_\ell Z}\mathcal{G}^{L*}_{\tilde{\chi}^0_1\tilde{\chi}^0_\ell G},$$
$$\psi_{RL} = \mathcal{G}_{h_iGZ}\mathcal{G}^R_{\tilde{\chi}^0_1\tilde{\chi}^0_\ell Z}\mathcal{G}^{R*}_{\tilde{\chi}^0_1\tilde{\chi}^0_\ell G},$$
$$\psi_{RR} = \mathcal{G}_{h_iGZ}\mathcal{G}^R_{\tilde{\chi}^0_1\tilde{\chi}^0_\ell Z}\mathcal{G}^{L*}_{\tilde{\chi}^0_1\tilde{\chi}^0_\ell G},$$

where

$$\mathcal{G}_{h_iGZ} = \begin{cases} \frac{g_2}{2c_W}s_{\beta-\alpha}; & h_i = h \\ \frac{g_2}{2c_W}c_{\beta-\alpha}; & h_i = H \end{cases}.$$

(3) $h_i = h/H$, $F = \tilde{\chi}^\pm_\ell$, $S = H^\pm$, $V = W^\pm$.

$$\psi_{LL} = \mathcal{G}_{h_iH^\pm W^\pm}\mathcal{G}^L_{\tilde{\chi}^0_1\tilde{\chi}^\pm_\ell W^\pm}\mathcal{G}^{R*}_{\tilde{\chi}^0_1\tilde{\chi}^\pm_\ell H^\pm},$$
$$\psi_{LR} = \mathcal{G}_{h_iH^\pm W^\pm}\mathcal{G}^L_{\tilde{\chi}^0_1\tilde{\chi}^\pm_\ell W^\pm}\mathcal{G}^{L*}_{\tilde{\chi}^0_1\tilde{\chi}^\pm_\ell H^\pm},$$
$$\psi_{RL} = \mathcal{G}_{h_iH^\pm W^\pm}\mathcal{G}^R_{\tilde{\chi}^0_1\tilde{\chi}^\pm_\ell W^\pm}\mathcal{G}^{R*}_{\tilde{\chi}^0_1\tilde{\chi}^\pm_\ell H^\pm},$$
$$\psi_{RR} = \mathcal{G}_{h_iH^\pm W^\pm}\mathcal{G}^R_{\tilde{\chi}^0_1\tilde{\chi}^\pm_\ell W^\pm}\mathcal{G}^{L*}_{\tilde{\chi}^0_1\tilde{\chi}^\pm_\ell H^\pm},$$

where $\mathcal{G}_{h_iH^\pm W^\pm} = \frac{g_2}{2}Y''_{h_i}$.

(4) $h_i = h/H$, $F = \tilde{\chi}^\pm_\ell$, $S = G^\pm$, $V = W^\pm$.

$$\psi_{LL} = \mathcal{G}_{h_iG^\pm W^\pm}\mathcal{G}^L_{\tilde{\chi}^0_1\tilde{\chi}^\pm_\ell W^\pm}\mathcal{G}^{R*}_{\tilde{\chi}^0_1\tilde{\chi}^\pm_\ell G^\pm},$$
$$\psi_{LR} = \mathcal{G}_{h_iG^\pm W^\pm}\mathcal{G}^L_{\tilde{\chi}^0_1\tilde{\chi}^\pm_\ell W^\pm}\mathcal{G}^{L*}_{\tilde{\chi}^0_1\tilde{\chi}^\pm_\ell G^\pm},$$
$$\psi_{RL} = \mathcal{G}_{h_iG^\pm W^\pm}\mathcal{G}^R_{\tilde{\chi}^0_1\tilde{\chi}^\pm_\ell W^\pm}\mathcal{G}^{R*}_{\tilde{\chi}^0_1\tilde{\chi}^\pm_\ell G^\pm},$$
$$\psi_{RR} = \mathcal{G}_{h_iG^\pm W^\pm}\mathcal{G}^R_{\tilde{\chi}^0_1\tilde{\chi}^\pm_\ell W^\pm}\mathcal{G}^{L*}_{\tilde{\chi}^0_1\tilde{\chi}^\pm_\ell G^\pm},$$

where

$$\mathcal{G}_{h_iG^\pm W^\pm} = \begin{cases} -\frac{g_2}{2}s_{\beta-\alpha}; & h_i = h \\ -\frac{g_2}{2}c_{\beta-\alpha}; & h_i = H \end{cases}.$$

Topology-1(f):

(1) $h_i = h/H$, $F = \tilde{\chi}^0_\ell$, $S = A$, $V = Z$.

$$\Xi_{LL} = \mathcal{G}_{h_iAZ}\mathcal{G}^L_{\tilde{\chi}^0_1\tilde{\chi}^0_\ell A}\mathcal{G}^{L*}_{\tilde{\chi}^0_1\tilde{\chi}^0_\ell Z},$$
$$\Xi_{LR} = -\mathcal{G}_{h_iAZ}\mathcal{G}^L_{\tilde{\chi}^0_1\tilde{\chi}^0_\ell A}\mathcal{G}^L_{\tilde{\chi}^0_1\tilde{\chi}^0_\ell Z},$$
$$\Xi_{RL} = \mathcal{G}_{h_iAZ}\mathcal{G}^R_{\tilde{\chi}^0_1\tilde{\chi}^0_\ell A}\mathcal{G}^{L*}_{\tilde{\chi}^0_1\tilde{\chi}^0_\ell Z},$$
$$\Xi_{RR} = -\mathcal{G}_{h_iAZ}\mathcal{G}^R_{\tilde{\chi}^0_1\tilde{\chi}^0_\ell A}\mathcal{G}^L_{\tilde{\chi}^0_1\tilde{\chi}^0_\ell Z}.$$

(2) $h_i = h/H$, $F = \tilde{\chi}^0_\ell$, $S = G$, $V = Z$.

$$\Xi_{LL} = \mathcal{G}_{h_iGZ}\mathcal{G}^L_{\tilde{\chi}^0_1\tilde{\chi}^0_\ell G}\mathcal{G}^{L*}_{\tilde{\chi}^0_1\tilde{\chi}^0_\ell Z},$$
$$\Xi_{LR} = -\mathcal{G}_{h_iGZ}\mathcal{G}^L_{\tilde{\chi}^0_1\tilde{\chi}^0_\ell G}\mathcal{G}^L_{\tilde{\chi}^0_1\tilde{\chi}^0_\ell Z},$$
$$\Xi_{RL} = \mathcal{G}_{h_iGZ}\mathcal{G}^R_{\tilde{\chi}^0_1\tilde{\chi}^0_\ell G}\mathcal{G}^{L*}_{\tilde{\chi}^0_1\tilde{\chi}^0_\ell Z},$$
$$\Xi_{RR} = -\mathcal{G}_{h_iGZ}\mathcal{G}^R_{\tilde{\chi}^0_1\tilde{\chi}^0_\ell G}\mathcal{G}^L_{\tilde{\chi}^0_1\tilde{\chi}^0_\ell Z}.$$

(3) $h_i = h/H$, $F = \tilde{\chi}^\pm_\ell$, $S = H^\pm$, $V = W^\pm$.

$$\Xi_{LL} = \mathcal{G}_{h_iH^\pm W^\pm}\mathcal{G}^L_{\tilde{\chi}^0_1\tilde{\chi}^\pm_\ell H^\pm}\mathcal{G}^{R*}_{\tilde{\chi}^0_1\tilde{\chi}^\pm_\ell W^\pm},$$
$$\Xi_{LR} = \mathcal{G}_{h_iH^\pm W^\pm}\mathcal{G}^L_{\tilde{\chi}^0_1\tilde{\chi}^\pm_\ell H^\pm}\mathcal{G}^{L*}_{\tilde{\chi}^0_1\tilde{\chi}^\pm_\ell W^\pm},$$
$$\Xi_{RL} = \mathcal{G}_{h_iH^\pm W^\pm}\mathcal{G}^R_{\tilde{\chi}^0_1\tilde{\chi}^\pm_\ell H^\pm}\mathcal{G}^{R*}_{\tilde{\chi}^0_1\tilde{\chi}^\pm_\ell W^\pm},$$
$$\Xi_{RR} = \mathcal{G}_{h_iH^\pm W^\pm}\mathcal{G}^R_{\tilde{\chi}^0_1\tilde{\chi}^\pm_\ell H^\pm}\mathcal{G}^{L*}_{\tilde{\chi}^0_1\tilde{\chi}^\pm_\ell W^\pm}.$$

(4) $h_i = h/H$, $F = \tilde{\chi}^\pm_\ell$, $S = G^\pm$, $V = W^\pm$.

$$\Xi_{LL} = \mathcal{G}_{h_iG^\pm W^\pm}\mathcal{G}^L_{\tilde{\chi}^0_1\tilde{\chi}^\pm_\ell G^\pm}\mathcal{G}^{R*}_{\tilde{\chi}^0_1\tilde{\chi}^\pm_\ell W^\pm},$$
$$\Xi_{LR} = \mathcal{G}_{h_iG^\pm W^\pm}\mathcal{G}^L_{\tilde{\chi}^0_1\tilde{\chi}^\pm_\ell G^\pm}\mathcal{G}^{L*}_{\tilde{\chi}^0_1\tilde{\chi}^\pm_\ell W^\pm},$$
$$\Xi_{RL} = \mathcal{G}_{h_iG^\pm W^\pm}\mathcal{G}^R_{\tilde{\chi}^0_1\tilde{\chi}^\pm_\ell G^\pm}\mathcal{G}^{R*}_{\tilde{\chi}^0_1\tilde{\chi}^\pm_\ell W^\pm},$$
$$\Xi_{RR} = \mathcal{G}_{h_iG^\pm W^\pm}\mathcal{G}^R_{\tilde{\chi}^0_1\tilde{\chi}^\pm_\ell G^\pm}\mathcal{G}^{L*}_{\tilde{\chi}^0_1\tilde{\chi}^\pm_\ell W^\pm}.$$

In the above, we have used the following:

$$C^L_{\ell k} = \mathcal{N}_{\ell 2}\mathcal{V}^*_{k1} - \frac{1}{\sqrt{2}}\mathcal{N}_{\ell 4}\mathcal{V}^*_{k2},$$
$$C^R_{\ell k} = \mathcal{N}^*_{\ell 2}\mathcal{U}_{k1} + \frac{1}{\sqrt{2}}\mathcal{N}^*_{\ell 3}\mathcal{U}_{k2},$$
$$N^L_{\ell n} = \frac{1}{2}(-\mathcal{N}_{\ell 3}\mathcal{N}^*_{n3} + \mathcal{N}_{\ell 4}\mathcal{N}^*_{n4}),$$
$$N^R_{\ell n} = -(N^L_{\ell n})^*,$$
$$Q_{k\ell} = \frac{1}{2}\mathcal{V}_{k1}\mathcal{U}_{\ell 2},$$
$$S_{k\ell} = \frac{1}{2}\mathcal{V}_{k2}\mathcal{U}_{\ell 1},$$
$$Q'^L_{\ell k} = c_\beta\left[\mathcal{N}^*_{\ell 4}\mathcal{V}^*_{k1} + \frac{1}{\sqrt{2}}\mathcal{V}^*_{k2}(\mathcal{N}^*_{\ell 2} + t_W\mathcal{N}^*_{\ell 1})\right],$$

$$
\begin{aligned}
Q'^{R}_{\ell k} &= s_\beta[\mathcal{N}_{\ell 3}\mathcal{U}_{k1} - \frac{1}{\sqrt{2}}\mathcal{U}_{k2}(\mathcal{N}_{\ell 2} + t_W\mathcal{N}_{\ell 1})],\\
Q''_{n\ell} &= \frac{1}{2}[\mathcal{N}_{n3}(\mathcal{N}_{\ell 2} - t_W\mathcal{N}_{\ell 1})\\
&\quad + \mathcal{N}_{\ell 3}(\mathcal{N}_{n2} - t_W\mathcal{N}_{n1})],\\
S''_{n\ell} &= \frac{1}{2}[\mathcal{N}_{n4}(\mathcal{N}_{\ell 2} - t_W\mathcal{N}_{\ell 1})\\
&\quad + \mathcal{N}_{\ell 4}(\mathcal{N}_{n2} - t_W\mathcal{N}_{n1})],\\
G^{\nu}_{nm1} &= -\frac{1}{\sqrt{2}}g_2(\mathcal{N}^*_{12} - t_W\mathcal{N}^*_{11})U^{\tilde{\nu}*}_{nm},\\
G^{e_L}_{nm1} &= \frac{1}{\sqrt{2}}g_2(\mathcal{N}^*_{12} + t_W\mathcal{N}^*_{11})W^{\tilde{e}*}_{nm}\\
&\quad - \frac{g_2}{\sqrt{2}M_W c_\beta}m_{e_n}\mathcal{N}^*_{13}W^{\tilde{e}*}_{n+3m},\\
G^{e_R}_{nm1} &= -\sqrt{2}g_2 t_W\mathcal{N}_{11}W^{\tilde{e}*}_{n+3m}\\
&\quad - \frac{g_2}{\sqrt{2}M_W c_\beta}m_{e_i}\mathcal{N}_{13}W^{\tilde{e}*}_{nm}.
\end{aligned}
$$

APPENDIX B: DIAGONALIZATION OF THE NEUTRALINO MASS MATRIX

We present the approximate analytical solutions for the eigenvalues of $\bar{\mathbb{M}}_{\tilde{\chi}^0}$ defined in Eq. (1) (see e.g., [108]) and the composition of the lightest neutralino, which will be relevant for the discussion. The 4×4 neutralino mass matrix in the basis $(\tilde{B}, \tilde{W}^0, \tilde{H}^0_d, \tilde{H}^0_u)$ can be read as

$$
\bar{\mathbb{M}}_{\tilde{\chi}^0} = \begin{pmatrix} M_1 & 0 & -M_Z s_W c_\beta & M_Z s_W s_\beta \\ 0 & M_2 & M_Z c_W c_\beta & -M_Z c_W s_\beta \\ -M_Z s_W c_\beta & M_Z c_W c_\beta & 0 & -\mu \\ M_Z s_W s_\beta & -M_Z c_W s_\beta & -\mu & 0 \end{pmatrix}. \tag{B1}
$$

The lightest neutralino $\tilde{\chi}^0_1$, in the above basis can be written as

$$
\tilde{\chi}^0_1 = \mathcal{N}_{11}\tilde{B} + \mathcal{N}_{12}\tilde{W}^0 + \mathcal{N}_{13}\tilde{H}^0_d + \mathcal{N}_{14}\tilde{H}^0_u. \tag{B2}
$$

In order to calculate the mass eigenvalues of Eq. (B1) and the compositions of $\tilde{\chi}^0_1$, N_{1j} [see Eq. (B2)], we rotate the neutralino mass matrix to a basis $(\tilde{B}, \tilde{W}^0, \tilde{H}^0_1, \tilde{H}^0_2)$, where $\tilde{H}^0_1 = \frac{\tilde{H}^0_u - \tilde{H}^0_d}{\sqrt{2}}$ and $\tilde{H}^0_2 = \frac{\tilde{H}^0_u + \tilde{H}^0_d}{\sqrt{2}}$. Then, we can write by orthogonal transformation,

$$
\mathbf{M} = \mathbf{U}\bar{\mathbb{M}}_{\tilde{\chi}^0}\mathbf{U}^T \tag{B3}
$$

$$
= \begin{pmatrix} M_1 & 0 & -\frac{1}{\sqrt{2}}M_Z s_W(s_\beta + c_\beta) & \frac{1}{\sqrt{2}}M_Z s_W(s_\beta - c_\beta) \\ 0 & M_2 & \frac{1}{\sqrt{2}}M_Z c_W(s_\beta + c_\beta) & -\frac{1}{\sqrt{2}}M_Z c_W(s_\beta - c_\beta) \\ -\frac{1}{\sqrt{2}}M_Z s_W(s_\beta + c_\beta) & \frac{1}{\sqrt{2}}M_Z c_W(s_\beta + c_\beta) & \mu & 0 \\ \frac{1}{\sqrt{2}}M_Z s_W(s_\beta - c_\beta) & -\frac{1}{\sqrt{2}}M_Z c_W(s_\beta - c_\beta) & 0 & -\mu \end{pmatrix}, \tag{B4}
$$

where the matrix $\mathbf{U}$ is given by

$$
\mathbf{U} = \begin{pmatrix} 1 & 0 & 0 & 0 \\ 0 & 1 & 0 & 0 \\ 0 & 0 & \frac{1}{\sqrt{2}} & -\frac{1}{\sqrt{2}} \\ 0 & 0 & \frac{1}{\sqrt{2}} & \frac{1}{\sqrt{2}} \end{pmatrix}. \tag{B5}
$$

We can write the matrix in Eq. (B4) in the following way:

$$
\begin{aligned}
\mathbf{M} &= \begin{pmatrix} M_1 & 0 & 0 & 0 \\ 0 & M_2 & 0 & 0 \\ 0 & 0 & \mu & 0 \\ 0 & 0 & 0 & -\mu \end{pmatrix} + \begin{pmatrix} 0 & 0 & a_1 & a_2 \\ 0 & 0 & a_3 & a_4 \\ a_1 & a_3 & 0 & 0 \\ a_2 & a_4 & 0 & 0 \end{pmatrix}\\
&= \mathbf{M}_D + \mathbf{M}_P.
\end{aligned} \tag{B6}
$$

The off-diagonal matrix $\mathbf{M}_P$ will be treated as perturbations as the diagonal eigenvalues in $\mathbf{M}_D$ are typically larger than M_Z. Now, we use time-independent perturbation theory to calculate the eigenvalues of $\mathbf{M}$. The eigenvectors of the unperturbed matrix $\mathbf{M}_D$ can be written as

$$
|\phi_1\rangle = \begin{pmatrix} 1 \\ 0 \\ 0 \\ 0 \end{pmatrix}, \quad |\phi_2\rangle = \begin{pmatrix} 0 \\ 1 \\ 0 \\ 0 \end{pmatrix},
$$

$$
|\phi_3\rangle = \begin{pmatrix} 0 \\ 0 \\ 1 \\ 0 \end{pmatrix}, \quad \text{and} \quad |\phi_4\rangle = \begin{pmatrix} 0 \\ 0 \\ 0 \\ 1 \end{pmatrix}, \tag{B7}
$$

with the mass eigenvalues at the zeroth-order (unperturbed eigenvalues) are given by

$$m^{(0)}_{\tilde{\chi}^0_1} = M_1, \quad m^{(0)}_{\tilde{\chi}^0_2} = M_2, \quad m^{(0)}_{\tilde{\chi}^0_3} = \mu, \quad m^{(0)}_{\tilde{\chi}^0_4} = -\mu. \tag{B8}$$

Now, the first-order corrections to the mass eigenvalues in the nondegenerate perturbation theory can be written as

$$\begin{aligned} m^{(1)}_{\tilde{\chi}^0_1} &= \langle \phi_1 | \mathbf{M}_P | \phi_1 \rangle = 0, \\ m^{(1)}_{\tilde{\chi}^0_2} &= \langle \phi_2 | \mathbf{M}_P | \phi_2 \rangle = 0, \\ m^{(1)}_{\tilde{\chi}^0_3} &= \langle \phi_3 | \mathbf{M}_P | \phi_3 \rangle = 0, \\ m^{(1)}_{\tilde{\chi}^0_4} &= \langle \phi_4 | \mathbf{M}_P | \phi_4 \rangle = 0. \end{aligned} \tag{B9}$$

Therefore, we see that the first-order corrections to the mass eigenvalues vanish. Let us now consider the second-order corrections, which for the nondegenerate perturbation theory read as

$$m^{(2)}_{\tilde{\chi}^0_n} = \sum_{\ell \neq n} \frac{|\langle \phi_\ell | \mathbf{M}_P | \phi_n \rangle|^2}{m^{(0)}_{\tilde{\chi}^0_n} - m^{(0)}_{\tilde{\chi}^0_\ell}}. \tag{B10}$$

Consequently, the second-order corrections are computed as follows:

$$\begin{aligned} m^{(2)}_{\tilde{\chi}^0_1} &= \sum_{\ell=2,3,4} \frac{|\langle \phi_\ell | \mathbf{M}_P | \phi_1 \rangle|^2}{m^{(0)}_{\tilde{\chi}^0_1} - m^{(0)}_{\tilde{\chi}^0_\ell}} = \frac{|a_1|^2}{m^{(0)}_{\tilde{\chi}^0_1} - m^{(0)}_{\tilde{\chi}^0_3}} + \frac{|a_2|^2}{m^{(0)}_{\tilde{\chi}^0_1} - m^{(0)}_{\tilde{\chi}^0_4}} \\ &= \frac{M_Z^2 s_W^2 (M_1 + \mu s_{2\beta})}{M_1^2 - \mu^2}, \end{aligned} \tag{B11}$$

$$\begin{aligned} m^{(2)}_{\tilde{\chi}^0_2} &= \sum_{\ell=1,3,4} \frac{|\langle \phi_\ell | \mathbf{M}_P | \phi_2 \rangle|^2}{m^{(0)}_{\tilde{\chi}^0_2} - m^{(0)}_{\tilde{\chi}^0_\ell}} = \frac{|a_3|^2}{m^{(0)}_{\tilde{\chi}^0_2} - m^{(0)}_{\tilde{\chi}^0_3}} + \frac{|a_4|^2}{m^{(0)}_{\tilde{\chi}^0_2} - m^{(0)}_{\tilde{\chi}^0_4}} \\ &= \frac{M_Z^2 c_W^2 (M_2 + \mu s_{2\beta})}{M_2^2 - \mu^2}, \end{aligned} \tag{B12}$$

$$\begin{aligned} m^{(2)}_{\tilde{\chi}^0_3} &= \sum_{\ell=1,2,4} \frac{|\langle \phi_\ell | \mathbf{M}_P | \phi_3 \rangle|^2}{m^{(0)}_{\tilde{\chi}^0_3} - m^{(0)}_{\tilde{\chi}^0_\ell}} = \frac{|a_1|^2}{m^{(0)}_{\tilde{\chi}^0_3} - m^{(0)}_{\tilde{\chi}^0_1}} + \frac{|a_3|^2}{m^{(0)}_{\tilde{\chi}^0_3} - m^{(0)}_{\tilde{\chi}^0_2}} \\ &= \frac{M_Z^2 (1 + s_{2\beta})(\mu - M_1 c_W^2 - M_2 s_W^2)}{2(\mu - M_1)(\mu - M_2)}, \end{aligned} \tag{B13}$$

$$\begin{aligned} m^{(2)}_{\tilde{\chi}^0_4} &= \sum_{\ell=1,2,3} \frac{|\langle \phi_\ell | \mathbf{M}_P | \phi_4 \rangle|^2}{m^{(0)}_{\tilde{\chi}^0_4} - m^{(0)}_{\tilde{\chi}^0_\ell}} = \frac{|a_2|^2}{m^{(0)}_{\tilde{\chi}^0_4} - m^{(0)}_{\tilde{\chi}^0_1}} + \frac{|a_4|^2}{m^{(0)}_{\tilde{\chi}^0_4} - m^{(0)}_{\tilde{\chi}^0_2}} \\ &= \frac{M_Z^2 (1 - s_{2\beta})(\mu + M_1 c_W^2 + M_2 s_W^2)}{2(\mu + M_1)(\mu + M_2)}. \end{aligned} \tag{B14}$$

Therefore, the masses of the neutralinos in the order $m_{\tilde{\chi}^0_1} < m_{\tilde{\chi}^0_2} < m_{\tilde{\chi}^0_3} < m_{\tilde{\chi}^0_4}$, can be expressed as

$$m_{\tilde{\chi}^0_1} = M_1 + \frac{M_Z^2 s_W^2 (M_1 + \mu s_{2\beta})}{M_1^2 - \mu^2} + \cdots, \tag{B15}$$

$$m_{\tilde{\chi}^0_2} = M_2 + \frac{M_Z^2 c_W^2 (M_2 + \mu s_{2\beta})}{M_2^2 - \mu^2} + \cdots, \tag{B16}$$

$$\begin{aligned} m_{\tilde{\chi}^0_3} = |\mu| &+ \frac{M_Z^2 (1 - s_{2\beta})(\mu + M_1 c_W^2 + M_2 s_W^2)\mathrm{sgn}(\mu)}{2(\mu + M_1)(\mu + M_2)} \\ &+ \cdots, \end{aligned} \tag{B17}$$

$$\begin{aligned} m_{\tilde{\chi}^0_4} = |\mu| &+ \frac{M_Z^2 (1 + s_{2\beta})(\mu - M_1 c_W^2 - M_2 s_W^2)\mathrm{sgn}(\mu)}{2(\mu - M_1)(\mu - M_2)} \\ &+ \cdots. \end{aligned} \tag{B18}$$

The matrix $\mathbf{M}$ can be diagonalized by an orthogonal transformation $\mathbf{M_{diag}} = \mathbf{V}\mathbf{M}\mathbf{V}^T$. Thus, the elements $\mathcal{N}_{1\ell}$ (in the original basis) is expressed as

$$\mathcal{N}_{k\ell} = \mathbf{V}_{kn} \mathbf{U}_{n\ell}. \tag{B19}$$

At the first order of nondegenerate perturbation theory we can write

$$\mathbf{V}^{(1)}_{kn} = \sum_{k \neq n} \frac{\langle \phi_n | \mathbf{M}_P | \phi_k \rangle}{m^{(0)}_{\tilde{\chi}^0_k} - m^{(0)}_{\tilde{\chi}^0_n}}. \tag{B20}$$

Now we can calculate the first-order corrections as

$$\mathbf{V}^{(1)}_{12} = \frac{\langle \phi_2 | \mathbf{M}_P | \phi_1 \rangle}{m^{(0)}_{\tilde{\chi}^0_1} - m^{(0)}_{\tilde{\chi}^0_2}} = 0, \tag{B21}$$

$$\begin{aligned} \mathbf{V}^{(1)}_{13} &= \frac{\langle \phi_3 | \mathbf{M}_P | \phi_1 \rangle}{m^{(0)}_{\tilde{\chi}^0_1} - m^{(0)}_{\tilde{\chi}^0_3}} = \frac{a_1}{m^{(0)}_{\tilde{\chi}^0_1} - m^{(0)}_{\tilde{\chi}^0_3}} \\ &= \frac{M_Z s_W (s_\beta + c_\beta)}{\sqrt{2}(\mu - M_1)}, \end{aligned} \tag{B22}$$

$$\begin{aligned} \mathbf{V}^{(1)}_{14} &= \frac{\langle \phi_4 | \mathbf{M}_P | \phi_1 \rangle}{m^{(0)}_{\tilde{\chi}^0_1} - m^{(0)}_{\tilde{\chi}^0_4}} = \frac{a_2}{m^{(0)}_{\tilde{\chi}^0_1} - m^{(0)}_{\tilde{\chi}^0_4}} \\ &= \frac{M_Z s_W (s_\beta - c_\beta)}{\sqrt{2}(\mu + M_1)}. \end{aligned} \tag{B23}$$

Since the first-order correction $\mathbf{V}^{(1)}_{12} = 0$, we need to calculate the second-order correction to $\mathbf{V}_{12}$. The second-order corrections can be written as

$$\mathbf{V}^{(2)}_{kn} = \sum_{m\neq k}\Bigg[\sum_{n\neq k}\frac{\langle\phi_n|\mathbf{M}_P|\phi_m\rangle\langle\phi_m|\mathbf{M}_P|\phi_k\rangle}{(m^{(0)}_{\tilde{\chi}^0_k}-m^{(0)}_{\tilde{\chi}^0_m})(m^{(0)}_{\tilde{\chi}^0_k}-m^{(0)}_{\tilde{\chi}^0_n})} - \frac{\langle\phi_n|\mathbf{M}_P|\phi_k\rangle\langle\phi_k|\mathbf{M}_P|\phi_k\rangle}{(m^{(0)}_{\tilde{\chi}^0_k}-m^{(0)}_{\tilde{\chi}^0_n})^2}\Bigg]. \tag{B24}$$

Therefore, we have

$$\mathbf{V}^{(2)}_{12} = \sum_{m=2,3,4}\frac{\langle\phi_2|\mathbf{M}_P|\phi_m\rangle\langle\phi_m|\mathbf{M}_P|\phi_1\rangle}{(m^{(0)}_{\tilde{\chi}^0_1}-m^{(0)}_{\tilde{\chi}^0_m})(m^{(0)}_{\tilde{\chi}^0_1}-m^{(0)}_{\tilde{\chi}^0_2})} - \frac{\langle\phi_2|\mathbf{M}_P|\phi_1\rangle\langle\phi_1|\mathbf{M}_P|\phi_1\rangle}{(m^{(0)}_{\tilde{\chi}^0_1}-m^{(0)}_{\tilde{\chi}^0_2})^2}, \tag{B25}$$

$$= \frac{\langle\phi_2|\mathbf{M}_P|\phi_3\rangle\langle\phi_3|\mathbf{M}_P|\phi_1\rangle}{(m^{(0)}_{\tilde{\chi}^0_1}-m^{(0)}_{\tilde{\chi}^0_3})(m^{(0)}_{\tilde{\chi}^0_1}-m^{(0)}_{\tilde{\chi}^0_2})} + \frac{\langle\phi_2|\mathbf{M}_P|\phi_4\rangle\langle\phi_4|\mathbf{M}_P|\phi_1\rangle}{(m^{(0)}_{\tilde{\chi}^0_1}-m^{(0)}_{\tilde{\chi}^0_4})(m^{(0)}_{\tilde{\chi}^0_1}-m^{(0)}_{\tilde{\chi}^0_2})}, \tag{B26}$$

$$= \frac{a_1 a_3}{(M_1-\mu)(M_1-M_2)} + \frac{a_2 a_4}{(M_1+\mu)(M_1-M_2)}, \tag{B27}$$

$$= -\frac{M_Z^2 s_{2W}(s_\beta+c_\beta)^2}{4(\mu-M_1)(M_2-M_1)} + \frac{M_Z^2 s_{2W}(s_\beta-c_\beta)^2}{4(\mu+M_1)(M_2-M_1)}. \tag{B28}$$

We derive the components of $\mathcal{N}_{1\ell}$,

$$\mathcal{N}_{11} \simeq 1, \tag{B29}$$

$$\mathcal{N}_{12} \simeq \mathbf{V}^{(2)}_{12} = -\frac{M_Z^2 s_{2W}(s_\beta+c_\beta)^2}{4(\mu-M_1)(M_2-M_1)} + \frac{M_Z^2 s_{2W}(s_\beta-c_\beta)^2}{4(\mu+M_1)(M_2-M_1)}, \tag{B30}$$

$$\mathcal{N}_{13} \simeq \frac{1}{\sqrt{2}}\mathbf{V}_{13} + \frac{1}{\sqrt{2}}\mathbf{V}_{14} = \frac{M_Z s_W(\mu s_\beta + M_1 c_\beta)}{\mu^2 - M_1^2}, \tag{B31}$$

$$\mathcal{N}_{14} \simeq -\frac{1}{\sqrt{2}}\mathbf{V}_{13} + \frac{1}{\sqrt{2}}\mathbf{V}_{14} = -\frac{M_Z s_W(\mu c_\beta + M_1 s_\beta)}{\mu^2 - M_1^2}. \tag{B32}$$

Finally, the masses and mixings of a binolike, winolike, and Higgsino-like neutralinos $\tilde{\chi}^0_i$ in the limit $\tan\beta \geq 10$ (in particular, $s_\beta \to 1$, $c_\beta \to 0$) take a simple form [assuming $\mathrm{sgn}(\mu) = +1$] in terms of the fundamental model parameters,

$$m_{\tilde{\chi}^0_1} \simeq M_1 + \frac{M_Z^2 s_W^2 M_1}{M_1^2-\mu^2}, \quad m_{\tilde{\chi}^0_2} \simeq M_2 + \frac{M_Z^2 c_W^2 M_2}{M_2^2-\mu^2}, \tag{B33}$$

$$m_{\tilde{\chi}^0_3} \simeq |\mu| + \frac{M_Z^2(\mu - M_1 c_W^2 - M_2 s_W^2)}{2(\mu-M_1)(\mu-M_2)}, \quad m_{\tilde{\chi}^0_4} \simeq |\mu| + \frac{M_Z^2(\mu + M_1 c_W^2 + M_2 s_W^2)}{2(\mu+M_1)(\mu+M_2)}, \tag{B34}$$

$$\mathcal{N}_{11} \simeq 1, \tag{B35}$$

$$\mathcal{N}_{12} \simeq -\frac{M_Z^2 s_{2W}}{4(\mu-M_1)(M_2-M_1)} + \frac{M_Z^2 s_{2W}}{4(\mu+M_1)(M_2-M_1)}, \tag{B36}$$

$$\mathcal{N}_{13} \simeq \frac{M_Z s_W \mu}{\mu^2 - M_1^2}, \tag{B37}$$

$$\mathcal{N}_{14} \simeq -\frac{M_Z s_W M_1}{\mu^2 - M_1^2}. \tag{B38}$$

$\tilde{\mathbf{B}}_{\tilde{\mathbf{H}}}$ LSP: The physical state $\tilde{\chi}^0_1$ becomes bino-Higgsino-like when $M_1 < |\mu| \ll M_2$ approximately holds. Since $\tilde{\chi}^0_2$ decoupled, masses for the Higgsino-like states can be approximated to

$$m_{\tilde{\chi}^0_{3,4}} \simeq |\mu| + \frac{M_Z^2 s_W^2}{2(\mu \mp M_1)}. \tag{B39}$$

Following SI direct detection limits, $\tilde{\chi}^0_1$ can only have moderate or minimal Higgsino components; thus, $m_{\tilde{\chi}^0_{1,3,4}}$ can be further simplified neglecting M_1 which results to

$$\Delta m(\tilde{\chi}^0_{3,4}, \tilde{\chi}^0_1) = m_{\tilde{\chi}^0_{3,4}} - m_{\tilde{\chi}^0_1} \simeq |\mu| - M_1 + \frac{M_Z^2 s_W^2}{2\mu} + \frac{M_Z^2 s_W^2 M_1}{\mu^2}. \tag{B40}$$

The other important mass splitting for our study is $\Delta m(\tilde{\chi}^\pm_1, \tilde{\chi}^0_1) = m_{\tilde{\chi}^\pm_1} - m_{\tilde{\chi}^0_1}$. Apart from the $\tilde{\chi}^0_1 - \tilde{\chi}^\pm_1$ coannihilations, the LHC limits on lighter charginos depend critically on the $\Delta m(\tilde{\chi}^\pm_1, \tilde{\chi}^0_1)$. Adapting the same route as before one obtains (assuming $|M_2\mu| > M_W^2 s_{2\beta}$),

$$m_{\tilde{\chi}_1^\pm} \simeq M_2 + M_W^2\left[\frac{M_2+\mu s_{2\beta}}{M_2^2-\mu^2}\right],$$
$$m_{\tilde{\chi}_2^\pm} \simeq |\mu| - M_W^2 \mathrm{sgn}(\mu)\left[\frac{\mu+M_2 s_{2\beta}}{M_2^2-\mu^2}\right]. \quad \text{(B41)}$$

In the limit of large $\tan\beta$ and heavy wino, the mass splitting between Higgsino-like chargino and $\tilde{\chi}_1^0$ can be approximated to

$$\Delta m(\tilde{\chi}_1^\pm, \tilde{\chi}_1^0) \equiv |\mu| - M_1 - \mathrm{sgn}(\mu)\frac{M_W^2\mu}{M_2^2} + \frac{M_Z^2 s_W^2 M_1}{\mu^2}. \quad \text{(B42)}$$

$\tilde{\mathbf{B}}_{\tilde{\mathbf{W}}\tilde{\mathbf{H}}}$ LSP: It refers to a limit $M_1 \leq M_2 < |\mu|$. Even after the latest LHC Run-2 data, the muon $g-2$ anomaly can still be accommodated with winos lighter than Higgsinos. The relevant mass splittings can be calculated from the above equations.

[1] G. Jungman, M. Kamionkowski, and K. Griest, Supersymmetric dark matter, Phys. Rep. **267**, 195 (1996).
[2] G. Bertone, D. Hooper, and J. Silk, Particle dark matter: Evidence, candidates and constraints, Phys. Rep. **405**, 279 (2005).
[3] N. Arkani-Hamed, A. Delgado, and G. Giudice, The well-tempered neutralino, Nucl. Phys. **B741**, 108 (2006).
[4] K. L. Chan, U. Chattopadhyay, and P. Nath, Naturalness, weak scale supersymmetry and the prospect for the observation of supersymmetry at the Tevatron and at the CERN LHC, Phys. Rev. D **58**, 096004 (1998).
[5] U. Chattopadhyay, A. Corsetti, and P. Nath, WMAP constraints, SUSY dark matter and implications for the direct detection of SUSY, Phys. Rev. D **68**, 035005 (2003).
[6] U. Chattopadhyay, D. Choudhury, M. Drees, P. Konar, and D. P. Roy, Looking for a heavy Higgsino LSP in collider and dark matter experiments, Phys. Lett. B **632**, 114 (2006).
[7] S. Akula, M. Liu, P. Nath, and G. Peim, Naturalness, supersymmetry and implications for LHC and dark matter, Phys. Lett. B **709**, 192 (2012).
[8] H. Baer, V. Barger, and A. Mustafayev, Implications of a 125 GeV Higgs scalar for LHC SUSY and neutralino dark matter searches, Phys. Rev. D **85**, 075010 (2012).
[9] J. Ellis and K. A. Olive, Revisiting the Higgs mass and dark matter in the CMSSM, Eur. Phys. J. C **72**, 2005 (2012).
[10] O. Buchmueller *et al.*, The CMSSM and NUHM1 after LHC Run 1, Eur. Phys. J. C **74**, 2922 (2014).
[11] H. Baer, V. Barger, P. Huang, D. Mickelson, M. Padeffke-Kirkland, and X. Tata, Natural SUSY with a bino- or wino-like LSP, Phys. Rev. D **91**, 075005 (2015).
[12] Y. He, L. Meng, Y. Yue, and D. Zhang, Impact of recent measurement of $(g-2)_\mu$, LHC search for supersymmetry, and LZ experiment on minimal supersymmetric standard model, Phys. Rev. D **108**, 115010 (2023).
[13] U. Chattopadhyay, D. Das, P. Konar, and D. P. Roy, Looking for a heavy wino LSP in collider and dark matter experiments, Phys. Rev. D **75**, 073014 (2007).
[14] J. Hisano, S. Matsumoto, M. Nagai, O. Saito, and M. Senami, Non-perturbative effect on thermal relic abundance of dark matter, Phys. Lett. B **646**, 34 (2007).
[15] A. Masiero, S. Profumo, and P. Ullio, Neutralino dark matter detection in split supersymmetry scenarios, Nucl. Phys. **B712**, 86 (2005).
[16] T. Cohen, M. Lisanti, A. Pierce, and T. R. Slatyer, Wino dark matter under siege, J. Cosmol. Astropart. Phys. 10 (2013) 061.
[17] B. Bhattacherjee, M. Ibe, K. Ichikawa, S. Matsumoto, and K. Nishiyama, Wino dark matter and future dSph observations, J. High Energy Phys. 07 (2014) 080.
[18] M. Baumgart, I. Z. Rothstein, and V. Vaidya, Constraints on Galactic wino densities from gamma ray lines, J. High Energy Phys. 04 (2015) 106.
[19] A. Hryczuk, I. Cholis, R. Iengo, M. Tavakoli, and P. Ullio, Indirect detection analysis: Wino dark matter case study, J. Cosmol. Astropart. Phys. 07 (**2014**) 031.
[20] M. Ibe, S. Matsumoto, S. Shirai, and T. T. Yanagida, Wino dark matter in light of the AMS-02 2015 data, Phys. Rev. D **91**, 111701 (2015).
[21] M. Beneke, A. Bharucha, F. Dighera, C. Hellmann, A. Hryczuk, S. Recksiegel, and P. Ruiz-Femenía, Relic density of wino-like dark matter in the MSSM, J. High Energy Phys. 03 (2016) 119.
[22] M. Beneke, A. Bharucha, A. Hryczuk, S. Recksiegel, and P. Ruiz-Femenia, The last refuge of mixed wino-Higgsino dark matter, J. High Energy Phys. 01 (2017) 002.
[23] M. Beneke, R. Szafron, and K. Urban, Sommerfeld-corrected relic abundance of wino dark matter with NLO electroweak potentials, J. High Energy Phys. 02 (2021) 020.
[24] M. Beneke, R. Szafron, and K. Urban, Wino potential and Sommerfeld effect at NLO, Phys. Lett. B **800**, 135112 (2020).
[25] G. Hinshaw *et al.* (WMAP Collaboration), Nine-year Wilkinson microwave anisotropy probe (WMAP) observations: Cosmological parameter results, Astrophys. J. Suppl. Ser. **208**, 19 (2013).
[26] N. Aghanim *et al.* (Planck Collaboration), Planck 2018 results. VI. Cosmological parameters, Astron. Astrophys. **641**, A6 (2020); **652**, C4(E) (2021).
[27] M. Chakraborti, U. Chattopadhyay, and S. Poddar, How light a higgsino or a wino dark matter can become in a compressed scenario of MSSM, J. High Energy Phys. 09 (2017) 064.

[28] J. L. Feng, K. T. Matchev, and T. Moroi, Focus points and naturalness in supersymmetry, Phys. Rev. D **61**, 075005 (2000).
[29] J. L. Feng, K. T. Matchev, and T. Moroi, Multi—TeV scalars are natural in minimal supergravity, Phys. Rev. Lett. **84**, 2322 (2000).
[30] J. L. Feng, K. T. Matchev, and F. Wilczek, Neutralino dark matter in focus point supersymmetry, Phys. Lett. B **482**, 388 (2000).
[31] U. Chattopadhyay, T. Ibrahim, and D. P. Roy, Electron and neutron electric dipole moments in the focus point scenario of SUGRA model, Phys. Rev. D **64**, 013004 (2001).
[32] S. P. Das, A. Datta, M. Guchait, M. Maity, and S. Mukherjee, Focus point SUSY at the LHC revisited, Eur. Phys. J. C **54**, 645 (2008).
[33] U. Chattopadhyay, A. Datta, A. Datta, A. Datta, and D. P. Roy, LHC signature of the minimal SUGRA model with a large soft scalar mass, Phys. Lett. B **493**, 127 (2000).
[34] H. Baer, T. Krupovnickas, A. Mustafayev, E.-K. Park, S. Profumo, and X. Tata, Exploring the BWCA (bino-wino co-annihilation) scenario for neutralino dark matter, J. High Energy Phys. 12 (**2005**) 011.
[35] U. Chattopadhyay, D. Das, A. Datta, and S. Poddar, Non-zero trilinear parameter in the mSUGRA model: Dark matter and collider signals at Tevatron and LHC, Phys. Rev. D **76**, 055008 (2007).
[36] U. Chattopadhyay and D. Das, Higgs funnel region of SUSY dark matter for small tan beta, RG effects on pseudoscalar Higgs boson with scalar mass non-universality, Phys. Rev. D **79**, 035007 (2009).
[37] U. Chattopadhyay, D. Das, and D. P. Roy, Mixed neutralino dark matter in nonuniversal Gaugino mass models, Phys. Rev. D **79**, 095013 (2009).
[38] U. Chattopadhyay, D. Das, D. K. Ghosh, and M. Maity, Probing the light Higgs pole resonance annihilation of dark matter in the light of XENON100 and CDMS-II observations, Phys. Rev. D **82**, 075013 (2010).
[39] M. Chakraborti, U. Chattopadhyay, S. Rao, and D. P. Roy, Higgsino dark matter in nonuniversal Gaugino mass models, Phys. Rev. D **91**, 035022 (2015).
[40] D. Feldman, Z. Liu, and P. Nath, Light Higgses at the Tevatron and at the LHC and observable dark matter in SUGRA and D branes, Phys. Lett. B **662**, 190 (2008).
[41] D. Feldman, Z. Liu, and P. Nath, Decoding the mechanism for the origin of dark matter in the early Universe using LHC data, Phys. Rev. D **78**, 083523 (2008).
[42] M. Drees and J. S. Kim, Minimal natural supersymmetry after the LHC8, Phys. Rev. D **93**, 095005 (2016).
[43] D. Barducci, A. Belyaev, A. K. M. Bharucha, W. Porod, and V. Sanz, Uncovering natural supersymmetry via the interplay between the LHC and direct dark matter detection, J. High Energy Phys. 07 (2015) 066.
[44] H. Baer, V. Barger, M. Savoy, and X. Tata, Multichannel assault on natural supersymmetry at the high luminosity LHC, Phys. Rev. D **94**, 035025 (2016).
[45] A. Chatterjee, J. Dutta, and S. K. Rai, Natural SUSY at LHC with right-sneutrino LSP, J. High Energy Phys. 06 (2018) 042.
[46] L. Randall and R. Sundrum, Out of this world supersymmetry breaking, Nucl. Phys. **B557**, 79 (1999).
[47] G. F. Giudice, M. A. Luty, H. Murayama, and R. Rattazzi, Gaugino mass without singlets, J. High Energy Phys. 12 (1998) 027.
[48] T. Gherghetta, G. F. Giudice, and J. D. Wells, Phenomenological consequences of supersymmetry with anomaly induced masses, Nucl. Phys. **B559**, 27 (1999).
[49] G. Aad *et al.* (ATLAS Collaboration), Search for squarks and gluinos in final states with jets and missing transverse momentum using 139 fb^{-1} of $\sqrt{s} = 13$ TeV pp collision data with the ATLAS detector, J. High Energy Phys. 02 (2021) 143.
[50] A. M. Sirunyan *et al.* (CMS Collaboration), Search for supersymmetry in proton-proton collisions at 13 TeV in final states with jets and missing transverse momentum, J. High Energy Phys. 10 (**2019**) 244.
[51] A. Canepa, Searches for supersymmetry at the Large Hadron Collider, Rev. Phys. **4**, 100033 (2019).
[52] M. Chakraborti, U. Chattopadhyay, A. Choudhury, A. Datta, and S. Poddar, Reduced LHC constraints for higgsino-like heavier electroweakinos, J. High Energy Phys. 11 (2015) 050.
[53] G. W. Bennett *et al.* (Muon $g-2$ Collaboration), Final report of the muon E821 anomalous magnetic moment measurement at BNL, Phys. Rev. D **73**, 072003 (2006).
[54] B. Abi *et al.* (Muon $g-2$ Collaboration), Measurement of the positive muon anomalous magnetic moment to 0.46 ppm, Phys. Rev. Lett. **126**, 141801 (2021).
[55] T. Aoyama *et al.*, The anomalous magnetic moment of the muon in the Standard Model, Phys. Rep. **887**, 1 (2020).
[56] M. Davier, A. Hoecker, B. Malaescu, and Z. Zhang, Reevaluation of the hadronic vacuum polarisation contributions to the Standard Model predictions of the muon $g-2$ and $\alpha(m_Z^2)$ using newest hadronic cross-section data, Eur. Phys. J. C **77**, 827 (2017).
[57] A. Keshavarzi, D. Nomura, and T. Teubner, Muon $g-2$ and $\alpha(M_Z^2)$: A new data-based analysis, Phys. Rev. D **97**, 114025 (2018).
[58] G. Colangelo, M. Hoferichter, and P. Stoffer, Two-pion contribution to hadronic vacuum polarization, J. High Energy Phys. 02 (2019) 006.
[59] M. Davier, A. Hoecker, B. Malaescu, and Z. Zhang, A new evaluation of the hadronic vacuum polarisation contributions to the muon anomalous magnetic moment and to $\boldsymbol{\alpha(m_Z^2)}$, Eur. Phys. J. C **80**, 241 (2020); **80**, 410(E) (2020).
[60] A. Keshavarzi, D. Nomura, and T. Teubner, $g-2$ of charged leptons, $\alpha(M_Z^2)$, and the hyperfine splitting of muonium, Phys. Rev. D **101**, 014029 (2020).
[61] A. Kurz, T. Liu, P. Marquard, and M. Steinhauser, Hadronic contribution to the muon anomalous magnetic moment to next-to-next-to-leading order, Phys. Lett. B **734**, 144 (2014).
[62] M. Hoferichter, B.-L. Hoid, and B. Kubis, Three-pion contribution to hadronic vacuum polarization, J. High Energy Phys. 08 (2019) 137.
[63] K. Melnikov and A. Vainshtein, Hadronic light-by-light scattering contribution to the muon anomalous magnetic moment revisited, Phys. Rev. D **70**, 113006 (2004).
[64] P. Masjuan and P. Sanchez-Puertas, Pseudoscalar-pole contribution to the $(g_\mu - 2)$: A rational approach, Phys. Rev. D **95**, 054026 (2017).

[65] G. Colangelo, M. Hoferichter, M. Procura, and P. Stoffer, Dispersion relation for hadronic light-by-light scattering: two-pion contributions, J. High Energy Phys. 04 (2017) 161.
[66] M. Hoferichter, B.-L. Hoid, B. Kubis, S. Leupold, and S. P. Schneider, Dispersion relation for hadronic light-by-light scattering: Pion pole, J. High Energy Phys. 10 (2018) 141.
[67] A. Gérardin, H. B. Meyer, and A. Nyffeler, Lattice calculation of the pion transition form factor with $N_f = 2 + 1$ Wilson quarks, Phys. Rev. D **100**, 034520 (2019).
[68] J. Bijnens, N. Hermansson-Truedsson, and A. Rodríguez-Sánchez, Short-distance constraints for the HLbL contribution to the muon anomalous magnetic moment, Phys. Lett. B **798**, 134994 (2019).
[69] G. Colangelo, F. Hagelstein, M. Hoferichter, L. Laub, and P. Stoffer, Longitudinal short-distance constraints for the hadronic light-by-light contribution to $(g-2)_\mu$ with large-N_c Regge models, J. High Energy Phys. 03 (2020) 101.
[70] G. Colangelo, M. Hoferichter, A. Nyffeler, M. Passera, and P. Stoffer, Remarks on higher-order hadronic corrections to the muon $g-2$, Phys. Lett. B **735**, 90 (2014).
[71] T. Blum, N. Christ, M. Hayakawa, T. Izubuchi, L. Jin, C. Jung, and C. Lehner, Hadronic light-by-light scattering contribution to the muon anomalous magnetic moment from lattice QCD, Phys. Rev. Lett. **124**, 132002 (2020).
[72] T. Aoyama, M. Hayakawa, T. Kinoshita, and M. Nio, Complete tenth-order QED contribution to the muon $g-2$, Phys. Rev. Lett. **109**, 111808 (2012).
[73] T. Aoyama, T. Kinoshita, and M. Nio, Theory of the anomalous magnetic moment of the electron, Atoms **7**, 28 (2019).
[74] A. Czarnecki, W. J. Marciano, and A. Vainshtein, Refinements in electroweak contributions to the muon anomalous magnetic moment, Phys. Rev. D **67**, 073006 (2003); **73**, 119901 (2006).
[75] C. Gnendiger, D. Stöckinger, and H. Stöckinger-Kim, The electroweak contributions to $(g-2)_\mu$ after the Higgs boson mass measurement, Phys. Rev. D **88**, 053005 (2013).
[76] D. P. Aguillard *et al.* (Muon $g-2$ Collaboration), Measurement of the positive muon anomalous magnetic moment to 0.20 ppm, Phys. Rev. Lett. **131**, 161802 (2023).
[77] Q. Wang *et al.* (PandaX-II Collaboration), Results of dark matter search using the full PandaX-II exposure, Chin. Phys. C **44**, 125001 (2020).
[78] E. Aprile *et al.* (XENON Collaboration), First dark matter search with nuclear recoils from the XENONnT experiment, Phys. Rev. Lett. **131**, 041003 (2023).
[79] E. Aprile *et al.* (XENON Collaboration), Dark matter search results from a one ton-year exposure of XENON1T, Phys. Rev. Lett. **121**, 111302 (2018).
[80] D. S. Akerib *et al.* (LUX Collaboration), Limits on spin-dependent WIMP-nucleon cross section obtained from the complete LUX exposure, Phys. Rev. Lett. **118**, 251302 (2017).
[81] X. Cui *et al.* (PandaX-II Collaboration), Dark matter results from 54-ton-day exposure of PandaX-II experiment, Phys. Rev. Lett. **119**, 181302 (2017).
[82] E. Aprile *et al.* (XENON Collaboration), Projected WIMP sensitivity of the XENONnT dark matter experiment, J. Cosmol. Astropart. Phys. 11 (**2020**) 031.
[83] C. Amole *et al.* (PICO Collaboration), Improved dark matter search results from PICO-2L Run 2, Phys. Rev. D **93**, 061101 (2016).
[84] D. S. Akerib *et al.* (LUX Collaboration), Results on the spin-dependent scattering of weakly interacting massive particles on nucleons from the Run 3 data of the LUX experiment, Phys. Rev. Lett. **116**, 161302 (2016).
[85] C. Fu *et al.* (PandaX-II Collaboration), Spin-dependent weakly-interacting-massive-particle–nucleon cross section limits from first data of PandaX-II experiment, Phys. Rev. Lett. **118**, 071301 (2017); **120**, 049902(E) (2018).
[86] J. Aalbers *et al.* (LUX-ZEPLIN Collaboration), First dark matter search results from the LUX-ZEPLIN (LZ) experiment, Phys. Rev. Lett. **131**, 041002 (2023).
[87] H. Baer, V. Barger, and H. Serce, SUSY under siege from direct and indirect WIMP detection experiments, Phys. Rev. D **94**, 115019 (2016).
[88] M. Badziak, M. Olechowski, and P. Szczerbiak, Is well-tempered neutralino in MSSM still alive after 2016 LUX results?, Phys. Lett. B **770**, 226 (2017).
[89] S. Profumo, T. Stefaniak, and L. Stephenson Haskins, The not-so-well tempered neutralino, Phys. Rev. D **96**, 055018 (2017).
[90] M. Abdughani, K.-I. Hikasa, L. Wu, J. M. Yang, and J. Zhao, Testing electroweak SUSY for muon $g-2$ and dark matter at the LHC and beyond, J. High Energy Phys. 11 (2019) 095.
[91] C. Cheung, L. J. Hall, D. Pinner, and J. T. Ruderman, Prospects and blind spots for neutralino dark matter, J. High Energy Phys. 05 (**2013**) 100.
[92] C. Cheung and D. Sanford, Simplified models of mixed dark matter, J. Cosmol. Astropart. Phys. 02 (2014) 011.
[93] P. Huang and C. E. M. Wagner, Blind spots for neutralino dark matter in the MSSM with an intermediate m_A, Phys. Rev. D **90**, 015018 (2014).
[94] D. Das, B. De, and S. Mitra, Cancellation in dark matter-nucleon interactions: The role of non-standard-model-like Yukawa couplings, Phys. Lett. B **815**, 136159 (2021).
[95] G. H. Duan, K.-I. Hikasa, J. Ren, L. Wu, and J. M. Yang, Probing bino-wino coannihilation dark matter below the neutrino floor at the LHC, Phys. Rev. D **98**, 015010 (2018).
[96] G. F. Giudice and A. Pomarol, Mass degeneracy of the Higgsinos, Phys. Lett. B **372**, 253 (1996).
[97] M. Drees, M. M. Nojiri, D. P. Roy, and Y. Yamada, Light Higgsino dark matter, Phys. Rev. D **56**, 276 (1997); **64**, 039901(E) (2001).
[98] M. Drees and M. Nojiri, Neutralino—Nucleon scattering revisited, Phys. Rev. D **48**, 3483 (1993).
[99] S. Bisal, A. Chatterjee, D. Das, and S. A. Pasha, Radiative corrections to aid the direct detection of the higgsino-like neutralino dark matter: Spin-independent interactions, arXiv:2311.09937.
[100] J. Hisano, S. Matsumoto, M. M. Nojiri, and O. Saito, Direct detection of the Wino and Higgsino-like neutralino dark matters at one-loop level, Phys. Rev. D **71**, 015007 (2005).
[101] J. Harz, B. Herrmann, M. Klasen, K. Kovařík, and L. P. Wiggering, Precision predictions for dark matter with DM@NLO in the MSSM, Eur. Phys. J. C **84**, 342 (2024).

[102] M. Klasen, K. Kovarik, and P. Steppeler, SUSY-QCD corrections for direct detection of neutralino dark matter and correlations with relic density, Phys. Rev. D **94**, 095002 (2016).
[103] M. Cirelli, N. Fornengo, and A. Strumia, Minimal dark matter, Nucl. Phys. **B753**, 178 (2006).
[104] J. Hisano, K. Ishiwata, N. Nagata, and T. Takesako, Direct detection of electroweak-interacting dark matter, J. High Energy Phys. 07 (2011) 005.
[105] J. Hisano, K. Ishiwata, and N. Nagata, A complete calculation for direct detection of Wino dark matter, Phys. Lett. B **690**, 311 (2010).
[106] J. Hisano, K. Ishiwata, and N. Nagata, Gluon contribution to the dark matter direct detection, Phys. Rev. D **82**, 115007 (2010).
[107] M. Drees, R. Godbole, and P. Roy, Theory and phenomenology of sparticles: An account of four-dimensional $N = 1$ supersymmetry in high energy physics (2004).
[108] J. F. Gunion and H. E. Haber, Two-body decays of neutralinos and charginos, Phys. Rev. D **37**, 2515 (1988).
[109] M. M. El Kheishen, A. A. Aboshousha, and A. A. Shafik, Analytic formulas for the neutralino masses and the neutralino mixing matrix, Phys. Rev. D **45**, 4345 (1992).
[110] V. D. Barger, M. S. Berger, and P. Ohmann, The supersymmetric particle spectrum, Phys. Rev. D **49**, 4908 (1994).
[111] M. W. Goodman and E. Witten, Detectability of certain dark matter candidates, Phys. Rev. D **31**, 3059 (1985).
[112] K. Griest, Cross-sections, relic abundance and detection rates for neutralino dark matter, Phys. Rev. D **38**, 2357 (1988); **39**, 3802(E) (1989).
[113] J. R. Ellis and R. A. Flores, Realistic predictions for the detection of supersymmetric dark matter, Nucl. Phys. **B307**, 883 (1988).
[114] R. Barbieri, M. Frigeni, and G. F. Giudice, Dark matter neutralinos in supergravity theories, Nucl. Phys. **B313**, 725 (1989).
[115] J. R. Ellis, A. Ferstl, and K. A. Olive, Reevaluation of the elastic scattering of supersymmetric dark matter, Phys. Lett. B **481**, 304 (2000).
[116] J. D. Vergados, On the direct detection of dark matter—exploring all the signatures of the neutralino-nucleus interaction, Lect. Notes Phys. **720**, 69 (2007).
[117] V. K. Oikonomou, J. D. Vergados, and C. C. Moustakidis, Direct detection of dark matter-rates for various wimps, Nucl. Phys. **B773**, 19 (2007).
[118] J. R. Ellis, K. A. Olive, and C. Savage, Hadronic uncertainties in the elastic scattering of supersymmetric dark matter, Phys. Rev. D **77**, 065026 (2008).
[119] P. Nath and R. L. Arnowitt, Event rates in dark matter detectors for neutralinos including constraints from the $b \to s\gamma$ decay, Phys. Rev. Lett. **74**, 4592 (1995).
[120] J. Hisano, Effective theory approach to direct detection of dark matter, in *Effective Field Theory in Particle Physics and Cosmology: Lecture Notes of the Les Houches Summer School*, edited by Sacha Davidson *et al.* (Oxford Academic, Oxford, 2020).
[121] T. Falk, A. Ferstl, and K. A. Olive, New contributions to neutralino elastic cross sections from cp violating phases in the minimal supersymmetric standard model, Phys. Rev. D **59**, 055009 (1999).
[122] M. Shifman, A. Vainshtein, and V. Zakharov, Remarks on Higgs-boson interactions with nucleons, Phys. Lett. B **78**, 443 (1978).
[123] A. Thomas, P. Shanahan, and R. Young, Strangeness in the nucleon: What have we learned?, Nuovo Cimento C **035N04**, 3 (2012).
[124] G. Belanger, F. Boudjema, A. Pukhov, and A. Semenov, micrOMEGAs$_3$: A program for calculating dark matter observables, Comput. Phys. Commun. **185**, 960 (2014).
[125] J. Alarcon, J. Martin Camalich, and J. Oller, The chiral representation of the πN scattering amplitude and the pion-nucleon sigma term, Phys. Rev. D **85**, 051503 (2012).
[126] A. Crivellin, M. Hoferichter, and M. Procura, Accurate evaluation of hadronic uncertainties in spin-independent WIMP-nucleon scattering: Disentangling two- and three-flavor effects, Phys. Rev. D **89**, 054021 (2014).
[127] M. Hoferichter, J. Ruiz de Elvira, B. Kubis, and U.-G. Meißner, High-precision determination of the pion-nucleon σ term from Roy-Steiner equations, Phys. Rev. Lett. **115**, 092301 (2015).
[128] D. Hooper, Particle dark matter, in *Proceedings of Theoretical Advanced Study Institute in Elementary Particle Physics on the Dawn of the LHC Era (TASI 2008): Boulder, USA* (World Scientific, Singapore, 2010), pp. 709–764.
[129] H. H. Patel, Package-X: A Mathematica package for the analytic calculation of one-loop integrals, Comput. Phys. Commun. **197**, 276 (2015).
[130] H. H. Patel, Package-X 2.0: A Mathematica package for the analytic calculation of one-loop integrals, Comput. Phys. Commun. **218**, 66 (2017).
[131] T. Hahn and M. Perez-Victoria, Automatized one loop calculations in four-dimensions and D-dimensions, Comput. Phys. Commun. **118**, 153 (1999).
[132] H. Eberl, M. Kincel, W. Majerotto, and Y. Yamada, One loop corrections to the chargino and neutralino mass matrices in the on-shell scheme, Phys. Rev. D **64**, 115013 (2001).
[133] T. Fritzsche and W. Hollik, Complete one loop corrections to the mass spectrum of charginos and neutralinos in the MSSM, Eur. Phys. J. C **24**, 619 (2002).
[134] W. Oller, H. Eberl, W. Majerotto, and C. Weber, Analysis of the chargino and neutralino mass parameters at one loop level, Eur. Phys. J. C **29**, 563 (2003).
[135] W. Oller, H. Eberl, and W. Majerotto, Precise predictions for chargino and neutralino pair production in e^+e^- annihilation, Phys. Rev. D **71**, 115002 (2005).
[136] M. Drees, W. Hollik, and Q. Xu, One-loop calculations of the decay of the next-to-lightest neutralino in the MSSM, J. High Energy Phys. 02 (**2007**) 032.
[137] A. C. Fowler and G. Weiglein, Precise predictions for Higgs production in neutralino decays in the complex MSSM, J. High Energy Phys. 01 (2010) 108.
[138] S. Heinemeyer, F. von der Pahlen, and C. Schappacher, Chargino decays in the complex MSSM: A full one-loop analysis, Eur. Phys. J. C **72**, 1892 (2012).
[139] A. Chatterjee, M. Drees, and S. Kulkarni, Radiative corrections to the neutralino dark matter relic density—An effective coupling approach, Phys. Rev. D **86**, 105025 (2012).

[140] A. Bharucha, S. Heinemeyer, F. von der Pahlen, and C. Schappacher, Neutralino decays in the complex MSSM at one-loop: A comparison of on-shell renormalization schemes, Phys. Rev. D **86**, 075023 (2012).
[141] T. Fritzsche, T. Hahn, S. Heinemeyer, F. von der Pahlen, H. Rzehak, and C. Schappacher, The implementation of the renormalized complex MSSM in FEYNARTS and FormCalc, Comput. Phys. Commun. **185**, 1529 (2014).
[142] A. Chatterjee, M. Drees, S. Kulkarni, and Q. Xu, On-shell renormalization of the chargino and neutralino masses in the MSSM, Phys. Rev. D **85**, 075013 (2012).
[143] N. Baro and F. Boudjema, Automatized full one-loop renormalization of the MSSM. II. The chargino-neutralino sector, the sfermion sector, and some applications, Phys. Rev. D **80**, 076010 (2009).
[144] S. Heinemeyer and F. von der Pahlen, Automated choice for the best renormalization scheme in BSM models, Eur. Phys. J. C **83**, 865 (2023).
[145] T. Fritzsche, T. Hahn, S. Heinemeyer, F. von der Pahlen, H. Rzehak, and C. Schappacher, The implementation of the renormalized complex MSSM in FEYNARTS and FormCalc, Comput. Phys. Commun. **185**, 1529 (2014).
[146] A. Denner, Techniques for calculation of electroweak radiative corrections at the one loop level and results for W physics at LEP-200, Fortsch. Phys. **41**, 307 (1993).
[147] K. Hagiwara, R. Liao, A. D. Martin, D. Nomura, and T. Teubner, $(g-2)_\mu$ and $\alpha(M_Z^2)$ re-evaluated using new precise data, J. Phys. G **38**, 085003 (2011).
[148] M. Steinhauser, Leptonic contribution to the effective electromagnetic coupling constant up to three loops, Phys. Lett. B **429**, 158 (1998).
[149] S. Amoroso *et al.*, Compatibility and combination of world W-boson mass measurements, Eur. Phys. J. C **84**, 451 (2024).
[150] H. Bahl, S. Heinemeyer, W. Hollik, and G. Weiglein, Theoretical uncertainties in the MSSM Higgs boson mass calculation, Eur. Phys. J. C **80**, 497 (2020).
[151] Y. S. Amhis *et al.* (HFLAV Collaboration), Averages of b-hadron, c-hadron, and τ-lepton properties as of 2018, Eur. Phys. J. C **81**, 226 (2021).
[152] W. Altmannshofer and P. Stangl, New physics in rare B decays after Moriond 2021, Eur. Phys. J. C **81**, 952 (2021).
[153] S. Kraml, S. Kulkarni, U. Laa, A. Lessa, W. Magerl, D. Proschofsky-Spindler, and W. Waltenberger, SMODELS: A tool for interpreting simplified-model results from the LHC and its application to supersymmetry, Eur. Phys. J. C **74**, 2868 (2014).
[154] J. Dutta, S. Kraml, A. Lessa, and W. Waltenberger, SMODELS extension with the CMS supersymmetry search results from Run 2, Lett. High Energy Phys. **1**, 5 (2018).
[155] C. K. Khosa, S. Kraml, A. Lessa, P. Neuhuber, and W. Waltenberger, SMODELS database update v1.2.3, Lett. High Energy Phys. **2020**, 158 (2020).
[156] G. Alguero, J. Heisig, C. K. Khosa, S. Kraml, S. Kulkarni, A. Lessa, H. Reyes-González, W. Waltenberger, and A. Wongel, Constraining new physics with SMODELS version 2, J. High Energy Phys. 08 (2022) 068.
[157] T. Albahri *et al.* (Muon $g-2$ Collaboration), Measurement of the anomalous precession frequency of the muon in the Fermilab muon $g-2$ experiment, Phys. Rev. D **103**, 072002 (2021).
[158] G. Colangelo, A. X. El-Khadra, M. Hoferichter, A. Keshavarzi, C. Lehner, P. Stoffer, and T. Teubner, Data-driven evaluations of Euclidean windows to scrutinize hadronic vacuum polarization, Phys. Lett. B **833**, 137313 (2022).
[159] A. Bazavov *et al.* (Fermilab Lattice, HPQCD, MILC Collaborations), Light-quark connected intermediate-window contributions to the muon $g-2$ hadronic vacuum polarization from lattice QCD, Phys. Rev. D **107**, 114514 (2023).
[160] C. Alexandrou *et al.* (Extended Twisted Mass Collaboration), Lattice calculation of the short and intermediate time-distance hadronic vacuum polarization contributions to the muon magnetic moment using twisted-mass fermions, Phys. Rev. D **107**, 074506 (2023).
[161] M. Cè *et al.*, Window observable for the hadronic vacuum polarization contribution to the muon $g-2$ from lattice QCD, Phys. Rev. D **106**, 114502 (2022).
[162] H. Wittig, Progress on $(g-2)_\mu$ from lattice QCD, in 57th Rencontres de Moriond on Electroweak Interactions and Unified Theories (2023), arXiv:2306.04165.
[163] F. V. Ignatov *et al.* (CMD-3 Collaboration), Measurement of the pion formfactor with CMD-3 detector and its implication to the hadronic contribution to muon $(g-2)$, arXiv:2309.12910.
[164] F. V. Ignatov *et al.* (CMD-3 Collaboration), Measurement of the $e^+e^- \to \pi^+\pi^-$ cross section from threshold to 1.2 GeV with the CMD-3 detector, arXiv:2302.08834.
[165] R. R. Akhmetshin *et al.* (CMD-2 Collaboration), Reanalysis of hadronic cross-section measurements at CMD-2, Phys. Lett. B **578**, 285 (2004).
[166] A. Anastasi *et al.* (KLOE-2 Collaboration), Combination of KLOE $\sigma(e^+e^- \to \pi^+\pi^-\gamma(\gamma))$ measurements and determination of $a_\mu^{\pi^+\pi^-}$ in the energy range $0.10 < s < 0.95$ GeV^2, J. High Energy Phys. 03 (2018) 173.
[167] M. Ablikim *et al.* (BESIII Collaboration), Measurement of the $e^+e^- \to \pi^+\pi^-$ cross section between 600 and 900 MeV using initial state radiation, Phys. Lett. B **753**, 629 (2016); **812**, 135982(E) (2021).
[168] J. P. Lees *et al.* (*BABAR* Collaboration), Precise measurement of the $e^+e^- \to \pi^+\pi^-(\gamma)$ cross section with the initial-state radiation method at *BABAR*, Phys. Rev. D **86**, 032013 (2012).
[169] J. L. Lopez, D. V. Nanopoulos, and X. Wang, Large $(g-2)$-mu in $SU(5) \times U(1)$ supergravity models, Phys. Rev. D **49**, 366 (1994).
[170] U. Chattopadhyay and P. Nath, Probing supergravity grand unification in the Brookhaven $g-2$ experiment, Phys. Rev. D **53**, 1648 (1996).
[171] T. Moroi, The Muon anomalous magnetic dipole moment in the minimal supersymmetric standard model, Phys. Rev. D **53**, 6565 (1996); **56**, 4424(E) (1997).
[172] U. Chattopadhyay, D. K. Ghosh, and S. Roy, Constraining anomaly mediated supersymmetry breaking framework via on going muon $g-2$ experiment at Brookhaven, Phys. Rev. D **62**, 115001 (2000).

[173] S. P. Martin and J. D. Wells, Muon anomalous magnetic dipole moment in supersymmetric theories, Phys. Rev. D **64**, 035003 (2001).
[174] S. Heinemeyer, D. Stockinger, and G. Weiglein, Two loop SUSY corrections to the anomalous magnetic moment of the muon, Nucl. Phys. **B690**, 62 (2004).
[175] D. Stockinger, The muon magnetic moment and supersymmetry, J. Phys. G **34**, R45 (2007).
[176] G.-C. Cho, K. Hagiwara, Y. Matsumoto, and D. Nomura, The MSSM confronts the precision electroweak data and the muon $g-2$, J. High Energy Phys. 11 (2011) 068.
[177] M. Endo, K. Hamaguchi, T. Kitahara, and T. Yoshinaga, Probing bino contribution to muon $g-2$, J. High Energy Phys. 11 (2013) 013.
[178] M. Endo, K. Hamaguchi, S. Iwamoto, and T. Yoshinaga, Muon $g-2$ vs LHC in supersymmetric models, J. High Energy Phys. 01 (2014) 123.
[179] M. Chakraborti, U. Chattopadhyay, A. Choudhury, A. Datta, and S. Poddar, The electroweak sector of the pMSSM in the light of LHC—8 TeV and other data, J. High Energy Phys. 07 (**2014**) 019.
[180] D. Chowdhury and N. Yokozaki, Muon $g-2$ in anomaly mediated SUSY breaking, J. High Energy Phys. 08 (2015) 111.
[181] K. Kowalska, L. Roszkowski, E. M. Sessolo, and A. J. Williams, GUT-inspired SUSY and the muon $g-2$ anomaly: Prospects for LHC 14 TeV, J. High Energy Phys. 06 (2015) 020.
[182] M. E. Gomez, S. Lola, R. Ruiz de Austri, and Q. Shafi, Confronting SUSY GUT with dark matter, sparticle spectroscopy and muon $(g-2)$, Front. Phys. **6**, 127 (2018).
[183] M. Chakraborti, S. Heinemeyer, I. Saha, and C. Schappacher, $(g-2)_\mu$ and SUSY dark matter: Direct detection and collider search complementarity, Eur. Phys. J. C **82**, 483 (2022).
[184] M. Chakraborti, S. Heinemeyer, and I. Saha, Improved $(g-2)_\mu$ measurements and wino/higgsino dark matter, Eur. Phys. J. C **81**, 1069 (2021).
[185] M. I. Ali, M. Chakraborti, U. Chattopadhyay, and S. Mukherjee, Muon and electron $(g-2)$ anomalies with non-holomorphic interactions in MSSM, Eur. Phys. J. C **83**, 60 (2023).
[186] M. Lindner, M. Platscher, and F. S. Queiroz, A call for new physics: The muon anomalous magnetic moment and lepton flavor violation, Phys. Rep. **731**, 1 (2018).
[187] K. Hagiwara, K. Ma, and S. Mukhopadhyay, Closing in on the chargino contribution to the muon $g-2$ in the MSSM: current LHC constraints, Phys. Rev. D **97**, 055035 (2018).
[188] M. Endo, K. Hamaguchi, S. Iwamoto, and T. Kitahara, Muon $g-2$ vs LHC Run 2 in supersymmetric models, J. High Energy Phys. 04 (**2020**) 165.
[189] M. Chakraborti, S. Heinemeyer, and I. Saha, Improved $(g-2)_\mu$ measurements and supersymmetry, Eur. Phys. J. C **80**, 984 (2020).
[190] A. Aboubrahim, M. Klasen, and P. Nath, What the Fermilab muon $g-2$ experiment tells us about discovering supersymmetry at high luminosity and high energy upgrades to the LHC, Phys. Rev. D **104**, 035039 (2021).
[191] P. Athron, C. Balázs, D. H. J. Jacob, W. Kotlarski, D. Stöckinger, and H. Stöckinger-Kim, New physics explanations of a $_\mu$ in light of the FNAL muon $g-2$ measurement, J. High Energy Phys. 09 (2021) 080.
[192] M. Van Beekveld, W. Beenakker, M. Schutten, and J. De Wit, Dark matter, fine-tuning and $(g-2)_\mu$ in the pMSSM, SciPost Phys. **11**, 049 (2021).
[193] M. Endo, K. Hamaguchi, S. Iwamoto, and T. Kitahara, Supersymmetric interpretation of the muon $g-2$ anomaly, J. High Energy Phys. 07 (2021) 075.
[194] M. Chakraborti, S. Heinemeyer, and I. Saha, The new MUON G-2 result and supersymmetry, Eur. Phys. J. C **81**, 1114 (2021).
[195] M. Chakraborti, L. Roszkowski, and S. Trojanowski, GUT-constrained supersymmetry and dark matter in light of the new $(g-2)_\mu$ determination, J. High Energy Phys. 05 (2021) 252.
[196] U. Chattopadhyay, A. Corsetti, and P. Nath, Theoretical status of muon $(g-2)$, AIP Conf. Proc. **624**, 230 (2002).
[197] U. Chattopadhyay and P. Nath, Interpreting the new Brookhaven muon $(g-2)$ result, Phys. Rev. D **66**, 093001 (2002).
[198] W. Porod, SPHENO, a program for calculating supersymmetric spectra, SUSY particle decays and SUSY particle production at e^+e^- colliders, Comput. Phys. Commun. **153**, 275 (2003).
[199] W. Porod and F. Staub, SPHENO3.1: Extensions including flavour, *CP*-phases and models beyond the MSSM, Comput. Phys. Commun. **183**, 2458 (2012).
[200] F. Staub, SARAH4: A tool for (not only SUSY) model builders, Comput. Phys. Commun. **185**, 1773 (2014).
[201] F. Staub, Exploring new models in all detail with SARAH, Adv. High Energy Phys. **2015**, 840780 (2015).
[202] H. G. Fargnoli, C. Gnendiger, S. Paßehr, D. Stöckinger, and H. Stöckinger-Kim, Non-decoupling two-loop corrections to $(g-2)_\mu$ from fermion/sfermion loops in the MSSM, Phys. Lett. B **726**, 717 (2013).
[203] H. Fargnoli, C. Gnendiger, S. Paßehr, D. Stöckinger, and H. Stöckinger-Kim, Two-loop corrections to the muon magnetic moment from fermion/sfermion loops in the MSSM: Detailed results, J. High Energy Phys. 02 (2014) 070.
[204] P. Athron, M. Bach, H. G. Fargnoli, C. Gnendiger, R. Greifenhagen, J.-h. Park, Sebastian Paßehr, D. Stöckinger, H. Stöckinger-Kim, and A. Voigt, GM2Calc: Precise MSSM prediction for $(g-2)$ of the muon, Eur. Phys. J. C **76**, 62 (2016).
[205] P. Athron, C. Balazs, A. Cherchiglia, D. H. J. Jacob, D. Stöckinger, H. Stöckinger-Kim, and A. Voigt, Two-loop prediction of the anomalous magnetic moment of the muon in the two-Higgs doublet model with GM2Calc 2, Eur. Phys. J. C **82**, 229 (2022).
[206] P. von Weitershausen, M. Schafer, H. Stockinger-Kim, and D. Stockinger, Photonic SUSY two-loop corrections to the Muon magnetic moment, Phys. Rev. D **81**, 093004 (2010).
[207] M. Bach, J.-h. Park, D. Stöckinger, and H. Stöckinger-Kim, Large muon $(g-2)$ with TeV-scale SUSY masses for $\tan\beta \to \infty$, J. High Energy Phys. 10 (2015) 026.
[208] A. Cherchiglia, P. Kneschke, D. Stöckinger, and H. Stöckinger-Kim, The muon magnetic moment in the

2HDM: Complete two-loop result, J. High Energy Phys. 01 (2017) 007; 10 (2021) 242(E).
[209] M. Aaboud *et al.* (ATLAS Collaboration), Search for electroweak production of supersymmetric particles in final states with two or three leptons at $\sqrt{s} = 13$ TeV with the ATLAS detector, Eur. Phys. J. C **78**, 995 (2018).
[210] A. M. Sirunyan *et al.* (CMS Collaboration), Search for electroweak production of charginos and neutralinos in multilepton final states in proton-proton collisions at $\sqrt{s} = 13$ TeV, J. High Energy Phys. 03 (2018) 166.
[211] M. Aaboud *et al.* (ATLAS Collaboration), Search for chargino-neutralino production using recursive jigsaw reconstruction in final states with two or three charged leptons in proton-proton collisions at $\sqrt{s} = 13$ TeV with the ATLAS detector, Phys. Rev. D **98**, 092012 (2018).
[212] G. Aad *et al.* (ATLAS Collaboration), Search for electroweak production of charginos and sleptons decaying into final states with two leptons and missing transverse momentum in $\sqrt{s} = 13$ TeV pp collisions using the ATLAS detector, Eur. Phys. J. C **80**, 123 (2020).
[213] G. Aad *et al.* (ATLAS Collaboration), Searches for electroweak production of supersymmetric particles with compressed mass spectra in $\sqrt{s} = 13$ TeV pp collisions with the ATLAS detector, Phys. Rev. D **101**, 052005 (2020).
[214] G. Aad *et al.* (ATLAS Collaboration), Search for direct production of electroweakinos in final states with one lepton, missing transverse momentum and a Higgs boson decaying into two b-jets in pp collisions at $\sqrt{s} = 13$ TeV with the ATLAS detector, Eur. Phys. J. C **80**, 691 (2020).
[215] G. Aad *et al.* (ATLAS Collaboration), Search for chargino-neutralino production with mass splittings near the electroweak scale in three-lepton final states in $\sqrt{s} = 13$ TeV pp collisions with the ATLAS detector, Phys. Rev. D **101**, 072001 (2020).
[216] G. Aad *et al.* (ATLAS Collaboration), Search for chargino–neutralino pair production in final states with three leptons and missing transverse momentum in $\sqrt{s} = 13$ TeV pp collisions with the ATLAS detector, Eur. Phys. J. C **81**, 1118 (2021).
[217] A. M. Sirunyan *et al.* (CMS Collaboration), Search for new physics in events with two soft oppositely charged leptons and missing transverse momentum in proton-proton collisions at $\sqrt{s} = 13$ TeV, Phys. Lett. B **782**, 440 (2018).
[218] A. M. Sirunyan *et al.* (CMS Collaboration), Combined search for electroweak production of charginos and neutralinos in proton-proton collisions at $\sqrt{s} = 13$ TeV, J. High Energy Phys. 03 (**2018**) 160.
[219] A. M. Sirunyan *et al.* (CMS Collaboration), Search for supersymmetric partners of electrons and muons in proton-proton collisions at $\sqrt{s} = 13$ TeV, Phys. Lett. B **790**, 140 (2019).
[220] A. M. Sirunyan *et al.* (CMS Collaboration), Search for supersymmetry in final states with two oppositely charged same-flavor leptons and missing transverse momentum in proton-proton collisions at $\sqrt{s} = 13$ TeV, J. High Energy Phys. 04 (2021) 123.
[221] A. Tumasyan *et al.* (CMS Collaboration), Search for supersymmetry in final states with two or three soft leptons and missing transverse momentum in proton-proton collisions at $\sqrt{s} = 13$ TeV, J. High Energy Phys. 04 (2022) 091.
[222] G. Aad *et al.* (ATLAS Collaboration), Search for direct production of charginos, neutralinos and sleptons in final states with two leptons and missing transverse momentum in pp collisions at $\sqrt{s} = 8$ TeV with the ATLAS detector, J. High Energy Phys. 05 (2014) 071.
[223] M. Aaboud *et al.* (ATLAS Collaboration), Search for electroweak production of supersymmetric states in scenarios with compressed mass spectra at $\sqrt{s} = 13$ TeV with the ATLAS detector, Phys. Rev. D **97**, 052010 (2018).
[224] W. Adam and I. Vivarelli, Status of searches for electroweak-scale supersymmetry after LHC Run 2, Int. J. Mod. Phys. A **37**, 2130022 (2022).
[225] G. Aad *et al.* (ATLAS Collaboration), Searches for new phenomena in events with two leptons, jets, and missing transverse momentum in 139 fb^{-1} of $\sqrt{s} = 13$ TeV pp collisions with the ATLAS detector, Eur. Phys. J. C **83**, 515 (2023).
[226] A. Tumasyan *et al.* (CMS Collaboration), Search for electroweak production of charginos and neutralinos at $\sqrt{s} = 13$ TeV in final states containing hadronic decays of WW, WZ, or WH and missing transverse momentum, Phys. Lett. B **842**, 137460 (2023).
[227] G. Aad *et al.* (ATLAS Collaboration), Search for charginos and neutralinos in final states with two boosted hadronically decaying bosons and missing transverse momentum in pp collisions at $\sqrt{s} = 13$ TeV with the ATLAS detector, Phys. Rev. D **104**, 112010 (2021).
[228] G. Aad *et al.* (ATLAS Collaboration), Search for direct pair production of sleptons and charginos decaying to two leptons and neutralinos with mass splittings near the W-boson mass in $\sqrt{s} = 13$ TeV pp collisions with the ATLAS detector, J. High Energy Phys. 06 (2023) 031.
[229] A. Tumasyan *et al.* (CMS Collaboration), Search for higgsinos decaying to two Higgs bosons and missing transverse momentum in proton-proton collisions at $\sqrt{s} = 13$ TeV, J. High Energy Phys. 05 (2022) 014.
[230] T. Hahn, Generating Feynman diagrams and amplitudes with FEYNARTS3, Comput. Phys. Commun. **140**, 418 (2001).
[231] J. Küblbeck, M. Böhm, and A. Denner, Feyn arts—Computer-algebraic generation of Feynman graphs and amplitudes, Comput. Phys. Commun. **60**, 165 (1990).
[232] T. Hahn and C. Schappacher, The implementation of the minimal supersymmetric standard model in FEYNARTS and FormCalc, Comput. Phys. Commun. **143**, 54 (2002).
[233] G. Belanger, F. Boudjema, A. Pukhov, and A. Semenov, MicrOMEGAs: A program for calculating the relic density in the MSSM, Comput. Phys. Commun. **149**, 103 (2002).
[234] G. Belanger, F. Boudjema, A. Pukhov, and A. Semenov, MicrOMEGAs 2.0: A program to calculate the relic density of dark matter in a generic model, Comput. Phys. Commun. **176**, 367 (2007).
[235] G. Belanger, F. Boudjema, A. Pukhov, and A. Semenov, Dark matter direct detection rate in a generic model with micrOMEGAs 2.2, Comput. Phys. Commun. **180**, 747 (2009).